UNIVERSITY OF GAZİANTEP
GRADUATE SCHOOL OF
NATURAL & APPLIED SCIENCES

NONLINEAR ANALYSIS OF CONVENTIONAL AND
BUCKLING RESTRAINED BRACED FRAMES UNDER NEAR-
FIELD GROUND MOTIONS

M. Sc. THESIS
IN
CIVIL ENGINEERING

BY
Nali M. AMEEN
June 2012

Nonlinear Analysis of Conventional and Buckling Restrained Braced Frames under Near-Field Ground Motions

M.Sc. Thesis
in
Civil Engineering
University of Gaziantep

Supervisor
Assist. Prof. Dr. Esra METE GÜNEYİSİ

By
Nali M. AMEEN
June 2012

T.C.
UNIVERSITY OF GAZİANTEP
GRADUATE SCHOOL OF
NATURAL & APPLIED SCIENCES
CIVIL ENGINEERING DEPARTMENT

Name of the thesis: Nonlinear Analysis of Conventional and Buckling Restrained Braced Frames under Near-Field Ground Motions

Name of the student: Nali M. AMEEN
Exam date: JUNE, 2012

Approval of the Graduate School of Natural and Applied Sciences

Prof. Dr. Ramazan KOÇ
Director

I certify that this thesis satisfies all the requirements as a thesis for the degree of Master of Science.

Prof. Dr. Mustafa GÜNAL
Head of Department

This is to certify that we have read this thesis and that in our opinion it is fully adequate, in scope and quality, as a thesis for the degree of Master of Science.

Asst. Prof. Dr. Esra METE GÜNEYİSİ
Supervisor

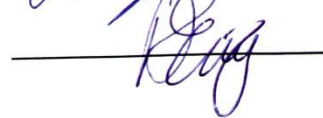Examining Committee Members   Signature

Asst. Prof. Dr. Esra METE GÜNEYİSİ   _____

Assoc. Prof. Dr. Mehmet GESOĞLU   _____

Asst. Prof. Dr. Ahmet ERKLİĞ   _____

I hereby declare that all information in this document has been obtained and presented in accordance with academic rules and ethical conduct. I also declare that, as required by these rules and conduct, I have fully cited and referenced all material and results that are not original to this work.

Nali M. AMEEN

ABSTRACT

NONLINEAR ANALYSIS OF CONVENTIONAL AND BUCKLING RESTRAINED BRACED FRAMES UNDER NEAR-FIELD GROUND MOTIONS

M. Ameen, Nali Nabaz
M.Sc. in Civil Engineering
Supervisor: Asst. Prof. Dr. Esra METE GÜNEYİSİ
June 2012, 121 pages

In this study, nonlinear static and dynamic analyses were performed to compare the structural response of different type of moment resisting frame buildings with diagonally conventional braces (CBs) and buckling restrained braces (BRBs) subjected to near-field ground motions. For the purpose of this study, two bare frames having two equal 6 m bays and a total height of 20 m were selected as case studies. The existing steel frames were designed according to two different cases. They were referred to as a) ordinary moment-resisting frames (OMRF), designed without any provision for preventing the collapse due to storey mechanism and b) special moment-resisting frames (SMRF), designed to fail after the global mechanism occurred. Then, conventional and buckling-restrained braces were inserted in the bays of the existing frames. For the braced frame structures, diagonal type with three different configurations was used. For the earthquake excitation, artificial pulses that were equivalent to Northridge and Kobe records were taken into consideration. Capacity curve, interstorey drift index, global damage index, base shear, top shear, damage index and plastification were evaluated for each frame system. The results exhibited a substantial improvement in the earthquake performance of the frames with the incorporation of conventional and especially buckling-restrained braces.

Keywords: Buckling-restrained brace, Diagonal brace, Earthquake, Frame, Nonlinear analysis, Structural response.

ÖZET

GELENEKSEL VE BURKULMASI ÖNLENMİŞ ÇAPRAZ ELEMANLI ÇERÇEVE YAPILARIN YAKIN ALAN DEPREMLERİ ETKİSİNDE DOĞRUSAL OLMAYAN ANALİZİ

M. Ameen, Nali Nabaz
Inşaat Mühendisliği Yüksek Lisans
Danışman: Yrd. Doç. Dr. Esra METE GÜNEYİSİ
Haziran 2012, 121 sayfa

Bu çalışmada, yakın alan yer hareketlerine maruz kalan değişik tipte geleneksel ve burkulması önlenmiş çaprazlarla güçlendirilmiş moment aktarabilen çerçevelere sahip binaların yapısal tepkilerini karşılaştırmak için doğrusal olmayan statik ve dinamik analizler yapılmıştır. Çalışmanın amacına yönelik olarak 6 m'lik iki eş açıklığa sahip toplam 20 m yüksekliğinde iki farklı çerçeve sistemi ömek çalışma olarak ele alınmıştır. Mevcut çelik çerçeveler iki farklı duruma göre tasarlanmıştır. Bunlar şu şekilde adlandırılmıştır: a) kat mekanizmasına bağlı göçmeyi engelleyecek özelliği bulunmayan sıradan moment aktaran çerçeve (SMAÇ) ve b) toplam mekanizma oluştuktan sonra göçmeye göre tasarlanmış özel moment aktaran çerçeve (ÖMAÇ). Daha sonra, geleneksel ve burkulması önlenmiş çaprazlar mevcut çerçeve açıklıklarına yerleştirilmiştir. Çaprazlı çerçeve yapılar için, üç farklı diyagonal şekli uygulanmıştır. Northridge ve Kobe deprem kayıtları yapay deprem şiddetini belirlemek için kullanılmıştır. Herbir çerçeve sistemi için kapasite eğrisi, katlararası öteleme indisi, genel hasar indisi, taban kesme kuvveti, tepe kesme kuvveti ve plastik mafsallaşma durumları değerlendirilmiştir. Elde edilen sonuçlara göre, geleneksel ve özellikle burkulması önlenmiş çerçevelerin deprem performanslarında önemli iyileştirmeler gözlenmiştir.

Anahtar kelimeler: Burkulması önlenmiş çapraz, Diyagonal çapraz, Deprem, Çerçeve, Doğrusal olmayan analiz, Yapısal tepki.

To My Parents

ACKNOWLEDGEMENT

TABLE OF CONTENTS

CONTENTS   **Page**

LIST OF FIGURES

LIST OF TABLES

LIST OF SYMBOLS/ABBREVIATIONS

CB	Conventional brace
BRB	Buckling restrained brace
CBF	Conventionally braced frame
BRBF	Buckling restrained braced frame
OMRF	Ordinary moment resisting frame
SMRF	Special moment resisting frame
UF-UF	Unbraced frames in two horizontal direction
UF-BF	Unbraced frames in one horizontal direction and braced frames in the other direction
BF-BF	Braced frames in both horizontal direction
MRF	Moment resisting frame
LLRS	Lateral load resisting system
k	Effective axial stiffness of the brace in the elastic range
A	Total area of the of the cross-section of the brace
E	Elastic modulus of members
L	Length of the brace
k_2	Effective axial stiffness of the brace in the post elastic range

E_t	Tangent modulus of elasticity of the bracing
δ	Axial deformation of the brace
δ_y	Axial deformation of the brace at yield stress
f_y	Nominal yield stress
A_g	Gross sectional area of braces
P_y	Nominal axial yield force of braces
P_{cr}	Buckling axial force of braces
Δ_{cr}	Axial deformation of the brace at the Buckling strength of brace
$\bar{P}_{cr}$	Residual force in the brace after buckling
α	Mass proportional damping coefficient
β	Stiffness proportional damping coefficient
ξ	Damping ratio
ω_i	Modal frequency of the structure in one direction
ω_j	Next modal frequency of the structure in the same direction
T_p	Pulse period (duration of a full velocity cycle)
t	Time
$V_{g_{max}}$	Maximum pulse velocity
$a_{g_{max}}$	Maximum pulse acceleration
$u_{g_{max}}$	Maximum pulse displacement
V_g	Ground velocity at any time

a_g	Ground acceleration at any time
u_g	Ground displacement at any time
LS	Life safety level
CP	Collapse prevention level
IO	Immediate occupancy level
δ_{max}	Maximum interstory drift
h	Storey height
D	Roof displacement
H	Total height of the building
Di	Damage Index of the ith storey
De	Effective damage index
ε_u	Ultimate strain of the brace
ε_{max}	Maximum strain experienced by the brace

CHAPTER 1

INTRODUCTION

1.1 General

Several recent destructive earthquakes, particularly the 1994 Northridge earthquake in California, the 1995 Hanshin-Awaji (Kobe) earthquake in Japan, and the 1999 Chi-Chi earthquake in Taiwan inflicted various levels of damage upon a large number of low-rise to medium-rise steel framed structures (FEMA 355E, 2000). The structural damage in steel structures was primarily caused by insufficient lateral load carrying capacity, poor detailing of connections, and local buckling occurring in connections and/or brace members (Bruneau et al., 1988; Mahin, 1988; Watanabe et al., 1988b; Nakashima et al., 1988; Tremblay et al., 1995; Tremblay et al., 1996; Naeim et al., 2000). The investigation of these negative consequences gave rise to serious discussion about seismic design philosophy and extensive research activity on the retrofit of existing steel framed buildings. Two retrofitting strategies emerged as being practical and efficient. The first one is to add new structural elements such as steel diagonal bracings providing the global stiffening and strengthening of the lateral load resisting systems (LLRS). The second one is to upgrade by selectively strengthening the deficient structural elements of the buildings including local modification of material properties and/or seismic details (Sarno et al., 2006). Generally, the first method is preferred and lateral force resisting elements such as steel braces are prevalently used to increase the seismic strength of framed building structures.

Considering the ease of construction and the relatively low cost, steel braces appear to be an attractive alternative to the other shear resisting members. Therefore, the bracing system becomes a very effective global upgrading strategy to enhance the global stiffness and strength of steel moment resisting framed structures. However, conventional braces (CBs) exhibit buckling deformation when loaded with large compression force (FEMA 450, 2003; Martinelli et al., 2003) and show unsymmetrical hysteresis behavior in tension and compression and typically the load resisting capacities are reduced when loaded monotonically in compression or cyclically (Qiang, 2005; Asgarian and Amirhesari, 2008). In order to overcome this problem, many research efforts have been conducted (Wakabayashi et al., 1973a; Kimura et al., 1976; Mochizuki et al., 1979; Fujimoto et al., 1988; Nagao et al., 1988), and as a result new type of brace called buckling restrained brace (BRB) with a perfect nonlinear behavior such as symmetrical hysteresis behavior, large energy dissipation and significant ductility has been developed, and that is by providing lateral support to ordinary braces that prevent buckling deformation; hence, the brace shows the same nonlinear behavior in both tension and compression.

Buckling restrained braces commonly found are made by encasing a core steel cross-shape or flat bar member into a steel tube and confined by infill concrete as shown in Figure 1.1 (Black et al., 2004; Sabelli et al., 2003). The two requirements to be met in the design of the BRBs, namely the axial strength to avoid material failure and flexural rigidity to avoid buckling, are provided by an axially loaded core and the sleeve surrounding it, respectively. The space between the core and the sleeve is filled with infill concrete or any other inert filler. The steel core member is designed to resist the axial forces with a full tension or compression yield capacity without the local or global flexural buckling failure.

When the brace is subjected to compression forces, an unbonding material placed between the core member and the infill concrete is required to reduce the friction. Thus, a BRB basically consists of three components, including steel core member, buckling restraining part, and the unbonding material.
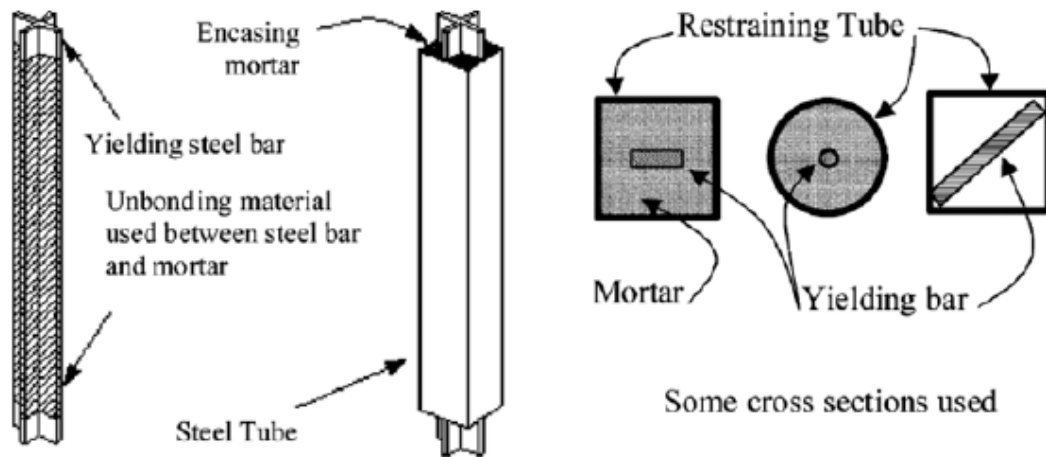
Figure 1.1 Some schematic details used for buckling restrained braces (Sabelli et al., 2003)

1.2 Objective and scope

The main objective of this study is to compare the seismic performance of different type of steel moment resisting framed buildings namely, special moment resisting frame (SMRF) and ordinary moment resisting frame (OMRF) equipped with diagonally CBs and BRBs subjected to near field ground motions and exploring the effect of improved nonlinear behavior of BRBs on performance and response of the building structures, also investigating the effect of buckling of the CBs on the response and behavior of the building structures when loaded with a large compressive force and finally judging on the rehabilitation strategy that would best improve the seismic performance of the buildings. For this, six-storey steel moment

resisting frames (MRFs) with lateral stiffness insufficient to satisfy code drift limitations were selected as case studies. Near-field ground motions based on Northridge and Kobe records were used. Then, series of nonlinear static and dynamic analyses were carried out for investigating the structural behavior of sample steel frames before and after retrofit.

1.3 Outline of the thesis

The major objective of this thesis is to provide a description through nonlinear analysis procedures of the various frame systems and assess their efficiency.

Chapter 1-Introduction: Aim and objectives of the thesis are introduced.

Chapter 2-Literature review: This chapter traces the historical background on practical application and previous studies on moment resisting frames, braced frames and their different types. Also, the negative consequences during severe earthquakes of each frame system discussed with an emphasis on available investigations on BRBs.

Chapter 3-Methodology: In this chapter, type of the frame systems and rehabilitation strategies that was used in this study is presented and the type of analysis procedures that has been carried out with the assumptions for modeling is discussed. Also it describes and discusses the ground motions used in this research.

Chapter 4-Result and discussion: This chapter present and discusses the results obtained from nonlinear static and dynamic analysis for assessing the structural performance of each frame system considered in this study in terms of capacity curves, interstorey drift index, and etc.

Chapter 5-Conclusion: General conclusions are drawn regarding the overall results from all chapters.

Appendix A-Constant ductility spectra: Reminds the reader on the theoretical background for computing constant ductility spectra, as presented in Chopra 2005.

Appendix B-Interstorey drift time history: Presents the nonlinear time-history analysis results in terms of interstorey for each floor level.

Appendix C-Roof displacement time history: Presents the nonlinear time-history analysis results in terms of roof displacement.

Appendix D-Base shear and top shear time history: Presents the nonlinear time-history analysis results in terms of base and top shear.

CHAPTER 2

LITERATURE REVIEW

2.1 Moment Resisting Frames

For more than hundred years ago steel moment resisting frames have been used, the first use of steel moment resisting frame was in 1885 in the 10 storey 138ft *Home insurance building* in Chicago, as shown in the Figure 2.1. At that era this building and many other tall buildings constructed with steel moment resisting frames by using "H" sections built up from zees and "L" sections, in these buildings typically large gusset plate were used and joined the beam and columns by angles and rivets. From 1900 to 1930, the use of the built up sections began to see decreasing and instead of them rolled "H" sections were used, for many years many tall structures such as *Newyork empire state building*, used such type of section profile. Following the second world war, engineers observed that it is not economic to utilize infill unreinforced masonry for the perimeter walls, as a result the walls began to be made of lighter materials such as; aluminum and modern glasses. The uses of gusset plates were ended, instead of that top and bottom flanges of the beam were connected to the column directly by angle and split tees. In 1950s, instead of angle and split tees, weld connections begun to be used, the top and the bottom flanges of the beams welded to the column flanges and the web of the beams were riveted the column flanges, however, by 1960's instead of rivet connections, high strength bolting begun to be used because they founded to be more economic compared to rivet connections.

Finally in the early 1970's engineers began to use the connection type known today as the welded unreinforced flange-bolted web (Ronald et al., 2009).

Figure 2.1 The Home Insurance Building – Chicago, IL, 1885, an early skyscraper
(Ronald et al., 2009)

In 1960 to 1970, Professor Egor Poper at University of California has shown that a perfect inelastic behavior could be obtained for steel structures during severe earthquakes by controlling the detailing and proportioning. Later, special design requirement, detailing and configurations were founded in the building codes in order to reduce seismic hazard in the high seismic risk regions (Ronald et al., 2009).

And finally a ductile steel frame was introduced as special moment resisting frame (SMRF) in the uniform building code (UBC), the term special refers to:

a) Special criteria are required in designing, and

b) Special performance during severe earthquakes.

At the beginning, the requirement for SMRF was to provide connections such that capable of developing of the strength of the connected members. However, later requirements introduced that

a) Weak beam/ strong column ratio,

b) Balance shear strength in the panel zones, and

c) Section compactness.

Must be provided, most of the steel structures constructed in 1960 to 1970 in western US were moment resisting frames and provided moment resisting connection and great distribution of lateral force and redundancy. However, engineers by 1980's begun to decrease the redundancy and to provide an economic meaning for the building structures through decreasing the moment resisting frame bays. In the aftermath of Northridge earthquake in Los angles, the brittle fracture of many modern special moment resisting frames had surprised the engineers and accelerated the research programs toward developing more robust moment resisting frames (Ronald et al., 2009).

A consortium of professional associations and researchers known as SAC Joint Venture engaged in a federally funded, multi-year program of research and development to determine the causes of this unanticipated behavior. The SAC research, conducted at a cost of $12 million over eight years, resulted in the basis for

the current design provisions for moment resisting frames contained in AISC 341 (AISC, 2005a), AISC 358 (AISC, 2005b), and AWS D1.8 (AWS, 2005).

2.2 Braced frames

Lessons learned with regard to steel moment resisting frames in the past earthquakes, accelerated the research efforts with the aim to enhance the braced frame structures as an alternative system. And that is due to ease of construction and the relatively low cost. Steel braces appear to be an attractive alternative to the other shear resisting members. Therefore, the bracing system becomes a very effective global upgrading strategy to enhance the global stiffness and the strength of steel moment resisting framed structures. Nonetheless, severe earthquakes, e.g. those in the 1985 Mexico (Osteraas and Krawinkler, 1989), 1989 Loma Prieta (Kim and Goel, 1992), 1994 Northridge (Tremblay et al,, 1995; Krawinkler et al., 1996), and 1995 Hyogo-ken Nanbu (AIJ, 1995; Hisatoku, 1995; Tremblay et al., 1995), demonstrates that buckling of the diagonal members and poor detailing of the connections (e.g. column to base, brace to beam, brace to column, beam to column) may erode seismic performance as a whole (Broderick et al., 1994; Elnashai et al.,1995; Nakashima et al., 1998; Watanabe et al., 1998b; Naeim et al., 2000).

After the 1995 Hyogoken-Nanbu (Kobe) earthquake, a survey was conducted by Youssef et al. (Youssef et al., 1995); according to the results of their study, the damage to structural members and connections with respect to structural type and the distribution of damage level is illustrated in Figure 2.2 (Di Sarno and Elnashai, 2009).

Damaged structures are categorized as having unbraced (UFs) or braced (BFs) frames. Thus, considering the two main framing directions of a structure, the surveyed buildings contain the following designations: UF-UF (unbraced frames in both horizontal directions), UB-BF (horizontally unbraced frames in one direction and braced frames in the other direction), and BF-BF (braced frames in both horizontal directions) (Youssef et al., 1995).
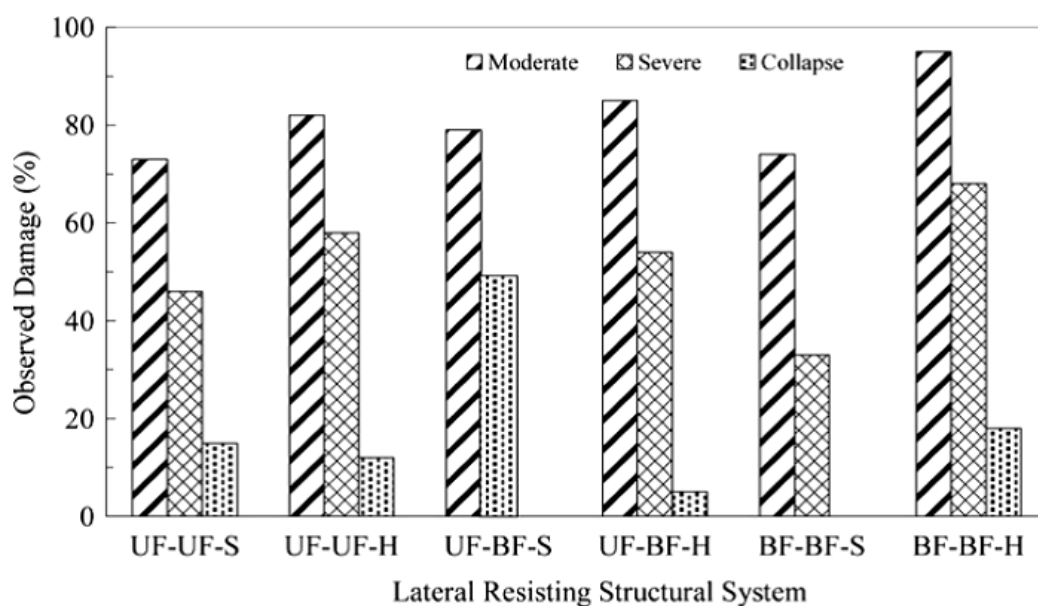
Figure 2.2 Distribution of damage level with respect to structural type (Di Sarno and Elnashai, 2009)

Most of the beams made with wide flange section and the columns with wide flange (H) sections, also some structural systems used square-tube sections (S). A total of 988 damaged building were considered in that survey; the statistics according to class of the frame were as follow:

a) 432 (43.7%) are UF-UF,

b) 134 (13.6%) are UF-BF,

c) 34 (3.4%) are BF-BF, and

d) 388 (39.3%) have an unidentified framing systems.

These statistics showed that few damages had occurred in the braced frames and most of the damages had occurred in the unbraced frames (Youssef et al., 1995).

Location of the damage, namely beams, columns, braces, beam to column connection and column bases, with the type of frame is shown in Figure 2.3. Following observations made from the collected data are as follows (FEMA 355E, 2000):

a) In the case of UFs most of the damage occurred in the column compared to other parts of the frames, while in the case of BFs most of the plastic deformation had concentrated in the brace elements,

b) Also UFs experienced significant damage in the column bases and the beam to column connections,

c) UFs utilized hollow sections for the columns had experienced significant damage in the beam to column connections, and

d) Columns made with wide flange sections experienced relevant damage in the case of UFs.

The observation and discussion made for the above surveyed data is representative for steel frames damaged by moderate to severe earthquake excitations (FEMA 355E, 2000).
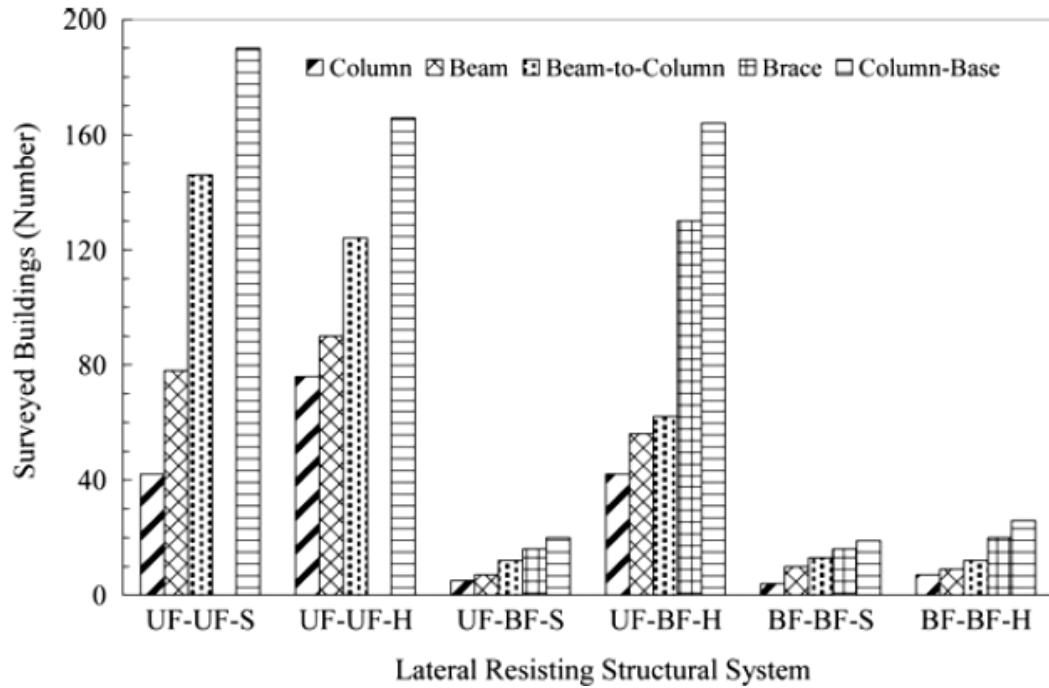
Figure 2.3 Damage to structural members and connections with respect to structural type (Di Sarno and Elnashai, 2009)

Buckling deformation of the braces may result in eroding the capacity of the structures, degradation of strength and stiffness and sudden change in the dynamic characteristics of the lateral load resisting system (LLRS) (Di Sarno and Elnashai, 2009). Figure 2.4 shows the brittle fracture for beam to column and brace to column connections that has resulted in reducing the performance and energy dissipation capacity under earthquake excitation. As a result care should be taken in the capacity design such that beam to column connections and the braces provide sufficient ductility (Bruneau et al., 1988; Nakashima et al.,2000; Tremblay, 2002; Broderick et al., 2005).
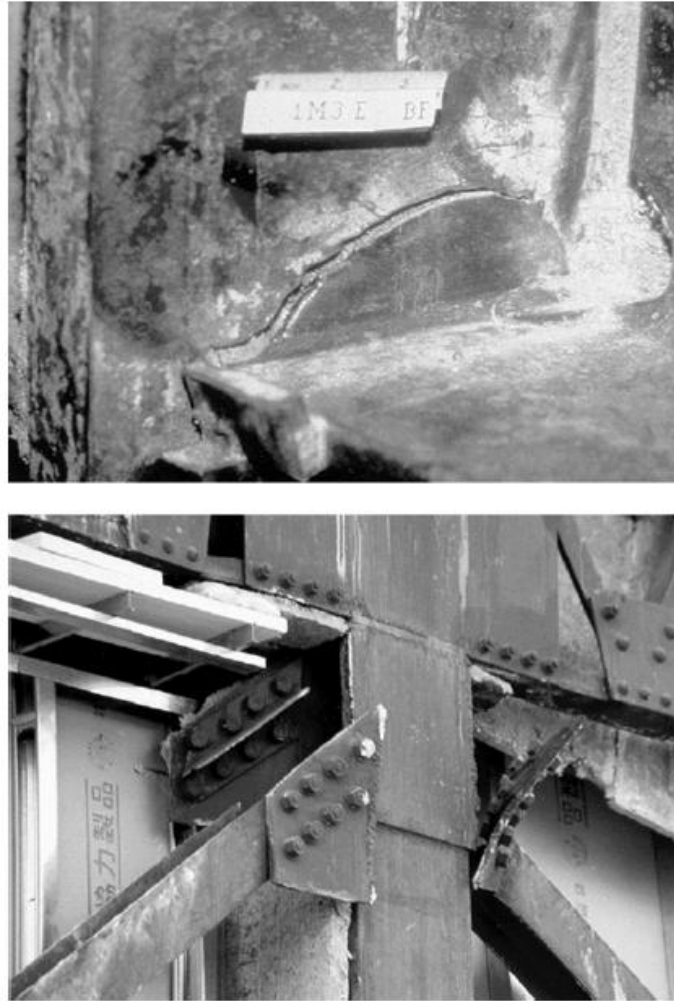
Figure 2.4 Fracture in beam-to-column connections in the Northridge earthquake (*top*) and web tear-out in bolted brace-to-column connections during the 1995 Kobe earthquake (*bottom*) (Di Sarno and Elnashai, 2009)

In response to many practical and economic issues, engineers are turning to the use of braced steel frames. Whenever hysteretic dampers are utilized, it is anticipated that the braces can increase the energy absorption of structures and/or reduce the demand imposed by earthquake loads. Structures are expected to resist safely the lateral load induced by an earthquake and avoid the risk of brittle failure if their energy absorption capacity is augmented. Design demands on structural and nonstructural component are conceived to be smaller than their capacity when global modification is applied as shown in Figure 2.5 (Bozorgnia and Bertero, 2004; Di Sarno and Elnashai, 2009).
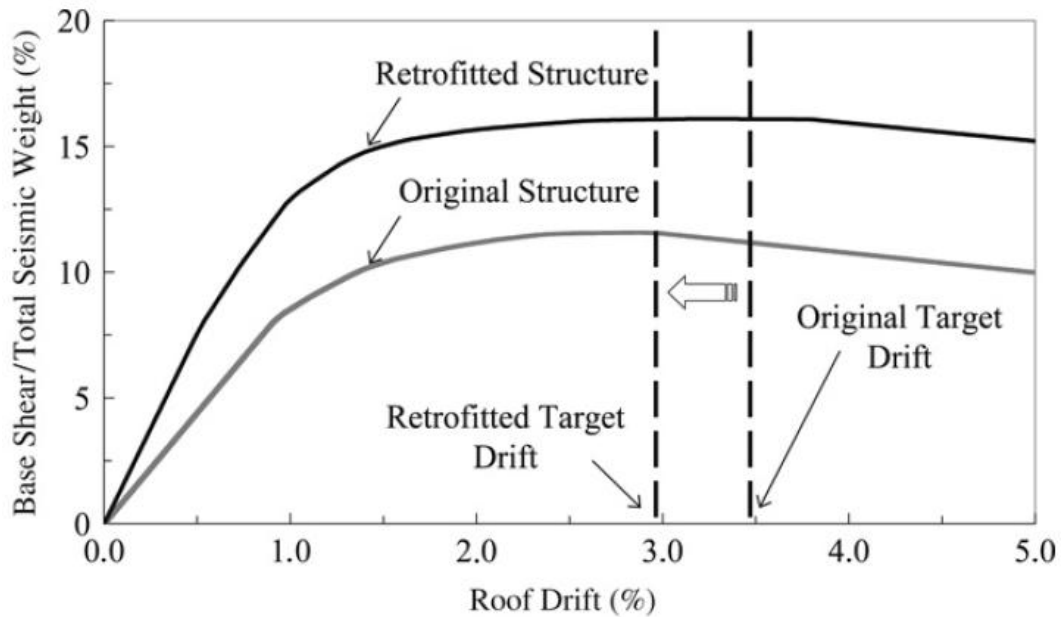
Figure 2.5 Characteristics of global intervention approaches in seismic retrofitting of structures (Di Sarno and Elnashai, 2009)

During severe earthquakes, large amount of kinetic energy would be fed to the structures, all building codes recognize that it is not economic to dissipate energy only through the elastic capacity of the materials. Thus, the best strategy to dissipate energy is to accept that yielding occurs in the structure but in such a way that plastic deformation would be concentrated at controlled locations or structural fuses and major structural members remain elastically (Deulkar et al., 2010).

In traditional braced frames, braces are considered the structural fuses that dissipate seismic energy through yielding in both tension and compression. However, due to potential problems and difficulties aroused from buckling deformation of the conventional braces (CB), the idea of buckling restrained brace (BRB) borne out to improve compressive capacity and achieve more favorable behavior, BRBs exhibit stable and balanced hysteresis behavior by accommodating ductile compression yielding before the onset of buckling (Asgarian and Amirhesari, 2008; Mahmoudi and Zaree, 2010).

2.2.1 Conventional braced frames

In order to resist lateral forces due to wind and earthquakes, conventionally braced frames (CBF) are considered to be one of the most efficient structural systems in steel construction.

In the past decades, engineers used conventional braces (CB) to control interstorey drift so that potential problems due to geometric nonlinearities and sudden fracture in the connections were mitigated. The CBs as LLRS were selected due to the fact they provide an economic means in steel construction, ease of construction and complete truss action (Rai and Goel, 2003).

However, CBFs had exhibited certain unfavorable modes in the severe earthquakes as a result of strength and stiffness degradation and excessive flexure of beams in chevron braced frames. These potential problems are due to buckling deformation and they have limited capacity in compression, as shown in Figure 2.6. Several researchers have tried to investigate the inelastic behavior of CBs when loaded cyclically, those analytical and experimental study has showed that the hysteresis behavior of such axially loaded members are characterized by gradual reduction in compressive capacity and deterioration of stiffness in tension. As a consequence of these behaviors, in the design process the brace selected for some stories are usually stronger than required while braces in the other stories have a capacity near from the design. These discrepancies lead to concentration of the earthquake damage in few 'weak' stories when some of the braces buckle prior to others. It is also observed that the buckling of the conventional braces results in a substantial damage to the adjacent nonstructural members (Sabelli et al., 2003; Mahmoudi and Zaree, 2010).

a) Behavior of conventional brace and buckling restrained brace tested in labaratory
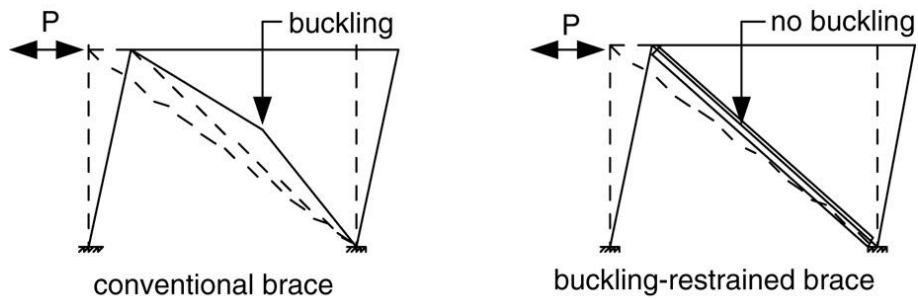
b) Schematic diagram showing behavior of conventional brace and buckling restrained brace

Figure 2.6 Behavior of conventional (CB) and buckling restrained brace (BRB) (Qiang, 2005)

Behavior of concentrically braced frames is strongly depending on the cyclic inelastic behavior of the braces. However, CBs have a complex hysteresis behavior when loaded cyclically, as shown in Figure 2.7, and that is due to following physical phenomena (Mahmoudi and Zaree, 2010):

a) Yielding in tension,

b) Buckling in compression,

c) Degradation of compressive capacity in post buckling range,

d) Degradation of axial stiffness, and

e) Low cycle fatigue fracture.

The previous physical factors make the analytical modeling complicated to be modeled accurately. Nevertheless, in practical analysis, accurate prediction is required in modeling the inelastic range for each component as stated in FEMA273 (FEMA273, 1997).

a)   b)
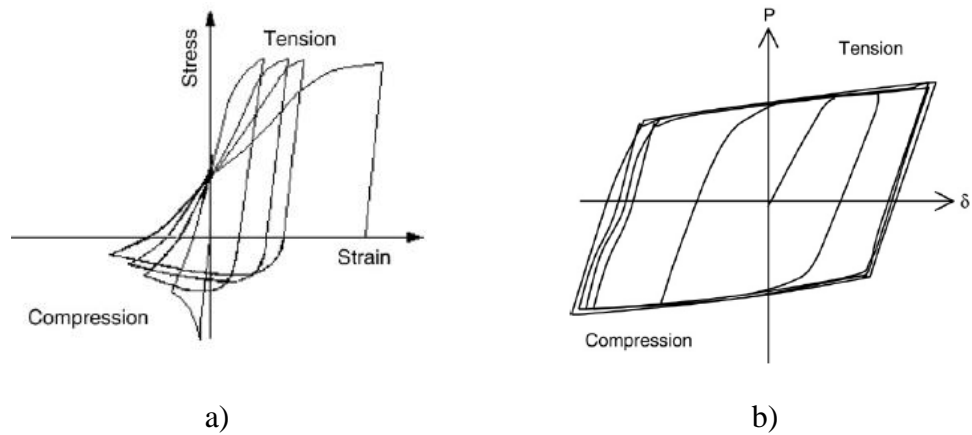
Figure 2.7 Hysteresis behavior of a) conventional brace and b) buckling restrained brace (Qiang, 2005)

2.2.2 Buckling restrained brace frames

Due to limited energy dissipation capacity and many other potential difficulties associated with utilizing conventional braces as a LLRS, as discussed previously. Researchers and engineers have been motivated to develop a new type of brace which exhibit more ideal elasto plastic behavior called buckling restrained brace (BRB). The concept of the BRB is simple, providing lateral support to the brace so that buckling deformation is prevented, as shown in Figure 2.8.

a)   b)

Figure 2.8 Schematic diagram of a) conventional brace and b) buckling restrained
brace

Previous researches (Saeki et al., 1995; Iwata et al., 2000; Yamaguchi et al,. 2000; Black et al., 2002) has shown that the BRBs exhibit symmetric hysteresis behavior with high energy dissipation capacity through stable tension-compression yield cycles, as shown in Figure 2.7.

The BRB is composed of a ductile steel core that carries the entire axial load of the brace and a sleeve surrounding it that provide flexural rigidity and stiffness to prevent global buckling, the space between the steel core and the sleeve is filled with grouting or any other inert filler. As seen in Figure 2.9, the BRB provides a slip surface between the core brace and the encasing unit so than no axial force would be transferred to the sleeve, as a result this assembly makes the steel core to deform longitudinally independent from the mechanism that restrains lateral and local buckling. The materials and geometry in this slip layer must be carefully designed and constructed to allow relative movement between the steel element and the concrete due to shearing and Poisson's effect, while simultaneously inhibiting local buckling of the steel as it yields in compression (Sabelli et al., 2003; Kumar et al., 2007; Deulkar et al., 2010).
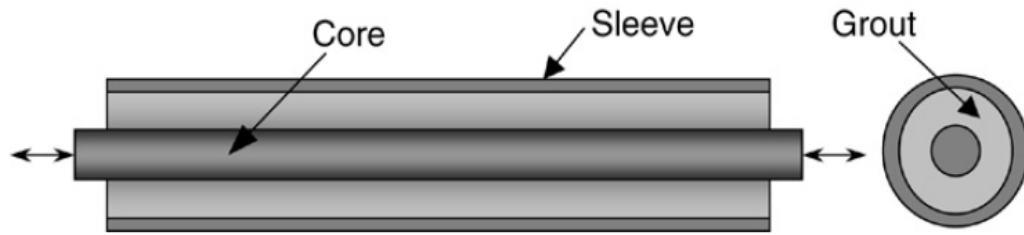
Figure 2.9 Nonbuckling bracing (Kumar et al., 2007)

Thus, as shown in Figure 2.10, basic BRB composition can be summarized as follow:

a) Steel core member (brace),

b) Projection of brace core beyond the buckling restrained unit,

c) Encasing unit (buckling restraining part), and

d) A debonding material between the brace and the encasing unit.
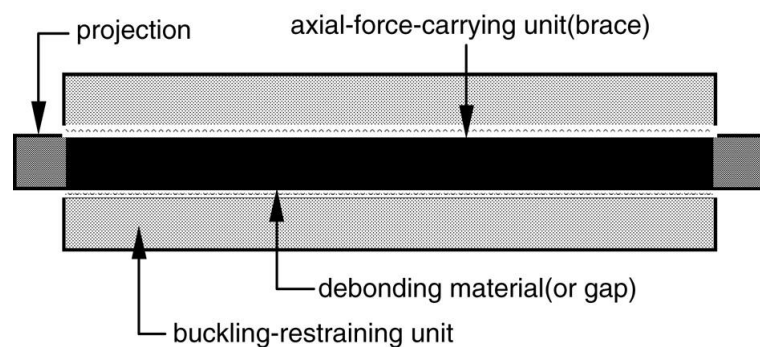
Figure 2.10 Composition of typical buckling-restrained brace (Qiang, 2005)

Previous researches (Kalyanaraman et al., 1994; Kalyanaraman et al., 1998a; Kalyanaraman et al., 1998b; Kalyanaraman et al., 2003) have shown that so long as the restraining unit has adequate elastic strength to prevent buckling under compression, the core brace can be subjected to a compressive strain well beyond the yield strain, without overall buckling of the strut. So as long as the compressive yield strength of the brace core smaller than the Euler buckling strength of the sleeve, the

sleeve does not buckle under compression. Thus, the core in non-buckling bracing can undergo considerable yielding, under both compression and tension, and absorb considerable energy, unlike conventional bracing. The basic structural framework in BRB frames is designed to remain elastic and all plastic deformation occurs in the braces (Sabelli et al., 2003).

Kalyanaraman et al. (1998a) have shown that the BRB has ability to control storey drift and energy absorption by varying the cross-sectional area of the steel core, the yield strength of the steel and the length of the core which is allowed to yield.

The BRBs subjected to many experimental tests (Nakashima et al., 2000; Tremblay, 2002; Bozorgnia and Bertero, 2004; Broderick et al., 2005), they have shown that due to the confinement effect of the restraining unit, the steel core brace can undergo an axial compressive strength about 10% to 15% greater than tensile capacity. Moreover, as shown in Figure 2.11, inelastic deformation (ductility) capacities are quite large such that the cumulative cyclic inelastic deformations often exceeding 300 times the initial yield deformation of the brace failure (Sabelli et al., 2003; Di Sarno and Elnashai, 2009).

To intentionally make the BRBs yield strength low to enhance energy dissipation, usually BRBs are manufactured with low yield steels, e.g. LYP100 and LYP235 with yield strength (f_y) equals to 100 MPa and 235 MPa, respectively (Sabelli, 2003; Qiang, 2005).
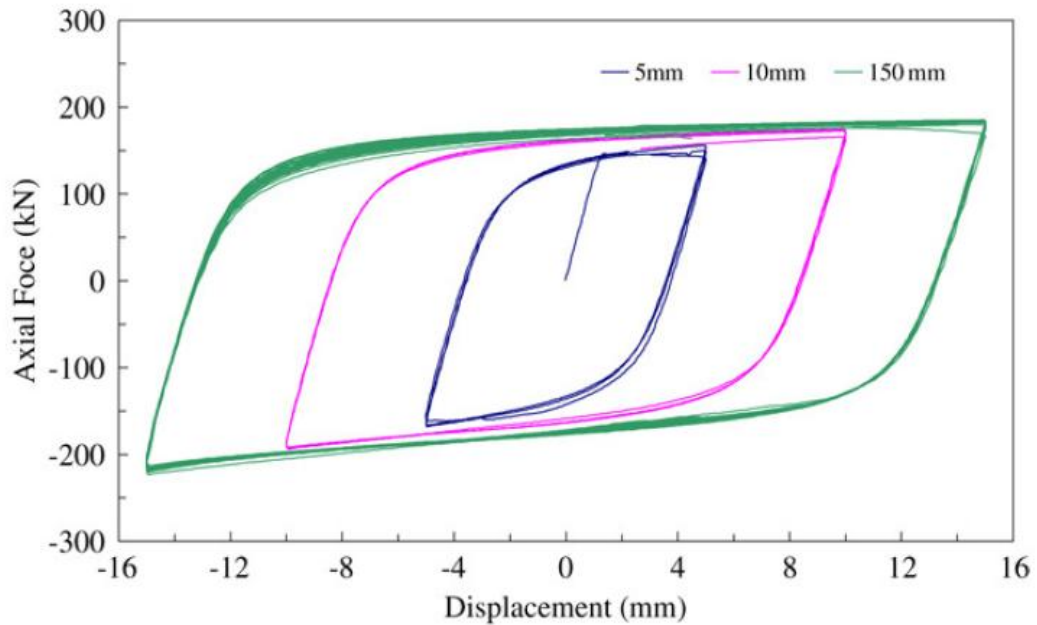
Figure 2.11 Response curve for typical unbonded brace (Di Sarno and Elnashai, 2009)

Buckling restrained braces are hysteresis dampers, as shown in Figure 2.11, very popular in US, Japan, and Italy since they are generally more cost effective than other types of passive protection devices used for seismic retrofitting, such as viscous dampers and high rubber bearing for base isolation (Soong and Dargush, 1998; Naeim and Kelly, 1999).

2.3 Previous researches on BRBs

Yoshino and Karino (1971) carried out the first research on the BRB. In their study, they tested two specimens that they called "*shear wall with braces*" under cyclic loading, each specimen consists of flat steel plate surrounded by reinforce concrete panels, the bond between them was broken by coating the steel plate with a debonding material, one of the specimens was provided with a 15 mm clearance between the panel lateral sides and the surrounding panel while no space is left in the second specimen.

A pioneering research carried out by Wakabayashi et al. (1973a), in their study, steel flat plates were used for the braces and they were surrounded by reinforced concrete panels with a debonding material between them. They concluded from the test result that breaking the bond between the brace and the surrounded panel would make the brace carry considerable axial force while the surrounding reinforced concrete panel served only to restrain the buckling deformation of the brace.

Their study consisted of the following muli-step experimental plan:

a) For examining the unbonding effect, tests on the debonding material were conducted,

b) Tests on the brace were conducted to explore the effects of strengthening of PC panels with steel reinforcement and reinforcement at boundaries and around the plates,

c) Reduced-scale tests on brace systems encased by PC panels, and

d) Tests on large-scale two-storey frames with the proposed brace systems.

Silicon resin, epoxy resin, vinyl tapes, etc. were tested for exploring the effect of debonding. Pull out tests were conducted on eleven samples with different debonding materials. The method of debonding of coating a layer of silicon resin on top of a layer of epoxy resin was utilized in the following tests.

Twenty one specimens with different details of the plate reinforcement and details between the exposed and embedded parts (styrol foam, gaps) were tested under monotonic compressive force, they found that it was important to put small styrol foam in the gap in order not to restrain the stiffened ends from deformation in the PC panels.

Fourteen specimens of X-brace and diagonal brace frame systems with a reduced scale of 1/5 were tested under cyclic loading in order to examine the hysteresis behavior, Figure 2.12 shows the test set up and the hysteresis behavior for one of the specimens used in the studies of Wakabayashi et al. (1973a; 1973b). They concluded from the test results that bonded braces exhibited a smaller load carrying capacity compared to unbonded braces. Maximum lateral drift angle in the case of unbonded brace was about of 0.03 rad which it was almost four times larger than that of the bonded brace.

In order to check the behavior of the BRB in real steel frames, two steel frame specimens (two stories and tow spans) with a scale of 1/2 were also tested for the final demonstration. As shown in Figure 2.13, they observed that the behavior the frames were stable, showed a spindle-hysteresis behavior and good energy dissipation capacity before local buckling occurs in the steel brace at a lateral angle of drift of 0.025 rad (Wakabayashi et al., 1973a; Wakabayashi et al., 1973b).
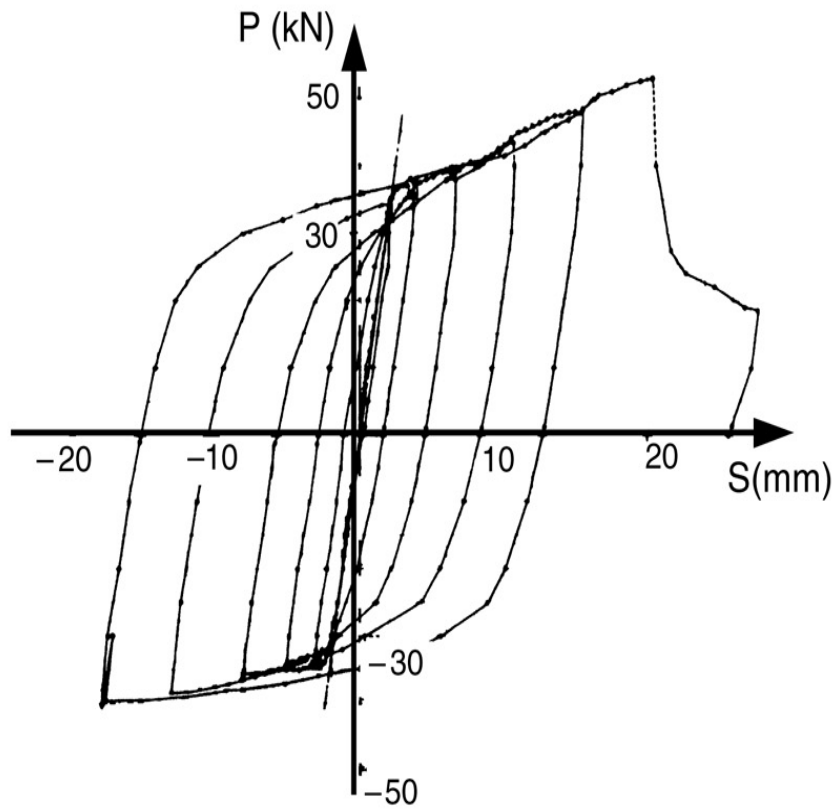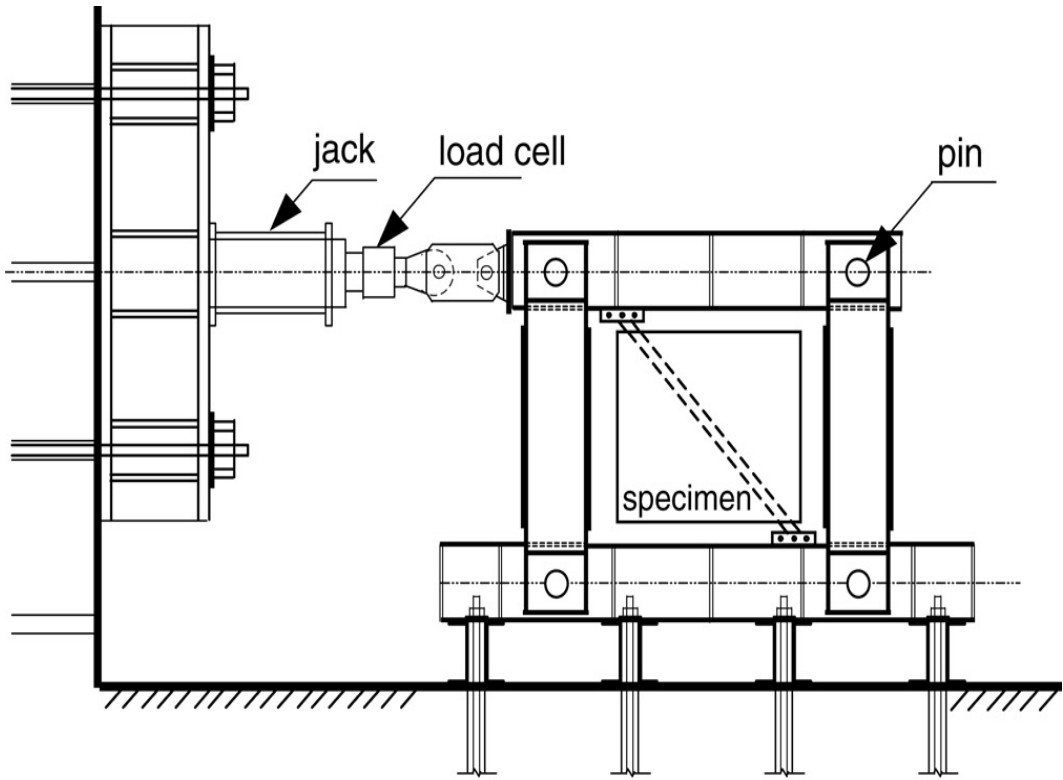
Figure 2.12 Buckling-restrained brace test setup and its hysteresis (Wakabayashi et al., 1973a; Wakabayashi et al., 1973b)
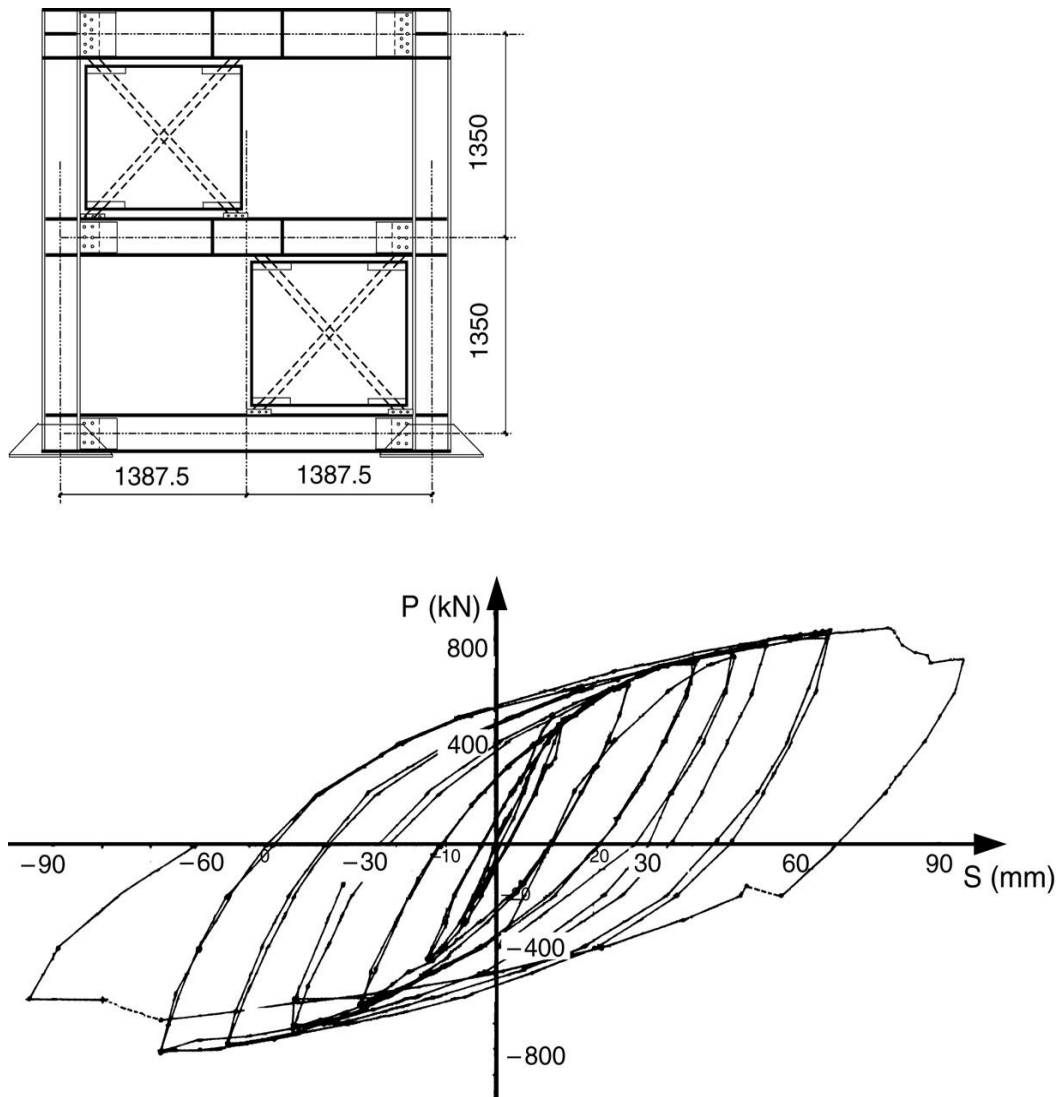
Figure 2.13 Frame test of X-shape BRB and its hysteresis (Wakabayashi et al., 1973a; Wakabayashi et al., 1973b)

Kimura et al. (1976) conducted the first test on steel braces surrounded by mortar-infilled steel tubes. However, no debonding materials were utilized for providing a slip surface for the brace, the encasing mortar infilled steel tube had showed some effect of preventing the buckling deformation of the steel brace core. The measured longitudinal strains in the steel tubes were approximately 10% to 15% of the longitudinal stain in the core braces. The test results had showed that the core brace could undergo an axial compressive strength greater than tensile strength.

25

In the subsequent research (Takeda and Kimura, 1979), they tested four specimens with full scale under cyclic loading but this time two of the specimens had some slit between the encasing mortar and the core brace, the results showed that the core brace would not exhibit any buckling deformation and dissipate a considerable energy if the ratio of the Euler limit of the steel tube to the yielding strength of the core brace is greater than 1.9.

Mochizuki et al. (Mochizuki et al., 1979; Mochizuki et al., 1980; Mochizuki et al., 1982) did some tests on the composite BRBs consisting of unbonded braces encased in reinforced concrete square cross-section members. In their study, a coefficient factor that represents the stiffness degradation of concrete panel after it cracks was used.

In the studies of Fujimoto et al. (1988) and Watanabe et al. (1988a), a slip surface was provided for the core brace so that no axial force would be transferred to the restraining unit. Figure 2.14 shows the dimension and cross-sections of the specimens and the test results, it could be seen from the test results that specimen No. 3 did not exhibit buckling deformation when loaded with a large compressive force and showed a spindle hysteresis behavior that dissipate large energy. On contrary, specimen No.4 due to insufficient restraining, global buckling had occurred before reaching its yield load.
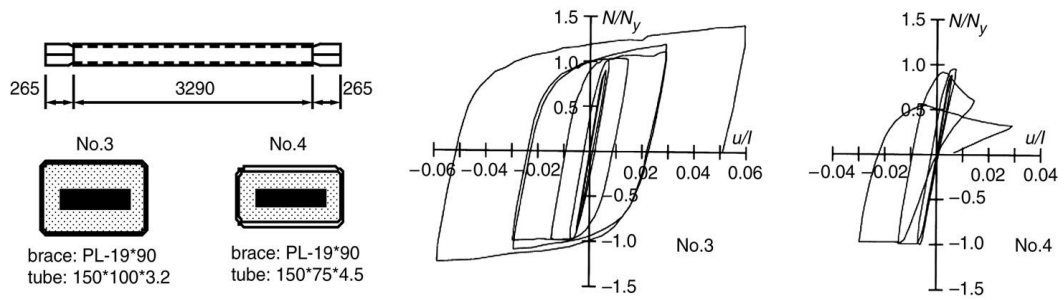
Figure 2.14 Dimensions and cross-sections of the specimens and the results
(Fujimoto et al., 1988)

Nagao et al. performed some experimental and theoretical analyses on composite BRBs composed of square steel tubes (braces) or H-section steel cores covered by reinforced concrete members (Nagao et al., 1988; Nagao et al., 1989; Nagao et al., 1990; Nagao et al., 1991; Nagao et al., 1992).

Kumar et al. (2007) presented the results of an analytical study carried out to understand the seismic behavior of multi-storied moment resisting and non-moment resisting frames designed with non-buckling bracing systems.

Lin et al. (2010) evaluated the seismic design and performance of eccentrically braced frames and buckling restrained braced frames in comparison with that of moment resisting frames.

As shown in the Figure 2.15, it was conducted on panel BRBs in order to confirm the global buckling restraining criterion. At that test, the steel plate brace was separated from the PC panels. Link devices were used to connect them together and they were installed at interval of 10 cm. Then, the steel plate was subjected to axial load. The aims of separating the PC panels from the steel plate brace were (Inoue et al., 1992; Inoue et al., 1993; Inoue et al., 2001):

a) To measure the force distribution of the brace directly, and

b) To adjust steel brace initial deflection arbitrarily.

As shown in Figure 2.15, the rod end and universal joint were installed at both ends of the linking device and to measure the force in the brace, load sensors were installed at each linking device. Linear bearing that could slide freely in the direction orthogonal to the steel plate plane was used to support the reinforced concrete panels. The initial deflection can be changed through the location-adjustable bolts shown in Figure 2.15.

Moment diagram and brace force distribution at the instance of buckling of the steel plate brace is shown in Figure 2.16. Bending moment M in the precast concrete panels was determined based on the force distribution in the steel plate brace. Force distribution of the brace was very complicated, but at the ends of the brace the value was large. The figure illustrates the bending moment distribution of the precast concrete (PC) panel and it is similar to the initial deflection distribution of the steel plate brace. At mid of the precast concrete panel, maximum bending moment occurred. Moreover, if the maximum moment is estimated as an equally distributed load, the bracing force is about 1.5% of yielding axial strength (Inoue et al., 1992).
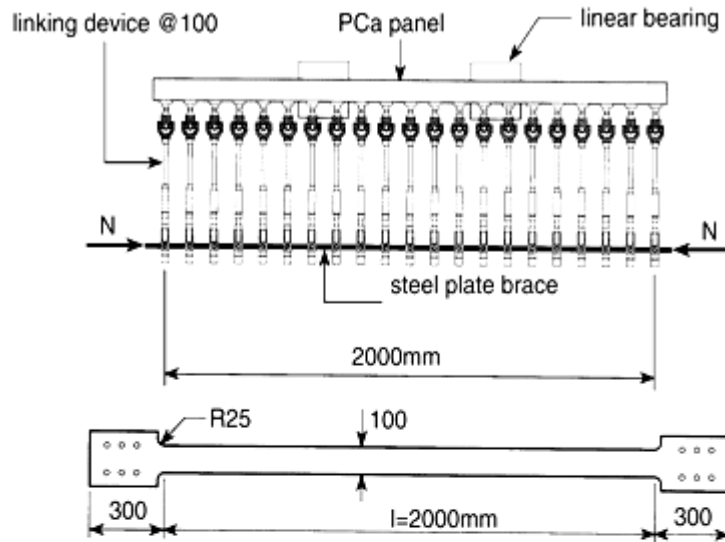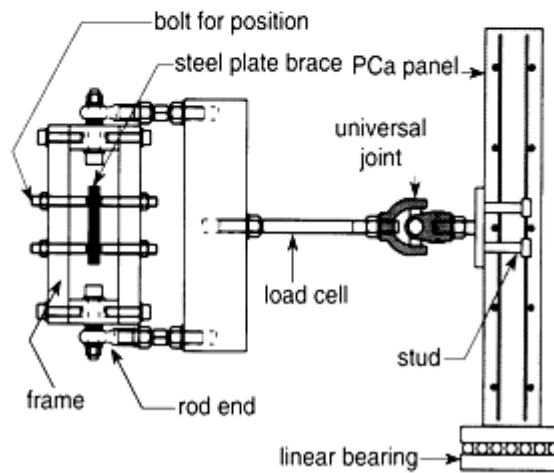
Figure 2.15 Test on panel BRB a) specimen and loading system and b) linkage between steel plate and PC panel (Inoue et al., 1992)
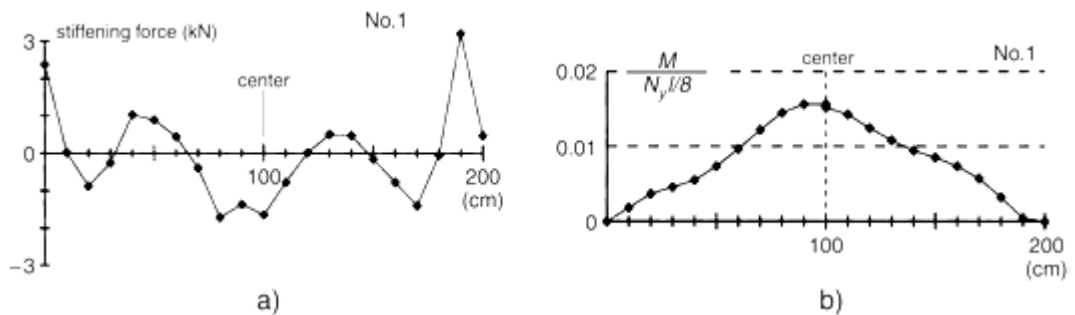

Figure 2.16 Distributions of stiffening force and bending moment at overall buckling (Specimen 1) a) stiffening force distribution and b) bending moment distribution of PC panel (Inoue et al., 1992)

Güneyisi (2012) performed an investigation on the seismic reliability of steel moment resisting framed buildings equipped with concentrically chevron braces and BRBs subjected to seismic excitations with the intention of understanding the structural and ground motion characteristics that influence their seismic fragility behavior. For this, a three-storey and eight-storey steel moment resisting frames (MRFs) designed with lateral stiffness insufficient to satisfy code drift limitations in zones with high seismic hazard were selected as a case study. Then, a series of nonlinear time history analyses were carried out for development of seismic fragility behavior of sample steel frames before and after retrofit. In the structural analysis, three sets of natural ground motions with different characteristics were employed. Moreover, seismic risk analysis of these frames were performed considering three sample locations, which lead to a more general conclusion about the effectiveness of using different bracing systems in the retrofitting strategy of existing steel framed buildings.

The fragility curves developed by using maximum inter-storey drift ratio for the original, conventionally braced, and buckling restrained braced three-storey and eight-storey frames under natural ground motions with low, intermediate, and high a/v ratios.

The fragility curves indicated that both the chevron brace and especially BRB systems improved the seismic behavior of the three-storey and eight-storey original structure by shifting fragility curves towards larger intensity values, which represented the reduction in probabilities of exceedance of damage. Among the sets of natural earthquake ground motions, the fragility curves developed from the

motions with low a/v ratio were the most, and with high a/v ratio were the least conservative.

According to the fragility curves developed under natural ground motions with high a/v ratio, the three-storey BRBF had a 2% probability of exceedance of light damage state for the first mode spectral acceleration of 0.65 g. However, according to the fragility curves developed under natural ground motions with low a/v ratio, it had a 75% probability of exceedance of light damage state for the first mode spectral acceleration value.

In that study, the fragility curves also developed for the retrofitted frames by using the structural demand parameters such as the out of plane buckling of columns and brace cyclic ductility demands.

From the results of the fragility analysis in terms of out-of-plane buckling of columns, it was observed that for three-storey conventionally and buckling restrained braced frames, maximum normalized column combined flexure and axial forces did not reach the limit value 1.0, thus fragility curves for the severe damage could not be achieved.

When the fragility curves developed by using the response parameter of maximum normalized brace cyclic ductility demand were compared with the fragility curves developed by using maximum storey drift, it was observed that for three-storey conventionally braced frames, the fragility curves in terms of brace cyclic ductility demand gave more conservative results. Thus, the median values found for the severe damage state by using maximum normalized brace cyclic ductility demand was less than the median values found by using maximum interstorey drift. In other words, for three-storey conventionally braced frame, maximum normalized brace

cyclic ductility demand was the governing failure mode for determination of the severe damage state. However, for the three-storey buckling restrained braced frame, the maximum interstorey drift ratio was the governing behavior for the determination of the severe damage state.

From the fragility curves developed for eight-storey frames, it was seen that for the severe damage state both using the response parameters of maximum normalized column combined flexure and axial forces, and maximum normalized cyclic ductility demand of braces yielded more conservative results in comparison to inter-storey drift ratio. Similar to the behavior of the three-storey conventionally braced frame and also for the eight-storey conventionally braced frame, maximum normalized brace cyclic ductility demand was the governing failure mode for determination of the severe damage state. However, it was also observed that compared to the three-storey conventionally braced frames, in the eight-storey conventionally braced frames, maximum cyclic ductility demand of braces could easily exceed the limit ductility of the braces and the advantage of BRBFs became much more pronounced. When the annual probability of exceedance of severe damage states of the eight-storey BRBF and CBF based on maximum normalized cyclic ductility demand were compared with each other, it was found that the seismic reliability of the BRBF was approximately 7 to 14 times better than that of CBF, depending mainly on the selection of the location.

Asgarian and Amirhesari (2008) presented the results of analytical study carried out to compare the seismic behavior of conventionally braced frame and buckling restrained brace frame when subjected to strong ground motion. Sabelli et al. (2003) conducted a research effort on behavior of concentrically braced steel frame to

identify improved design procedures and code provisions. Kumar et al. (2007) investigated the effect of tailoring the strength and stiffness of BRBs on performance of steel frames. Di Sarno and Elnashai (2009) also performed an analytical study to investigate and compare the seismic performance of special concentrically braced frames (SCBF), buckling restrained braced frame (BRBF), and mega braced frame (MBF).

However, few studies have investigated the seismic performance of CBFs and BRBFs under the effect of near field ground motions (Tirca and Tremblay, 2004; Ren *et al.*, 2008). For instance, in the study of Tirca and Tremblay (2004), the effect of building height and ground motion type on seismic behavior of zipper braced steel frames was examined. In the another study forwarded by Ren et al. (2008), the seismic damage assessment of steel frame structures with buckling restrained braces under near-field ground motions was performed and discussed. Therefore, further analytical researches are still required to compare the performance of such systems and to investigate the effect of different configurations for the braces and frame types when subjected to near field ground motions.

2.4 BRB configurations

As shown in Figures 2.17 and 2.18, in general, BRBs categorized into two main and wide covering types:

a) One typical type is a steel brace restrained by reinforce concrete or combination of concrete and outer steel member, and

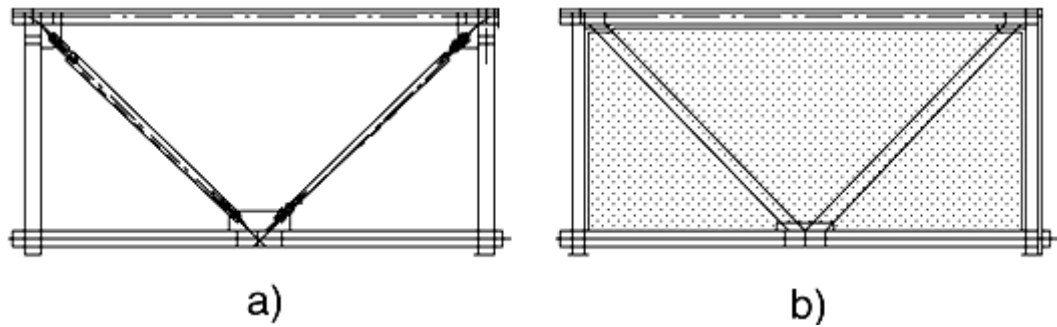b) The second one is a steel plate restrained by PC panels.

Figure 2.17 View of buckling-restrained braces in frame system a) typical BRB configuration and b) panel BRB configuration (Qiang, 2005)

Figure 2.19 illustrates some typical cross-sections of the BRBs proposed by various researchers (Qiang, 2005). It is seen that the cross-section of the steel core member is usually bi-axially symmetric, can be a cruciform, an H or a flat bar shape. The buckling restraining part can be constructed from mortar filled in the tube, reinforced concrete, reinforced concrete covered with fiber reinforced polymer (FRP) or all-metallic steel tubes.

Figure 2.18 Photos of buckling-restrained braces a) typical tube BRB and b) panel BRB (Qiang, 2005)
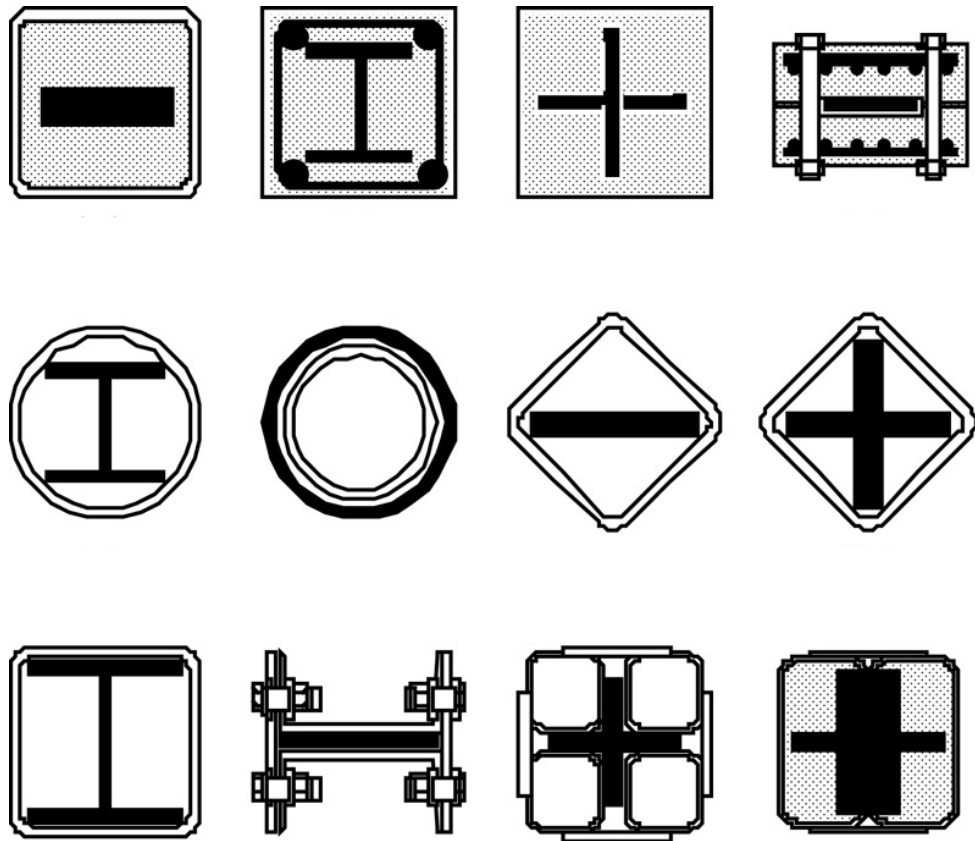
Fig. 2.19 Cross-sections of BRBs (Qiang, 2005)

2.5 Application of BRBs

As discussed previously, the early invention of BRB was in Japan by Wakabayashi et al., and then many researches took place on the behavior of BRB. As a result of its superior behavior, it was implemented in practical applications; such as: "*Raguza Tower*" a 26 storey building in Osaka which had utilized BRBs encased by PC panels*," Passage Garden"* and "*Harumi 1 chome*" in shibuya, Tokyo. Utilized BRB encased by reinforce concrete member (Qiang, 2005).

High-rise steel building implementation of dampers in Japan from 1995-1999 is shown in Figure 2.20. It can be observed form the figure that 60% of high-rise steel buildings utilized BRBs.

Percentage of the three main types of hysteresis dampers which include BRBs, seismic wall, and shear panels implemented in Japan in 2000 is illustrated in Figure 2.21. It can be seen from the figure that BRBs were the most widely used among the other types.
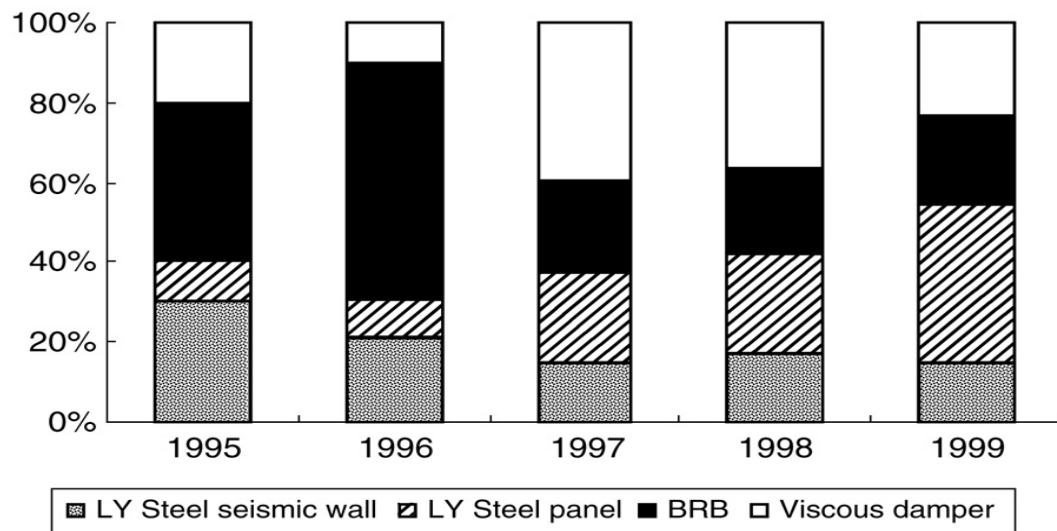
Figure 2.20 BRBs occupation in high-rise steel building from 1993 to 1999 in Japan (BCJ, 2002)
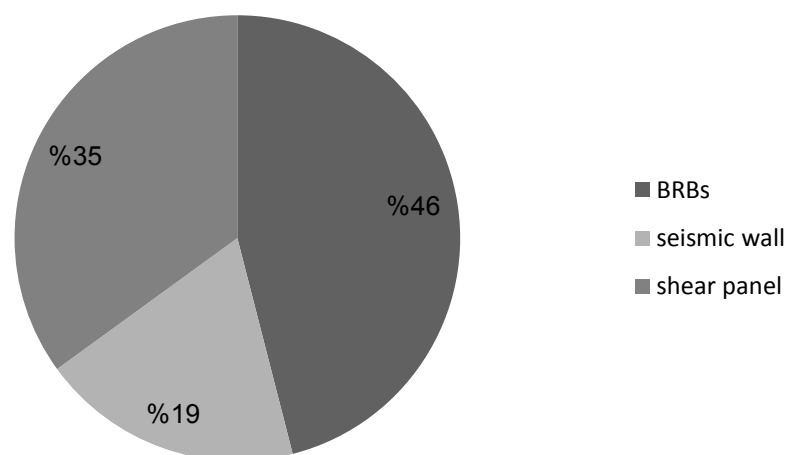
Figure 2.21 Percentage of three types of dampers of high-rise steel building in 2000 in Japan (Qiang, 2005)

Implementation of BRBs was not ended in Japan but also transferred to the other countries such as USA, Italy, and etc. The first application in USA was in 1999 for the new laboratory building at University of California Davis. However, nine years later many new high-rise steel buildings and the seismic retrofit of existing buildings utilized BRBs. Now about 150 building structures in USA utilized BRBs as seismic load resisting systems. Construction projects to date include those manufactured by *Corebrace*, *Nippon Steel Corporation*, *Star Seismic* (Walterio and López, 2008). Figure 2.22 and Figure 2.23 shows some of the projects in USA manufactured by *Corebrace*

Figure 2.22 Use of BRB in world market center III, Las Vegas, Nevada
(Corebrace, 2002)

Figure 2.23 Use of BRB in SME steel corporate headquarter, West Jordan, Utah.
(Corebrace, 2002)

CHAPTER 3

METHODOLOGY

3.1 Description of the analytical models

In this study, two types of steel frame structures were considered. The first one was a special moment resisting frame (SMRF) (AISC, 2005a), designed to generate global mechanism during inelastic response, and the second frame was an ordinary moment resisting frame (OMRF) (AISC, 2005b) designed without any provision for preventing the collapse due to storey mechanism. These frames were first designed by Tirca et al. (2003). The beams were built with IPE profiles while the columns were taken as HEB profiles. The column and the beam sections varied at the third storey so that the structures were divided into two 3-storey tiers. The frames had 6 stories and two equal 6 m bays, the storey height in the models was 3.2 m for all the floors except in the first floor in which the storey height was 4 m. Section profiles for the unbraced frames are shown in Table 3.1 and dynamic properties of OMRF and SMRF are presented in Table 3.2.

Table 3.1 Characteristics of the unbraced frames

Type of frame	Columns				Beams	
	1-3 stories		4-6 stories		1-3 stories	4-6 stories
	external	internal	external	internal		
OMRF	HE240B	HE260B	HE200B	HE220B	IPE360	IPE300
SMRF	HE260B	HE280B	HE220B	HE240B	IPE360	IPE300

Table 3.2 Dynamic properties of the unbraced and braced frames

Frame	Period (s)			Modal participating mass ratio		
	T_{s1}	T_{s2}	T_{s3}	α_1	α_2	α_3
OMRF	1.16	0.42	0.23	0.822	0.127	0.029
OMRF-conf-1	0.64	0.24	0.14	0.808	0.134	0.030
OMRF-conf-2	0.63	0.23	0.14	0.811	0.133	0.027
OMRF-conf-3	0.65	0.24	0.14	0.804	0.140	0.029
SMRF	1.09	0.39	0.21	0.817	0.127	0.033
SMRF-conf-1	0.65	0.22	0.13	0.850	0.104	0.028
SMRF-conf-2	0.64	0.22	0.13	0.854	0.101	0.027
SMRF-conf-3	0.65	0.23	0.13	0.846	0.109	0.027

Then, conventional and buckling restrained braces were inserted to these frames with different configurations (i.e. configuration-1, configuration-2, and configuration-3). In Figure 3.1, the elevation view of unbraced and braced frames in configuration considered is shown. Total of 28 cases were analyzed in this study (4 unbraced cases and 24 braced frames with conventional and buckling restrained brace) as shown in Figure 3.2. The dynamic properties of these braced frames are also given in Table 3.2. The cross-sectional area of the cores of the BRBs in OMRF-Tp1.4-BRB-conf-1 and SMRF-Tp1.4-BRB-conf-1 were designed considering the interstorey index in these frames coincides with the target index of 1.5% given in SEAOC (SEAOC, 1999) provisions. Then, for purpose of comparison, the same cross-sectional areas were used in the other frame cases. Properties of the braces are shown in Table 3.3.

From Table 3.2, it was observed that the first two modes captured most of the response of the structure which was about 97%. However, in this study, 18 modes were included in the modal-time-history so that an accuracy of about 100% could be obtained.

Also it was observed that the fundamental periods of the unbraced frames were shorter than braced frames which it was an indication that the braced frames were stiffer than unbraced frames. However, CBFs and BRBFs had the same fundamental period because in this study the same cross-sectional area for CBs and BRBs were utilized.

For beams and columns elements, the yield strength and modulus of elasticity were presumed to be 50 ksi (corresponding to ASTM A992) and 200 GPa, respectively. However, for the braces, a steel material with yield strength of 30 ksi (corresponding to ASTM, A36, Group 4) was utilized. Using low yield steels for the braces was to enhance energy dissipation of BRBs.
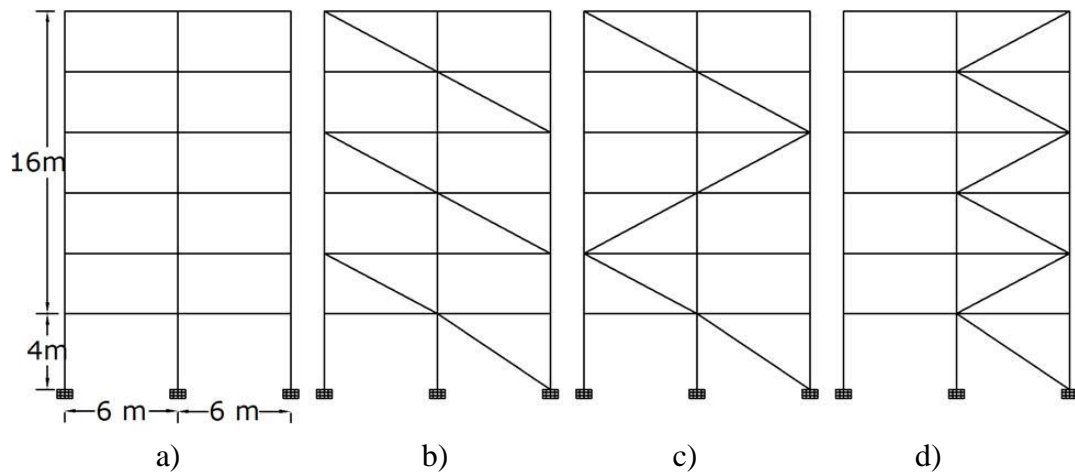
Figure 3.1 Typical model: a) unbraced frame (Tirca et al., 2003), b) configuration-1, c) configuration-2, and d) configuration-3

Table 3.3 Characteristics of the braces used

Storey No.	OMRF-Tp1.4-BRB-conf-1			SMRF-Tp1.4-BRB-conf-1		
	Designation	Area (mm^2)	Inertia (mm^4*10^6)	Designation	Area (mm^2)	Inertia (mm^4*10^6)
1	HSS 3×.203	1,077	0.691	HSS 3×.152	819	0.541
2	HSS 3×.188	993	0.645	HSS 3×.134	722	0.483
3	HSS 3×.188	993	0.645	HSS 3×.134	722	0.483
4	HSS 3×.125	677	0.454	HSS 3×.125	677	0.454
5	HSS 3×.125	677	0.454	HSS 3×.125	677	0.454
6	HSS 3×.125	677	0.454	HSS 3×.125	677	0.454

Each model in the current study was named according to the frame type, pulse period (T_p), brace type, and configuration of the braces. For example, model name "OMRF-Tp1.4-BRB-conf-1" referred to the model that utilized ordinary moment resisting frame (OMRF) section profiles for beams and columns and subjected to earthquake excitation with pulse period (Tp) of 1.4 s and buckling restrained braces (BRB) with the first configuration was inserted to the frame.

The performance of unbraced frames and various braced frames subjected to near field ground motions was investigated by nonlinear static and dynamic analyses using the finite element program of SAP2000, non-linear version 14 (CSI Analysis Reference Manual, 2009).

In the nonlinear static analysis (pushover analysis), concentrated incremental static lateral loads were applied at each floor using triangular distribution through the height of the structure. The structure models were based on the centerline dimensions that beams and columns span between the nodes at the intersections of beam and column centerlines and no cardinal points or insertion points were used for the modeling purpose. Columns and beams were modeled as frame element and braces were modeled as nonlinear link (NLLink).
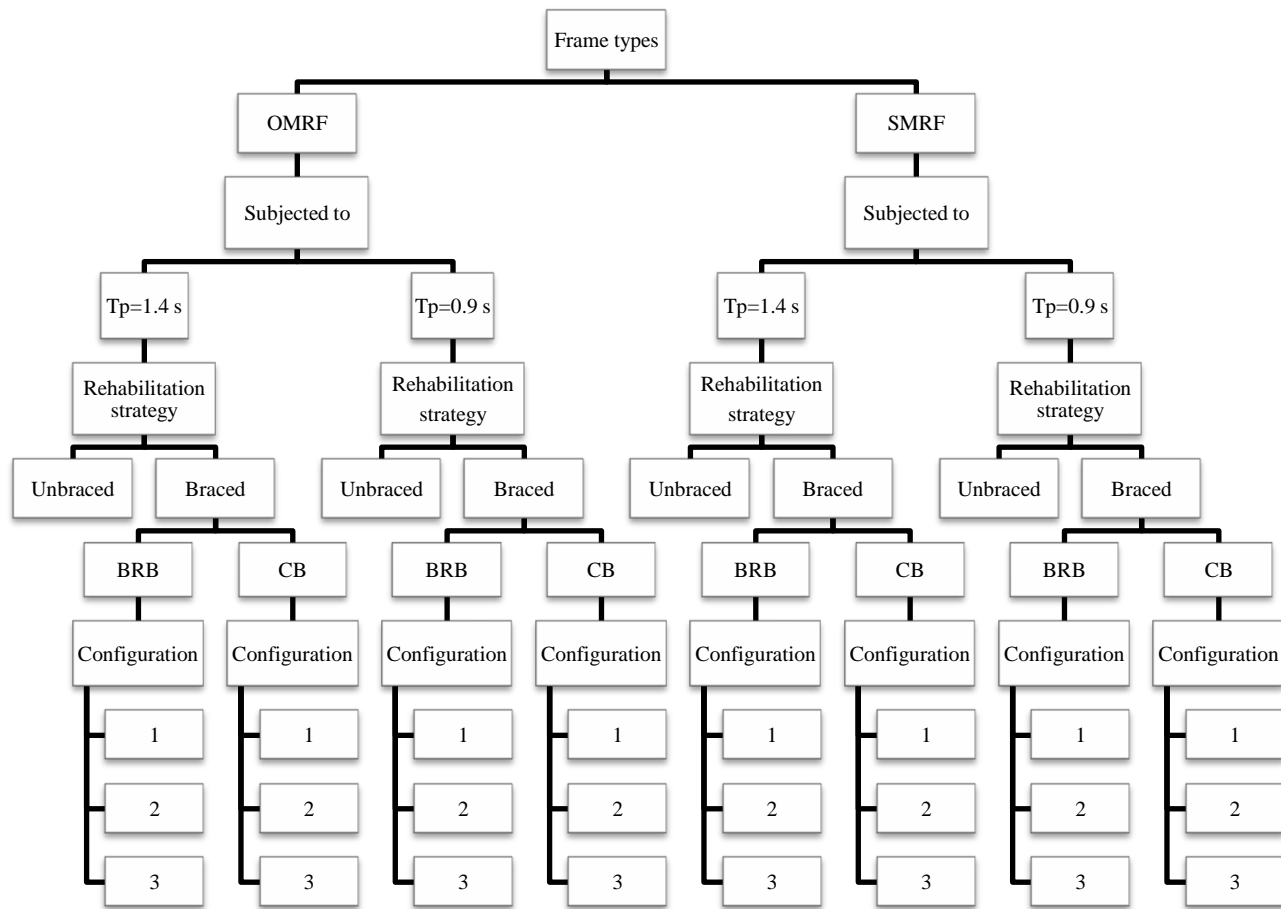
Figure 3.2 Tree diagram showing 28 different frame cases considered in this study

3.2 Nonlinear behavior of structural elements

The nonlinear behavior of a building structure depends on the nonlinear responses of the elements that are used in the lateral force resisting system. Therefore, before applying any nonlinear analysis method on a building structure, the nonlinear behavior of such elements must be clearly described and evaluated.

In FEMA-356 (FEMA 356, 2000), the generalized load deformation relation of a structural member while exhibiting nonlinear behavior is shown in Figure 3.1. After the member yields (when applied load/yield load proportion (Q/Qy) is equal to 1), the subsequent strain hardening accommodates the strain hardening in the load-deformation relation as the member deforms toward the expected strength. The horizontal axis of this diagram may either express curvature or strain.
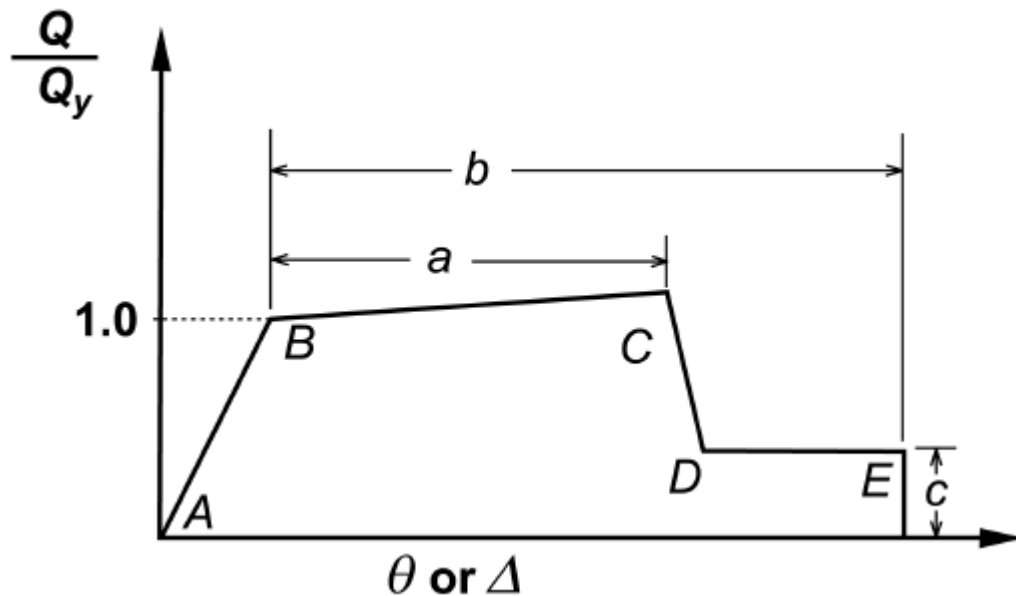
Figure 3.3 The generalized load deformation relation while exhibiting nonlinear behavior of a structural member (FEMA 356, 2000)

Point A corresponds to unloaded condition and point B represents yielding of the element. The ordinate at C corresponds to nominal strength and abscissa at C corresponds to the deformation at which significant strength degradation begins. The drop from C to D represents the initial failure of the element and resistance to lateral loads beyond point C is usually unreliable. The residual resistance from D to E allows the frame elements to sustain gravity loads. Beyond point E, the maximum deformation capacity, gravity load can no longer be sustained.

ATC-40 and FEMA-356 codes also define the acceptance criteria depending on the plastic hinge rotations by considering various performance levels. In Figure 3.4, the acceptance criteria on a force versus deformation diagram are given. In this diagram, the points marked as IO, LS and CP represent immediate occupancy, life safety and collapse prevention, respectively.
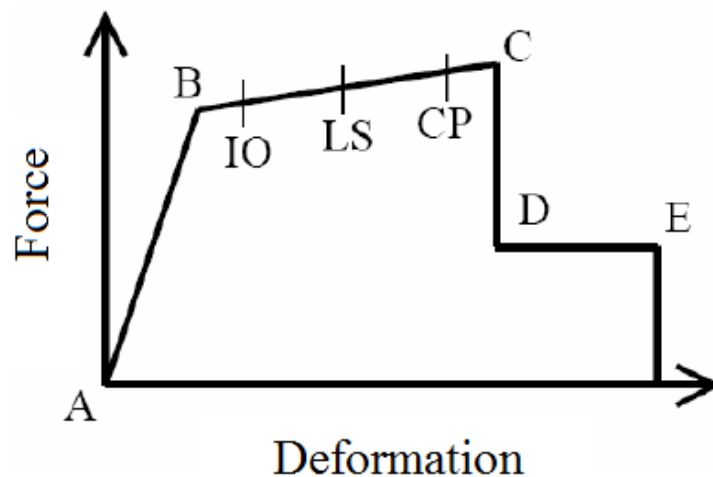
Figure 3.4 Acceptance criteria on a force versus deformation diagram (FEMA 356, 2000)

Hinges can be assigned at any number of locations (potential yielding points) along the span of the frame element as well as element ends. Uncoupled moment (M2 and M3), torsion (T), axial force (P) and shear (V2 and V3) force-displacement relations

can be defined. As the column axial load changes under lateral loading, there is also a coupled P-M2-M3 (PMM) hinge which yields based on the interaction of axial force and bending moments at the hinge location. Also, more than one type of hinge can be assigned at the same location of a frame element.

There are three types of hinge properties in SAP2000. They are default hinge properties, user-defined hinge properties and generated hinge properties. Only default hinge properties and user-defined hinge properties can be assigned to frame elements. When these hinge properties (default and user-defined) are assigned to a frame element, the program automatically creates a new generated hinge property for each and every hinge.

Default hinge properties could not be modified and they are section dependent. When default hinge properties are used, the program combines its built-in default criteria with the defined section properties for each element to generate the final hinge properties. The built-in default hinge properties for steel and concrete members are based on ATC-40 (ATC 40, 1996) and FEMA-273 (FEMA273, 1997) criteria.

User-defined hinge properties can be based on default properties or they can be fully user-defined. When user-defined properties are not based on default properties, then the properties can be viewed and modified. The generated hinge properties are used in the analysis. They could be viewed, but they could not be modified.

In this study, axial force-moment interaction (P-M3) according to FEMA356 (FEMA356, 2000) was defined for determining the nonlinear hinge properties of a columns, such hinges required that the axial force vs. moment interaction diagram to be calculated. When an axial force and corresponding moment value of a loading was formed outside the plotted interaction diagram, this column exhibited nonlinear

behavior. Plastic hinge moment capacity (M3) according to FEMA356 (FEMA356, 2000) was introduced for plastic hinges of the beam elements. As an example, the interaction diagrams for the column HE260B is given in Figure 3.5.
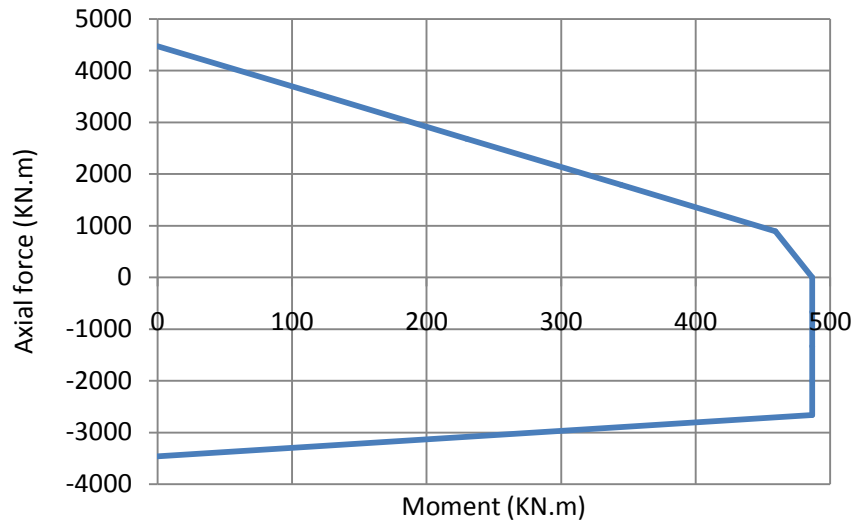
Figure 3.5 A typical P-M$_3$ interaction diagram of column HE260B

For modeling, the nonlinear behavior of BRBs elasto-plastic force deformation property (Kumar et al., 2007) was used, as shown in Figure 3.6. And 3% of strain hardening is considered.
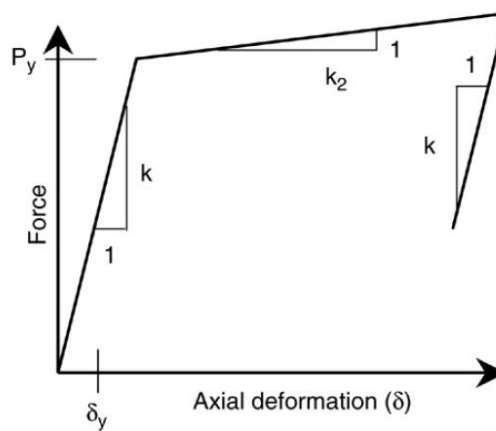
Figure 3.6 Constitutive model of bracings (Kumar et al., 2007)

The effective axial stiffness, in the elastic and post elastic range, is given by

$$k = AE/L \qquad for\ \delta < \delta_y \tag{3.1}$$

$$k_2 = (AE_t)/L \qquad for\ \delta \geq \delta_y \tag{3.2}$$

Where:

A = Total cross-sectional area

E = Modulus of elasticity

L = Length of brace

E_t = Tangent modulus of elasticity

$$\delta = \frac{f_y A}{k}$$

For modeling, the nonlinear behavior of CBs (Figure 3.7), the phenomenological model proposed by Jain and Jeol (1980), which was also presented in (FEMA 274, 1997), was used. The values of the modeling parameters were selected based on Table 5-8 of (FEMA 273, 1997).

a) Tension brace   b) Compression brace
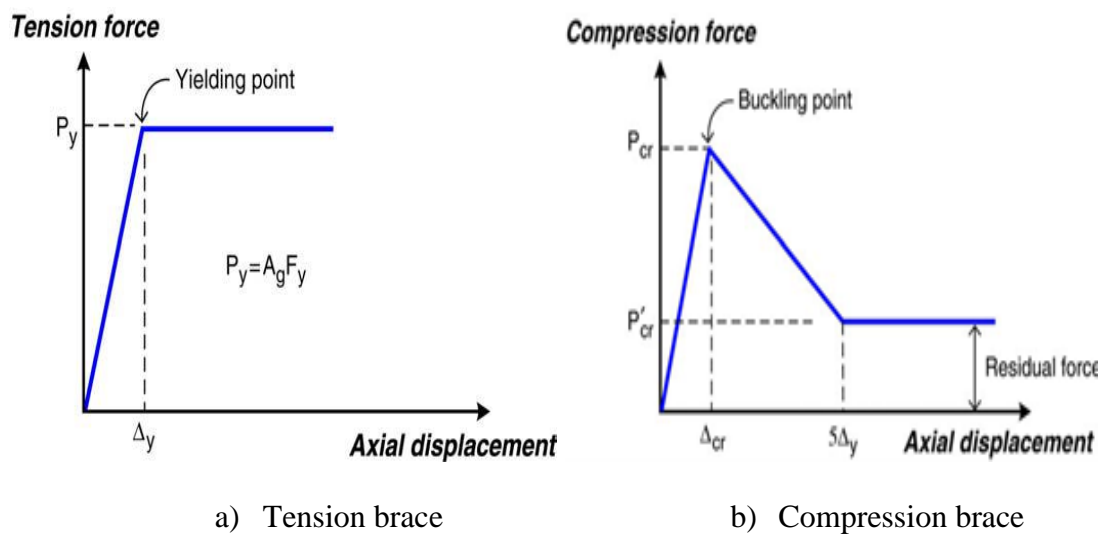
Figure 3.7 Simplified analysis model for force–displacement relationship of brace (Kim and Choi, 2005).

3.3 Nonlinear static pushover analysis

Nonlinear static pushover analysis has become the most commonly used method to determine the nonlinear behavior of the building structures in the recent years. In this simplified method, a capacity curve is obtained which shows the relation of base shear and roof displacement. This curve represents the behavior of the building structure under increasing base shear forces. As the capacities of the members of the lateral force resisting system exceed their yield limits during the increasing of the base shear forces, the slope of the force-deformation curve will change, and hence the nonlinear behavior can be represented (Altuntop, 2007).

In the pushover analysis, the applied lateral forces to a model are increased in a regular manner depending on the initial load pattern. Member forces are calculated for each step and the stiffness of the members whose capacities are exceeded is changed according to the hinge properties in the next step of the analysis. This process ends when the structure becomes unstable. Figure 3.8 displays a typical pushover curve as an example.
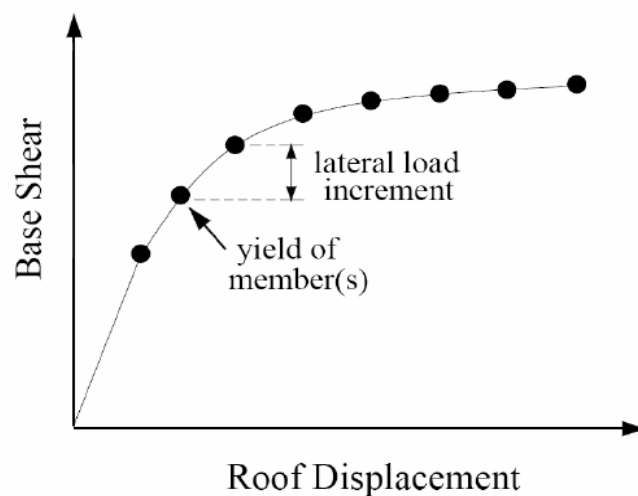
Figure 3.8. An example pushover curve of a building structure (Sermin, 2005)

The pushover analysis can be performed considering the control over the force or displacement. Force control option was useful when the magnitude of the load was known clearly, and the structure was expected to support that load. The displacement control was useful when the magnitude of the load was unknown and displacements were searched.

In this study, the pushover analysis was carried out in these following steps:

- The model representing the building structure was created and vertical loads (dead load and live load), member properties and member nonlinear behaviors were defined and assigned to the model,

- Hinge properties were defined and these properties were assigned to the member ends,

- Lateral load patterns to be used in the pushover analyses were assigned,

- An initial force controlled pushover loading to be used for the lateral load increment analyses, was applied to the model as a pushover case. This pushover load case was composed of the dead loads and reduced live loads,

- A new displacement controlled pushover case was defined considering the lateral load pattern which was defined above for the incremental pushover analysis starting from the initial pushover case.

3.4 Nonlinear time history analysis

In order to examine the exact nonlinear behavior of building structures, nonlinear time history analysis has to be carried out. In this method, the structure is subjected to real ground motion records. This makes this analysis method quite different from all of the other approximate analysis methods as the inertial forces were directly

determined from these ground motions and the responses of the building either in deformations or in forces are calculated as a function of time, considering the dynamic properties of the building structure.

In this study, the nonlinear time-history analysis was carried out as follows:

- The model representing the building structure was created and vertical loads (dead load and live load), member properties and member nonlinear behaviors were defined and assigned to the model,

- Floor masses were assigned to the model,

- Hinge properties were defined and these properties were assigned to the member ends considering end-offsets,

- The ground motion record was defined as a function of acceleration versus time,

- An initial loading was applied to the model like it was done in the pushover analyses to represent the initial case. This case composed of the dead loads and reduced live loads.

Hereafter, the analysis and the time history parameters were defined in order to perform a nonlinear time history analysis by means of SAP2000.

In the current study, a critical damping ratio of 2% was considered for all analysis of SMRF and OMRFs, so that other sources of energy dissipation during elastic and inelastic responses were accounted. Hilber-Hughes-Taylor direct integration method has been adopted and Rayleigh damping was used in this study; in order to calculate the mass and stiffness proportional damping coefficients (α and β) the first and the third modes were used.

$$\alpha = \zeta(2\omega_i \omega_j/(\omega_i + \omega_j)) \tag{3.3}$$

$$\beta = 2\zeta/(\omega_i + \omega_j) \tag{3.4}$$

For purpose of comparison, it was crucial that the unbraced and braced frames had the same damping ratio. To accomplish this, Nonlinear time history analysis was performed in two steps, in the first step; an Eigen value analysis was performed to determine the natural periods and mode shapes of the frames, in the second step; the correct α and β damping coefficients were evaluated based on these natural periods. Gravity loads consisting of dead loads and 30% of the live loads were considered in the dynamic analysis.

3.5 Ground motions used in this study

Ordinary earthquake excitations impose smaller demand compared to near-field ground motions. Records obtained in near fault areas may be characterized by large amplitude pulse in velocity and displacement time history, long-period pulse, and capable of causing severe damage to structures. This holds true particularly in ground motion time histories of fault-normal component with 'forward' directivity, in which most of the seismic energy reaches within a short time at the beginning of the earthquake, and that is due to the fact the fault rapture propagates toward the site at a speed close to the shear wave velocity (Alavi and Krawinkler, 2004) on other hand.
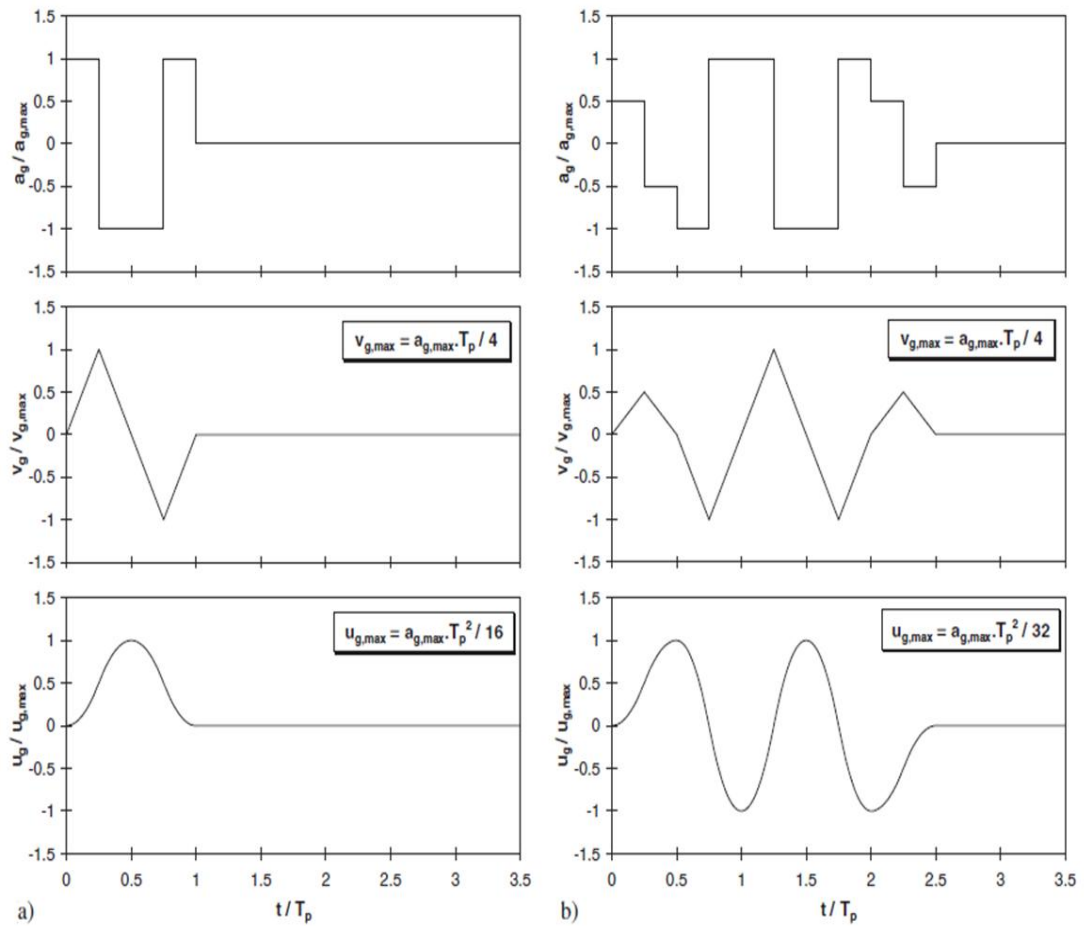
Figure 3.15 Acceleration, velocity and displacement time histories of basic pulses: a) pulse P2 and b) pulse P3 (Alavi and Krawinkler, 2004)

Ground motions with 'backward' directivity characterized by low amplitude pulse, long duration of motion and long period, and they do not exhibit pulse characteristics. It is important to be pointed out that velocity spectrum of some of near fault ground motions contain more than one peak value, this predominant peak velocity spectrum is utilized to evaluate the pulse period T_p (duration of full velocity cycle). Simulating near-fault ground motion in the forward directivity region with simple pulse model with reasonable accuracy greatly facilitate the process of analysis and design of the structures. Many pulse shapes has been developed by the researchers (Alavi and Krawinkler, 2004), but the three basic pulse shape and commonly used pulses are: half pulse (P1), full pulse (P2), and multiple pulse (P3).

In Figure 3.5, acceleration, velocity and displacement time history for pulse P2 and P3 are shown, and P1 which is not presented in the Figure 3.5 is the first half of pulse P2.

Previous researches have shown that square pulse shape could adequately represent other pulse shapes like triangular pulse shape. Some other studies investigated the other different pulse shapes like sine wave acceleration pulses that could simulate both fault-parallel and fault-perpendicular components of the earthquake excitations with forward directivity (Alavi and Krawinkler, 2004). The great advantage of using rectangular pulse shapes is that they are not a complex definition of the peak acceleration and they provide a simple relationship between the peak velocity and the peak acceleration.

These artificial pulses are defined by two parameters: the pulse period T_p, and intensity of the earthquake, that is maximum ground acceleration or maximum ground velocity, these parameters are related to each other as seen in the equation:

$$V_{gmax} = a_{gmax} \ T_P/4 \tag{3.5}$$

In this study, the same artificial accelerograms generated by (Tirca et al., 2003) was used, and that was by utilizing pulse shape P2 with maximum ground acceleration of 0.35g and a pulse period Tp of 1.4 s and 0.9 s to simulate the Northridge and Kobe earthquakes, respectively. It was shown that the equivalent pulse P2 adequately represented the Northridge and Kobe earthquakes (Tirca et al., 2003).

CHAPTER 4

RESULTS AND DISCUSSION

4.1 General

In this section, the results for unbraced frames (UFs), conventionally braced frames (CBFs), and buckling restrained braced frames (BRBFs) obtained from nonlinear static and dynamic analysis were given and discussed comparatively. In the present study, a total of 28 different cases were taken into account and structural performance of unbraced and braced frame systems having different type of brace and configuration under the effect of near-fault ground motions were evaluated. Performance characteristics in terms of capacity curves, interstory drift index, global damage index, base shear, top shear, damage index, and plastification were given.

4.1.1 Capacity curves

The capacity curves (pushover curves) were evaluated for different frame type, brace type, and brace configurations. Figures 4.1-4.3 shows the comparison of the capacity curves. It was pointed out that the BRBFs were much stiffer and showed a better performance compared to the CBFs, also putting the stiffness of the CBFs in perspective with unbraced frames (UFs), it was apparent that in general the former was much stiffer than later. However, in some cases (i.e. SMRF-CB-conf-1 and OMRF-CB-conf-1), there was a slight difference in the pushover curves, and that was due to the fact in the first configuration most of the braces would be under the compression force, and they would exhibit buckling deformation and strength

degradation when maximum capacity was exceeded. Whereas, in the second and third configurations, the differences in the pushover curves were more noticeable because some of the braces were under compression force while the others were under tension force.

It was observed that the capacity curves in general for unbraced frames were bilinear since at the beginning the structure was globally in the elastic stage and provided a linear elastic slope, and then when the base shear was exceeded, some structural members (beams and columns) would yield and induce a change in the slope of the capacity curve. However, in the case of the braced frames, the pushover curves were tri-linear. The first change in the elastic slope was due to the yielding of the braces and the second change was due to the yielding of the structural members. Therefore, the length of the second slope was the delay between the yielding of the brace and the structural members. Also, it was seen that generally the yielding of the brace members occurred at constant roof displacement.

The pushover curves for CBFs and BRBFs followed the same path at the initial steps and that was due to the fact that both CBFs and BRBFs had the same initial stiffness with the same cross-sectional area. However, after yielding of the braces, the pushover curves would follow different path for each of CBF and BRBF. Because conventional braces (CBs) would exhibit buckling and strength degradation while buckling retrained braces (BRBs) did not buckle out and carry an increasing load in the inelastic range.
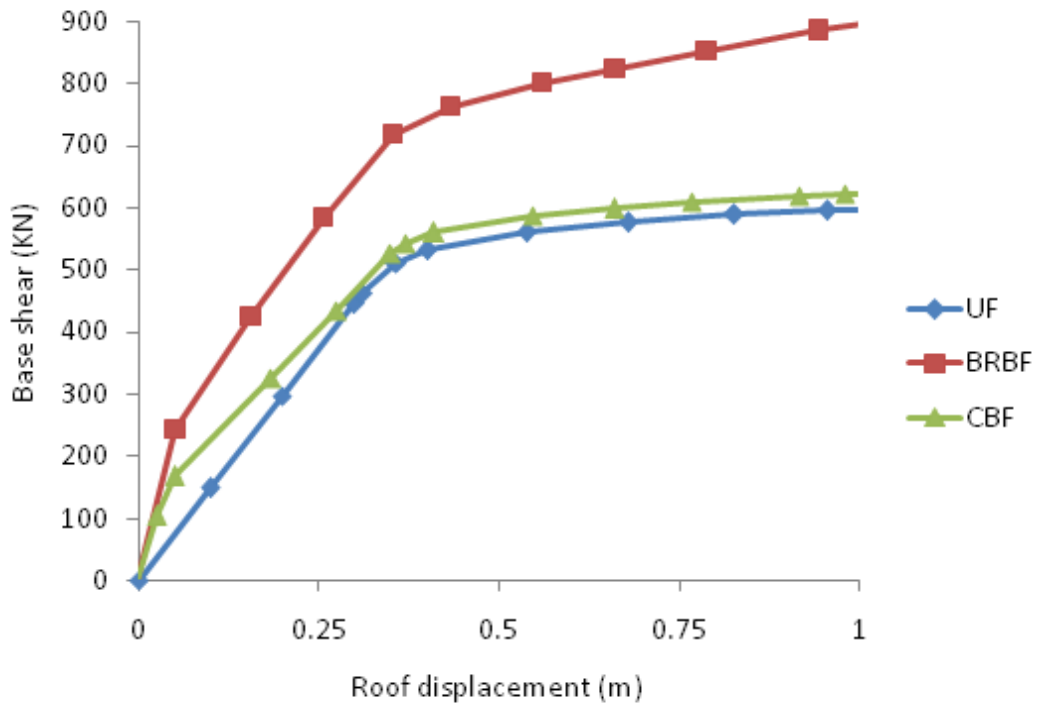
a)
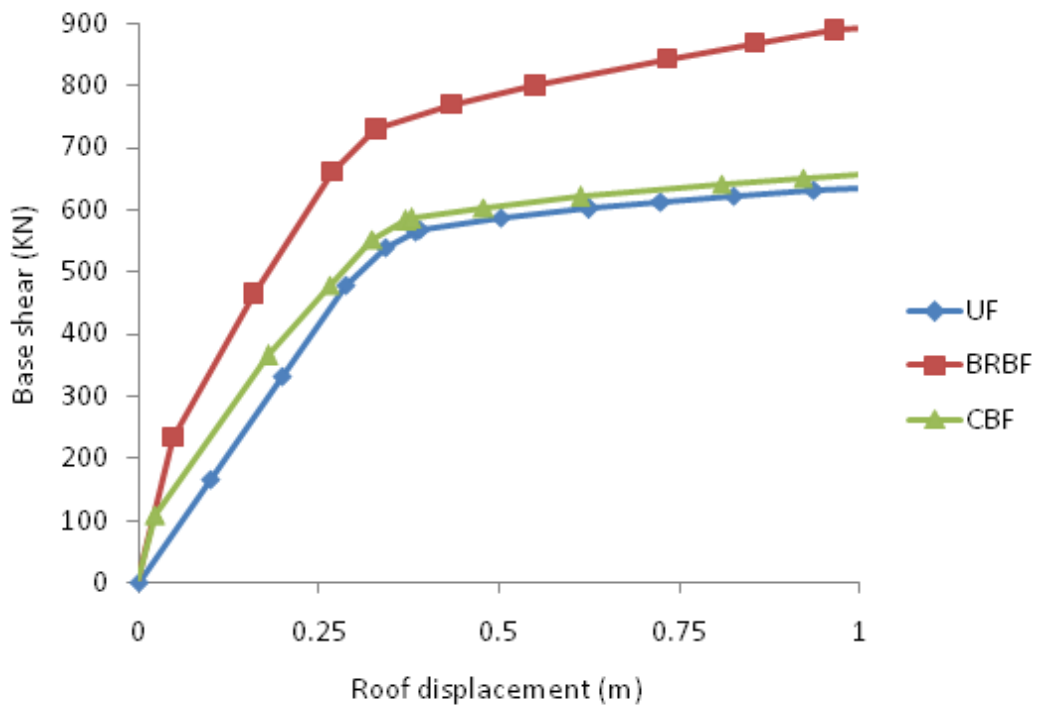
b)

Figure 4.1 Capacity curves for unbraced and braced frames with configuration-1: a) OMRFs and b) SMRFs
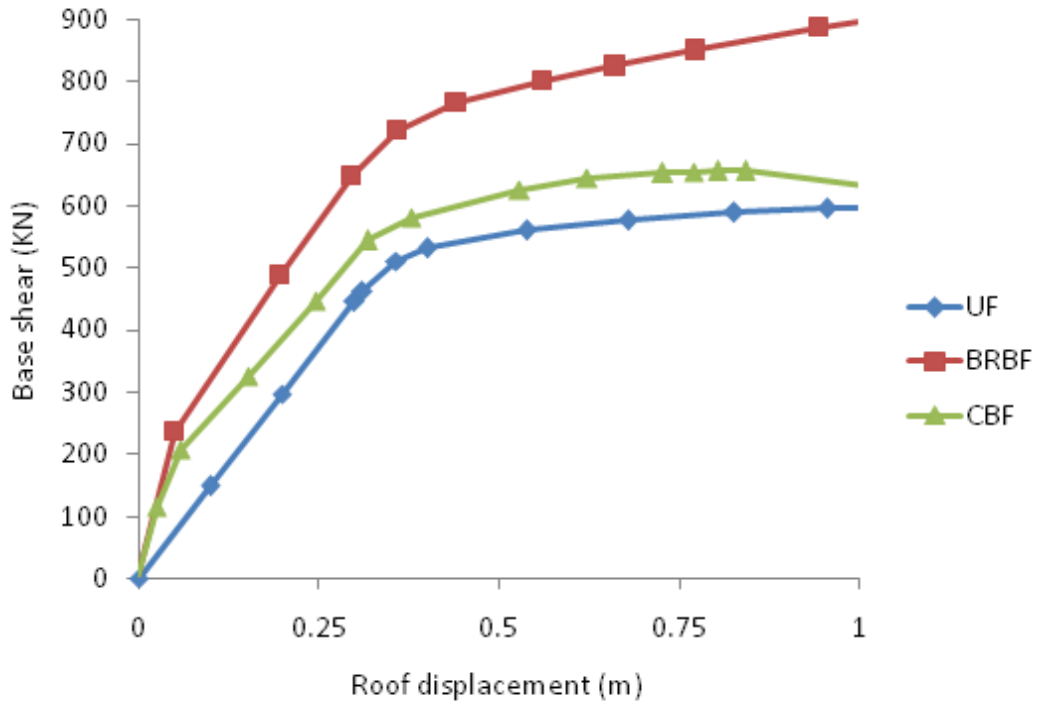
a)
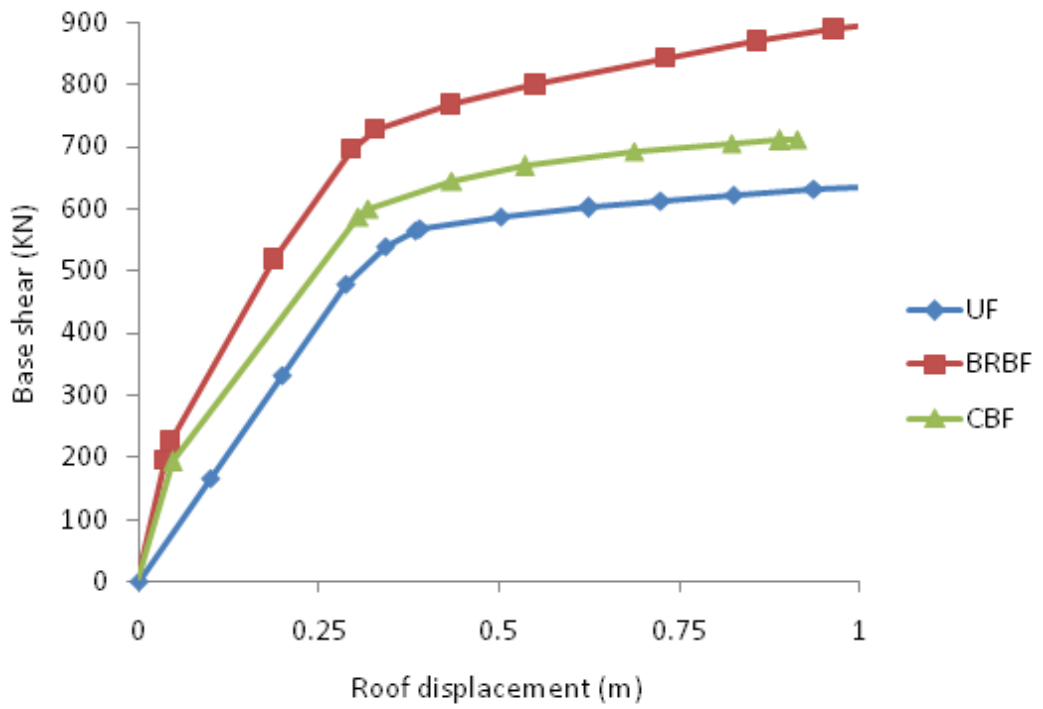
b)

Figure 4.2 Capacity curves for unbraced and braced frames with configuration-2: a) OMRFs and b) SMRFs
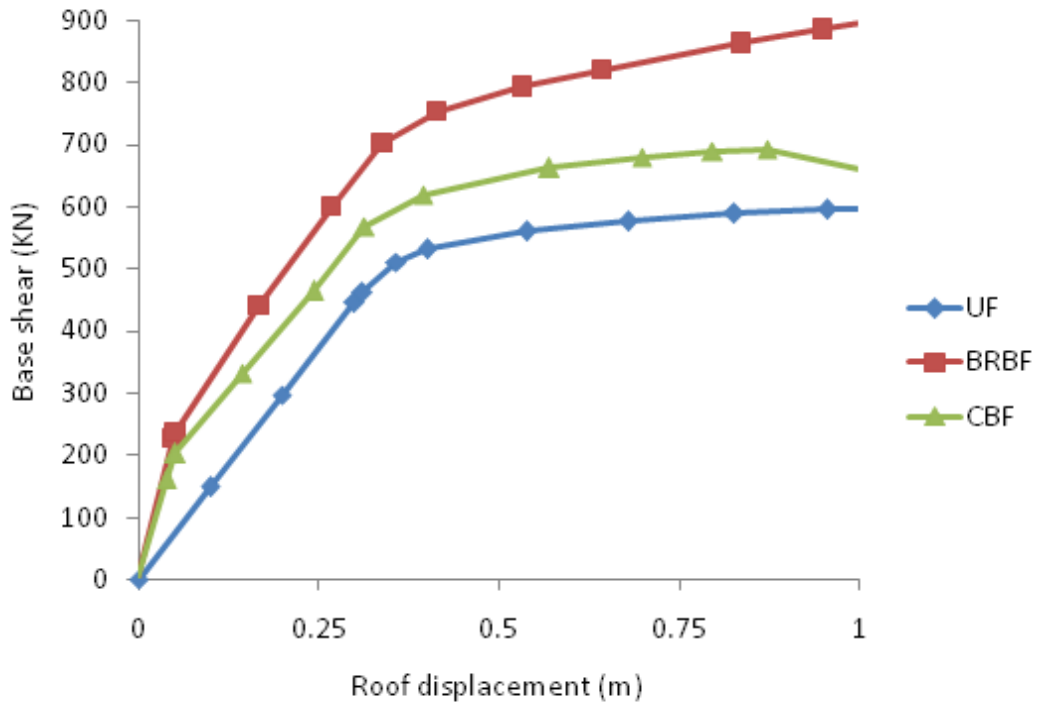
a)
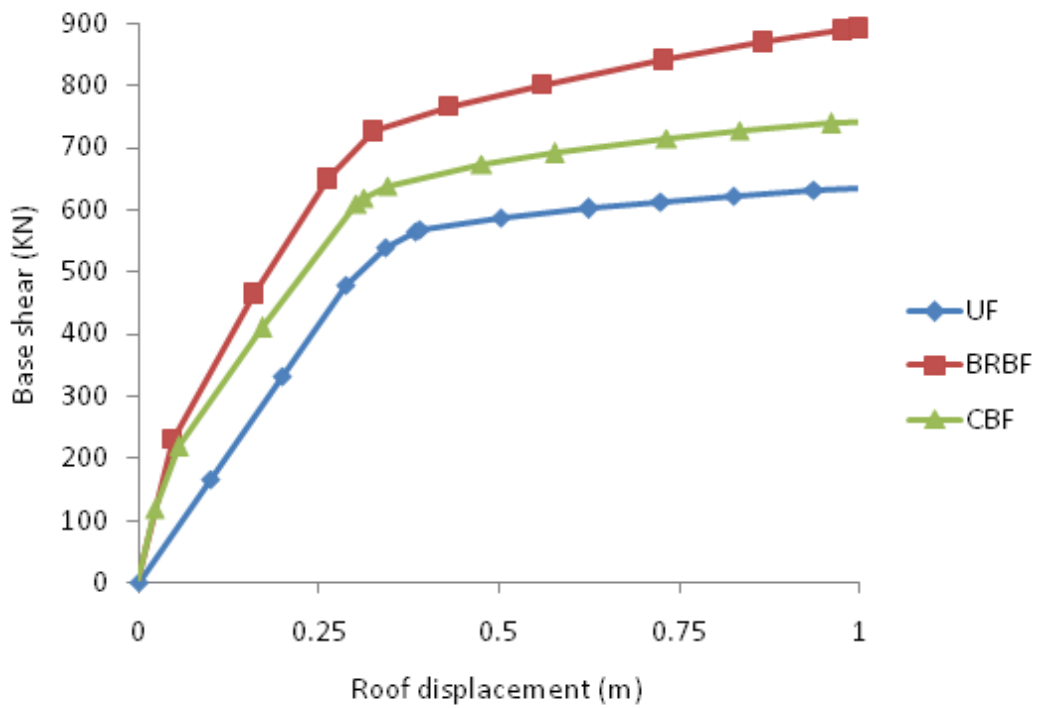
b)

Figure 4.3 Capacity curves for unbraced and braced frames with configuration-3: a)
OMRFs and b) SMRFs

4.1.2 Interstorey index

The maximum interstorey drift (δ_{max}) divided by the storey height (h) is defined as *maximum interstorey index*. This index is a good indication of the damages experienced by the structural members. However, some building codes like FEMA 273 in section 2.5.1 (FEMA273, 1997) state that the value of this index could be used for design purposes and should not be used in the post-earthquake safety evaluation process and it will not supersede the local deformation limit of the structural members. Drift limit requirements depend on the building code and analysis procedure that has been utilized. In this study, 0.35g was considered as the acceleration for life safety level (LSL), this index was limited to 1.5% for LSL according to (SEAOC, 1999) requirements.

The maximum interstorey index was assessed for both CB and BRB frames subjected to equivalent pulses to Northridge and Kobe earthquakes discussed previously by taking the maximum values presented in Appendix A. Figures 4.4 and 4.5 compare maximum interstorey index for CB and BRB frames with different configuration, frame type, and earthquake time history.

Comparison of maximum interstorey index of the frames indicated that this index for CB was considerably greater than for BRB, it could be seen in the response plots, both unprotected and CB frames did not meet SEAOC limitations and in some cases (i.e. OMRF-CB subjected to Tp=1.4 s) was even two times higher than the limit. Moreover, a better performance could be observed in CB and especially BRB frames compared to unbraced frames (UFs). Because of the sensitivity of structural response to the pulse period value Tp, the maximum interstorey indexes were greater for

earthquake excitations with a larger pulse period as it could be observed in the response plots for equivalent pulses to Northridge and Kobe records.

On the other hand, SMRFs in case of unbraced condition and braced one with CB showed a better performance compared to OMRFs, the strength of OMRF braced with CBs was recognized to drop quickly when yielding occurred in girders connected to braces due to unbalanced forces developed by buckling of braces under compression. However, SMRFs braced with CBs retained a relevant amount of strength even after the initial buckling of a brace (Kim et al., 2011). In the case of frames with BRBs, it was observed that BRBs did not exhibit buckling deformations, then they led to uniform development of forces in girders in both OMRFs and SMRFs, as a result, a rapid dropping in strength of frames did not occur that might lead to catastrophic failure.

It was also observed from the figures that there was a slight difference between the interstorey indexes of the frames with different configurations. However, some brace configurations were performing better than the others. For example, the interstorey index in the braces in the second configuration (conf-2) was more compared to the other configurations (conf-1 and conf-3) and that was due to the fact that in the second configuration all the brace were supporting the seismic loads in one direction or in other words they would either support compression load or tension load. This held particularly true in the case of CBs because of their different load carrying capacity in compression and tension. However, the differences in the interstorey index for different configurations in the case of BRBFs were very small because BRBs had the same load carrying capacity in both compression and tension.
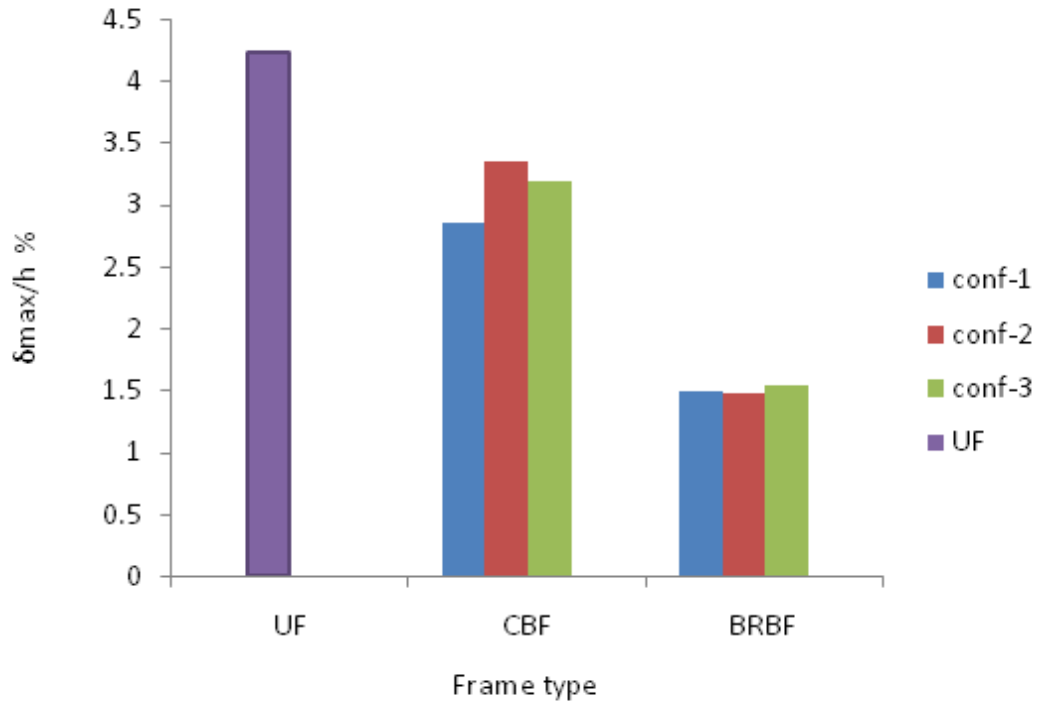
a)
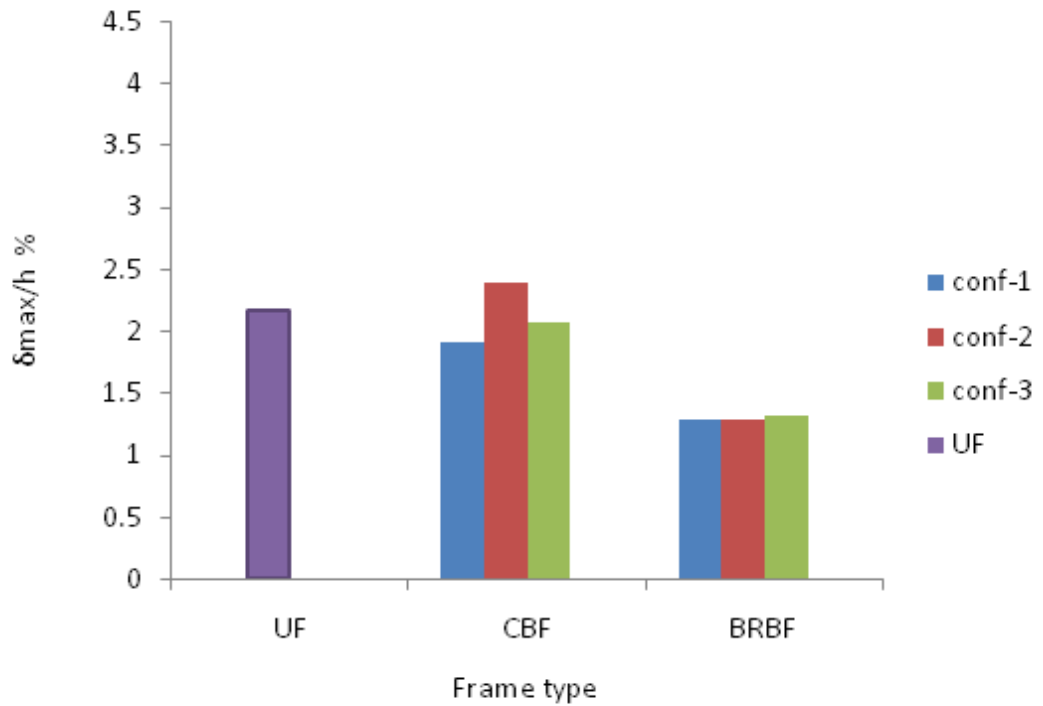
b)

Figure 4.4 Maximum interstorey index for OMRF: a) T_p=1.4 s and b) T_p=0.9 s
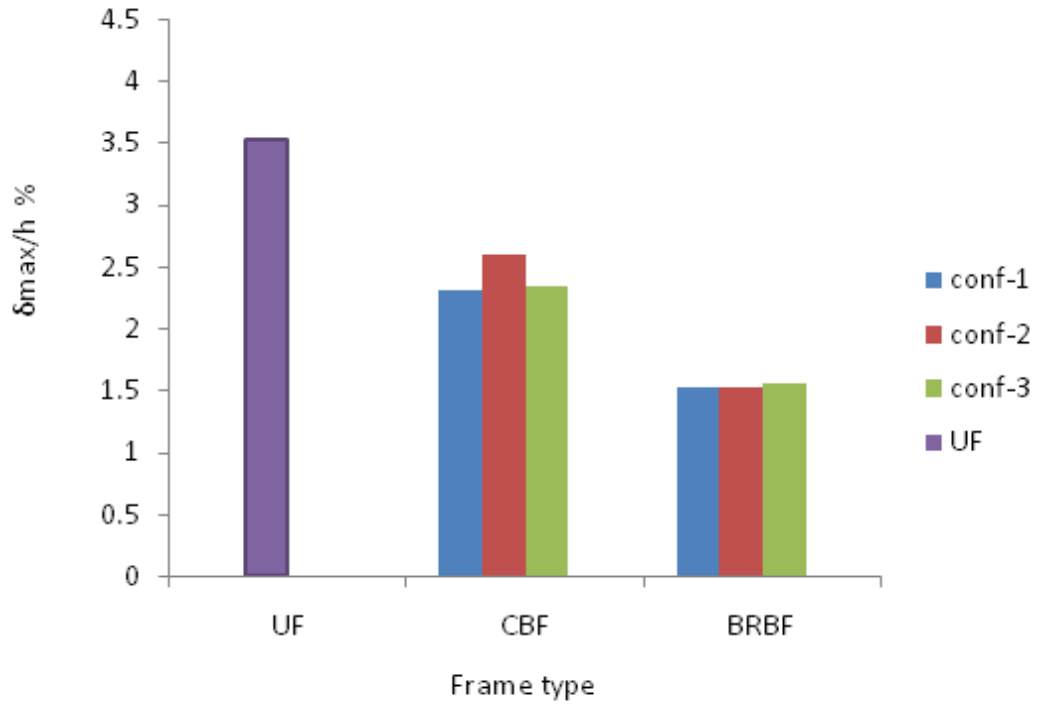
a)
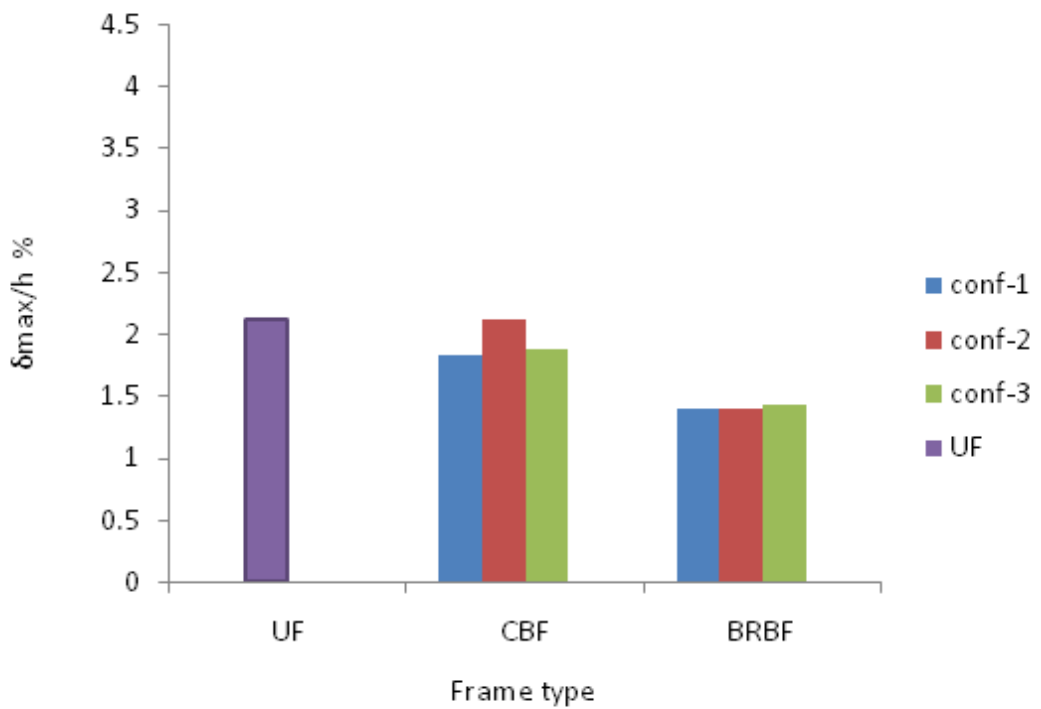
b)

Figure 4.5 Maximum interstorey index for SMRF: a) T_p=1.4 s and b) T_p=0.9 s

4.1.3 Global damage index

The ratio of the roof displacement (D) over the total height of the building (H) is defined as the *global damage index*. The global damage index was assessed for both CB and BRB frames subjected to equivalent pulses to Northridge and Kobe earthquakes by taking the maximum values of roof displacement time histories presented in Appendix C.

Figures 4.6-4.7 compare the global damage index for CB and BRB frames with different configuration, frame type, and earthquake time history. Comparison of global damage index of the frames revealed that the global index for CB was greater than that for BRB, and CB frames showed better performance in comparison to unbraced frames (UFs). The use of CBs resulted in reductions of 15-25%. However, the use of BRBs resulted in further reductions of 39-54%. These global deformations depend mainly upon the characteristics of earthquake ground motions, especially frequency content.

As seen in the results of the interstorey index, because of the sensitivity of structural response with the pulse period value T_p, as the pulse periods became larger, greater global damage index was introduced as it was observed in the response plots for equivalent pulses to Northridge and Kobe inputs.

From the result of this index, it was evident that the various configurations had a small effect on global performance of the structures, especially in the case of BRBs. That was due to similar behavior of BRBs in both compression and tension. However, due to distinct load carrying capacity of CBs in compression and tension, the difference in the global damage index was more noticeable.
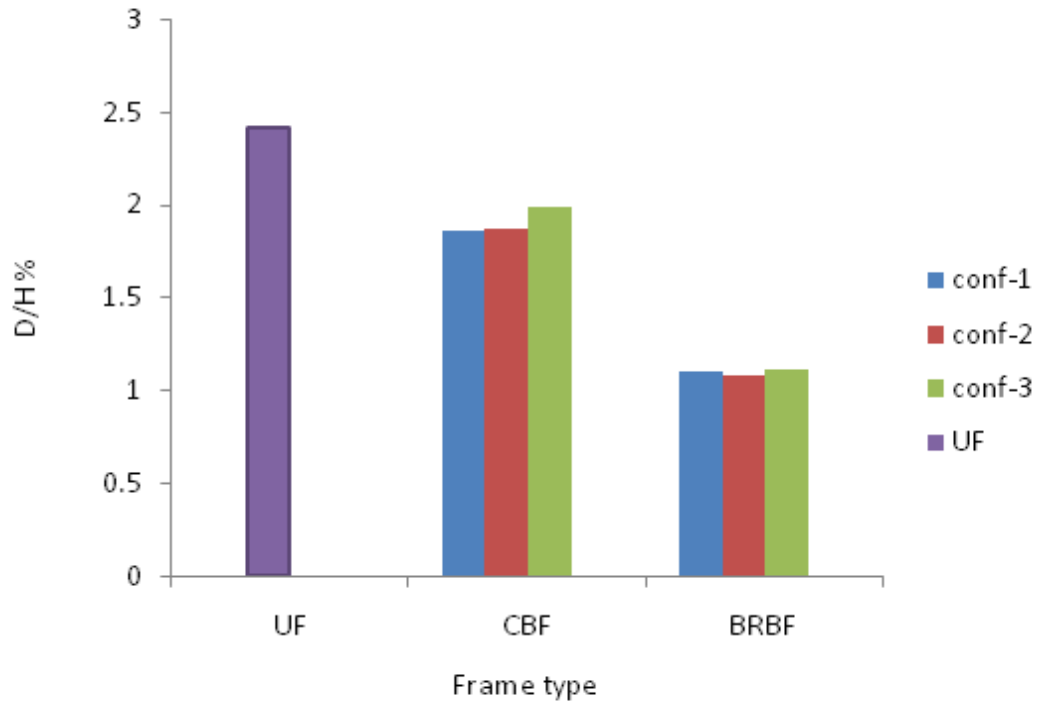
a)
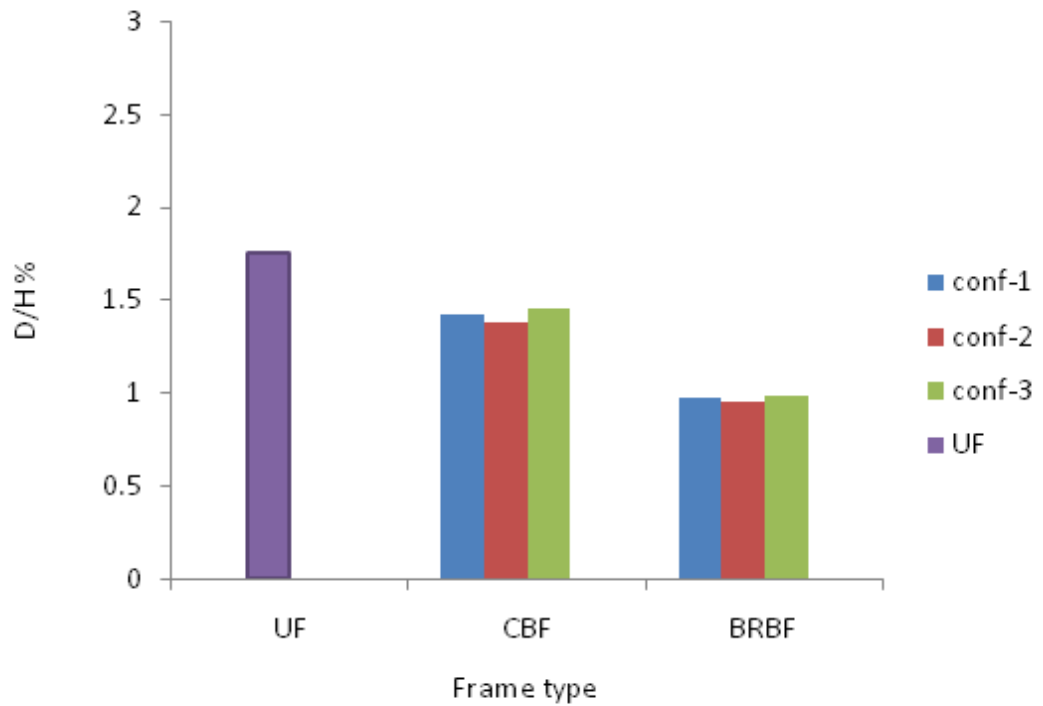
b)

Figure 4.6 Global damage index for OMRF: a) $T_p=1.4$ s and b) $T_p=0.9$ s
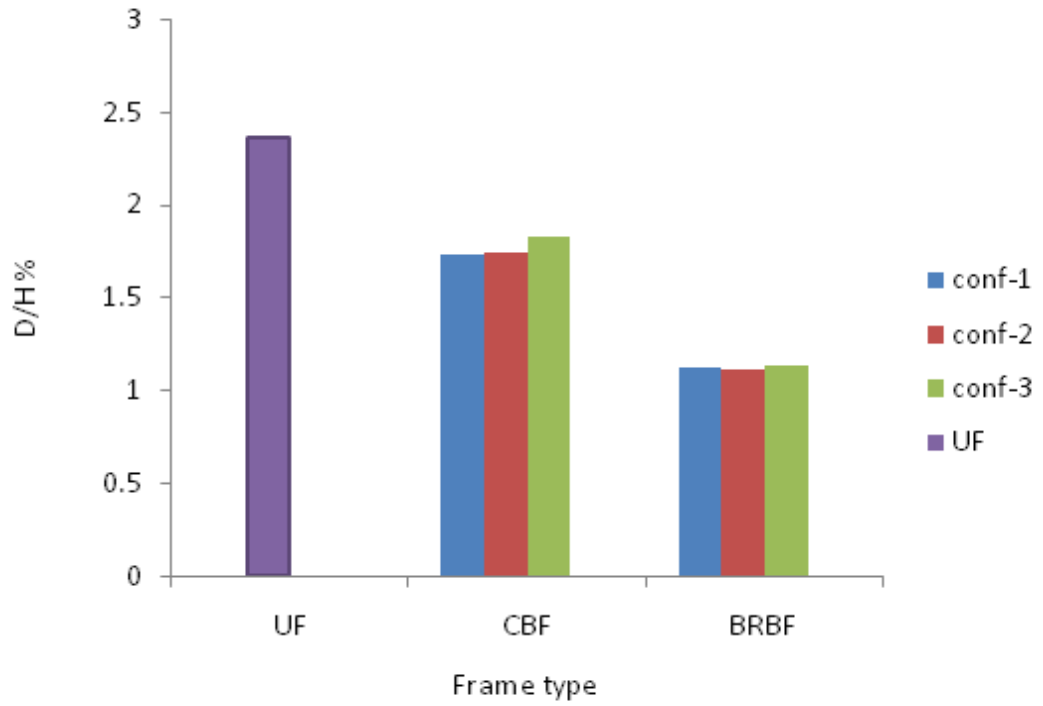
a)
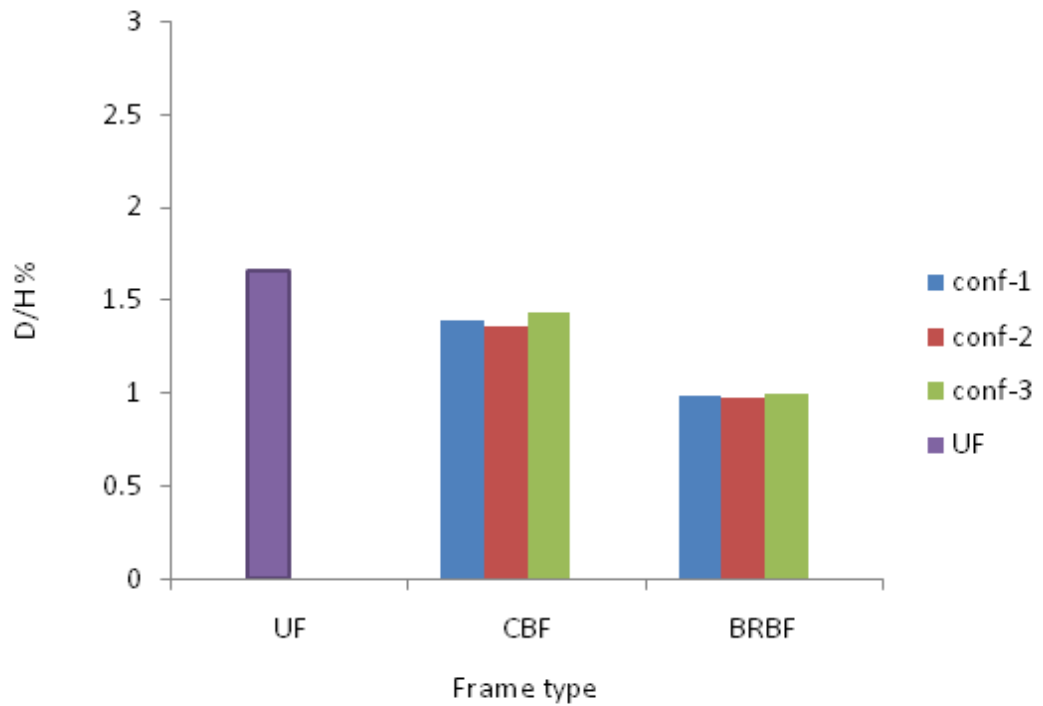
b)

Figure 4.7 Global damage index for SMRF: a) T_p=1.4 s and b) T_p=0.9 s

4.1.4 Base shear and top shear

The base and top shear were evaluated for both CB and BRB frames subjected to artificial accelerations equivalent to Northridge and Kobe earthquakes. Figures 4.8-4.11 compare the base shear and top shear for CB and BRB frames with different configuration, frame type, and earthquake time history.

Maximum base and top shear was assessed for both CB and BRB frames subjected to equivalent pulses to Northridge and Kobe earthquakes by taking the maximum values of base and top shear time histories presented in Appendix D.

Strength of frame, peak ground acceleration, and earthquake type affected the variation of base shear forces. Position of the fundamental period of the frame with respect to earthquake excitation acceleration spectrum defined this variation in the elastic stage. Nevertheless, the base and top shear distribution were affected significantly by T_s/T_p ratio. Putting the severity of pulse P2 with T_p=1.4 s in perspective with T_p=0.9 s, due to value of the pulse velocity period larger base shear could be observed in the former pulse.

Total base shear was increased in the presence of braces, but the columns were not influenced so much by this increment, because most of the shear forces were supported by the braces. As explained clearly in the section 4.1.7 Plastification in the frames, most of the plastic hinges was formed in the braces, however, in the case of CB frames, some plastic hinges was developed in the columns because when conventional braces exhibited buckling deformation their strength was degraded and then most of the shear forces would be supported by the columns. Total top shear was decreased in the presence of braces. However, in some cases (i.e. OMRF-CB) was even increased.

67
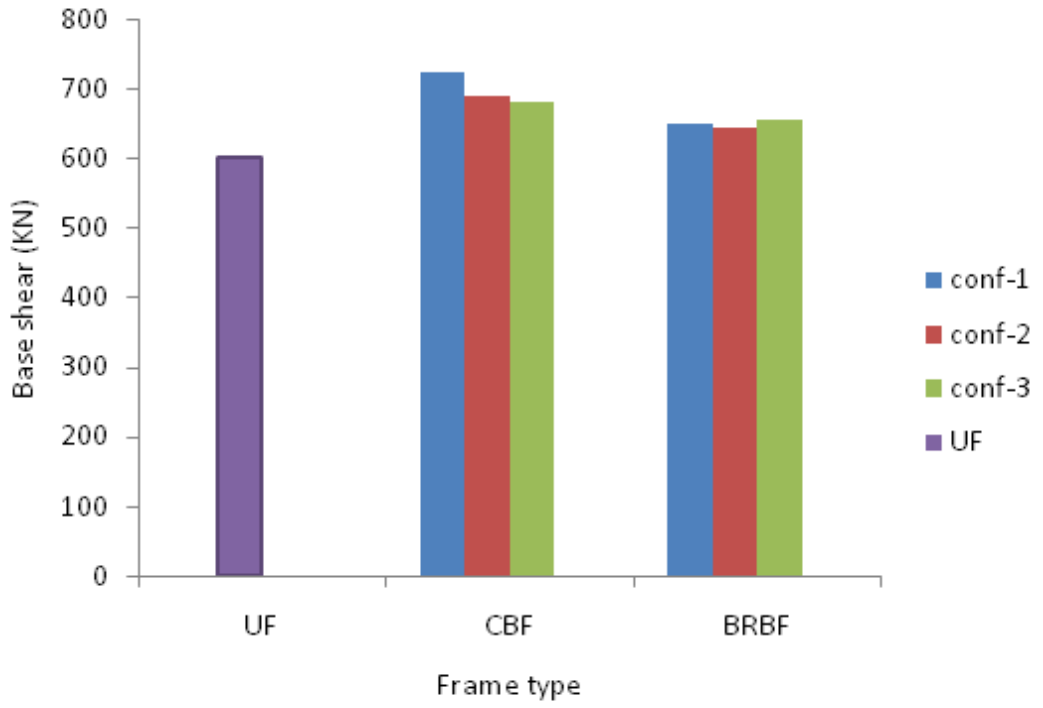
a)
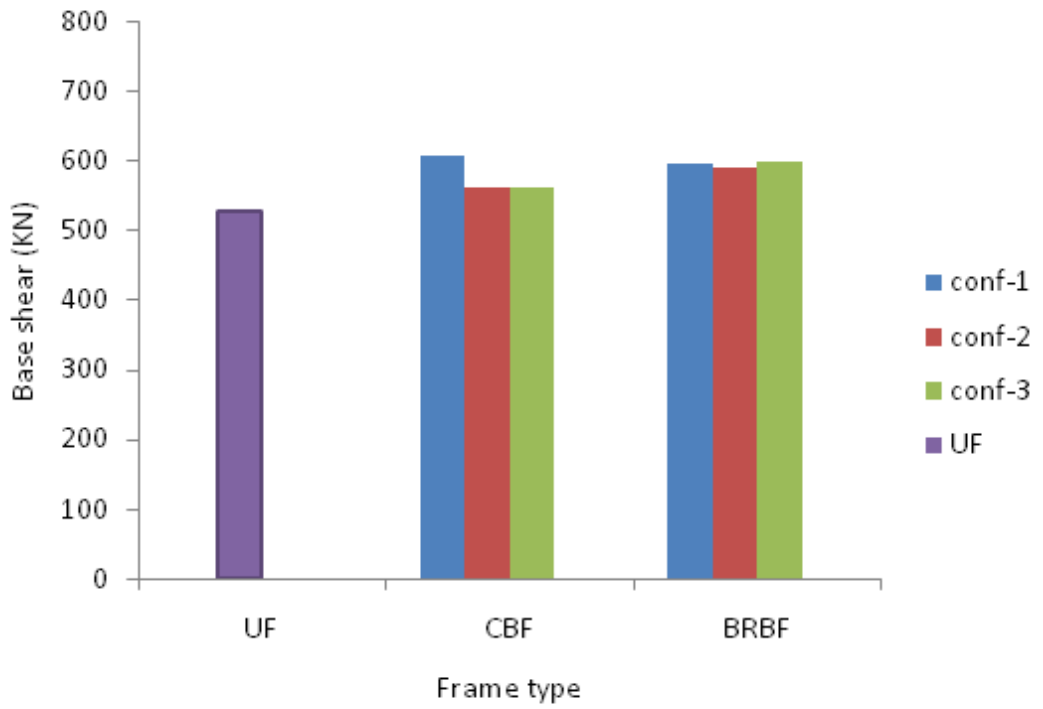
b)

Figure 4.8 Base shear for OMRF: a) $T_p=1.4$ s and b) $T_p=0.9$ s
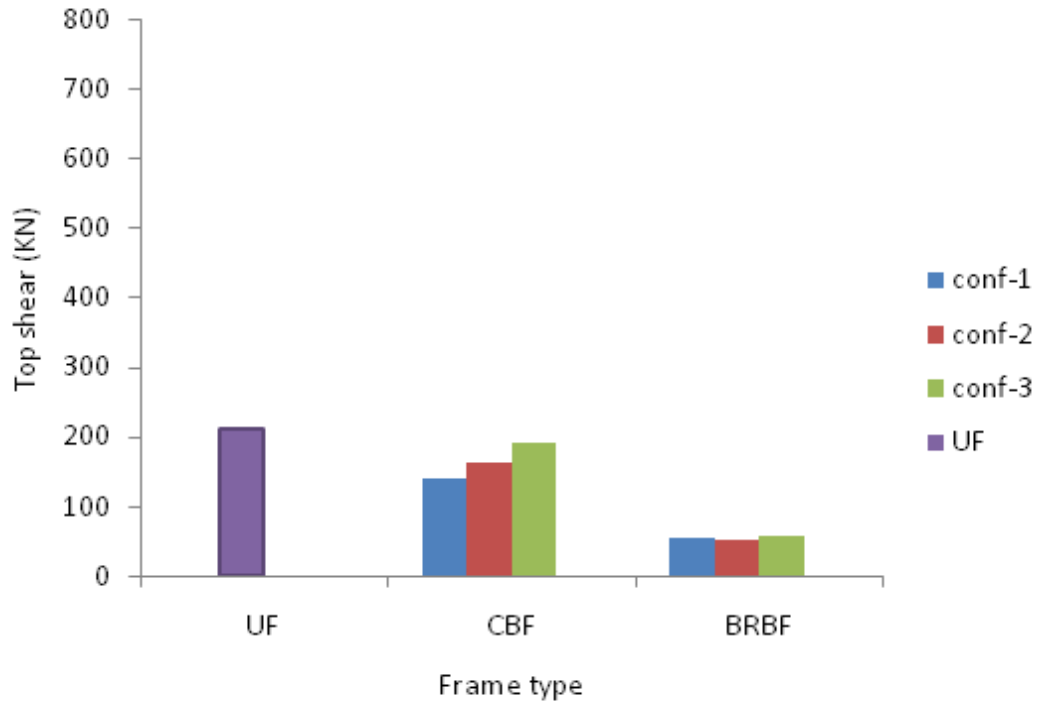
a)
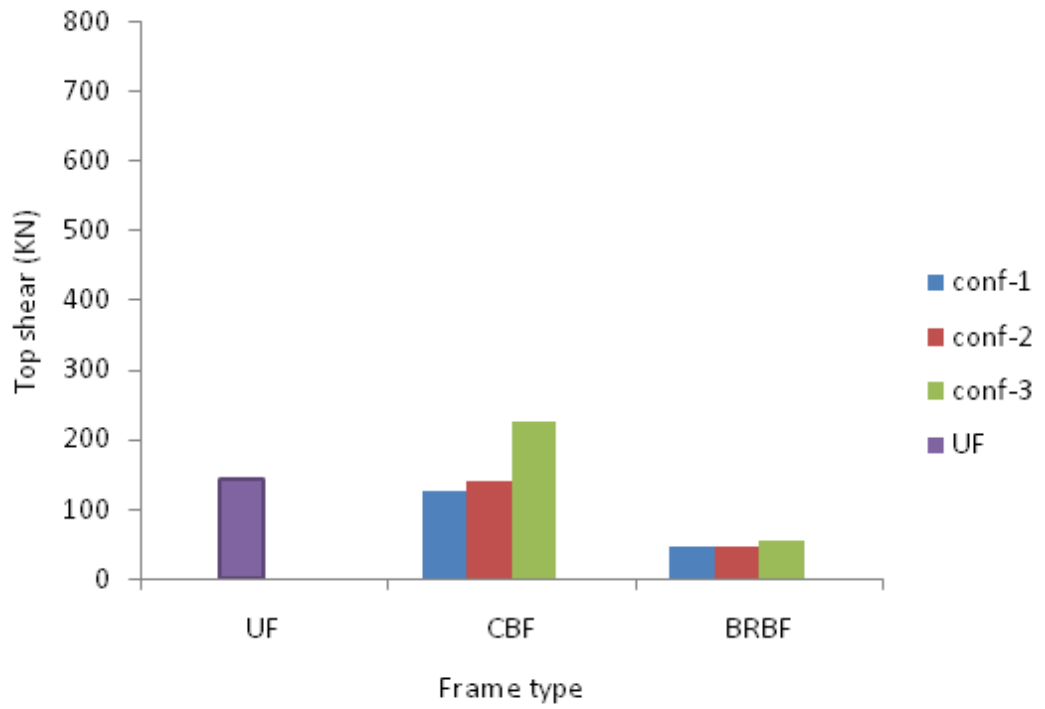
b)

Figure 4.9 Top shear for OMRF: a) T_p=1.4 s and b) T_p=0.9 s
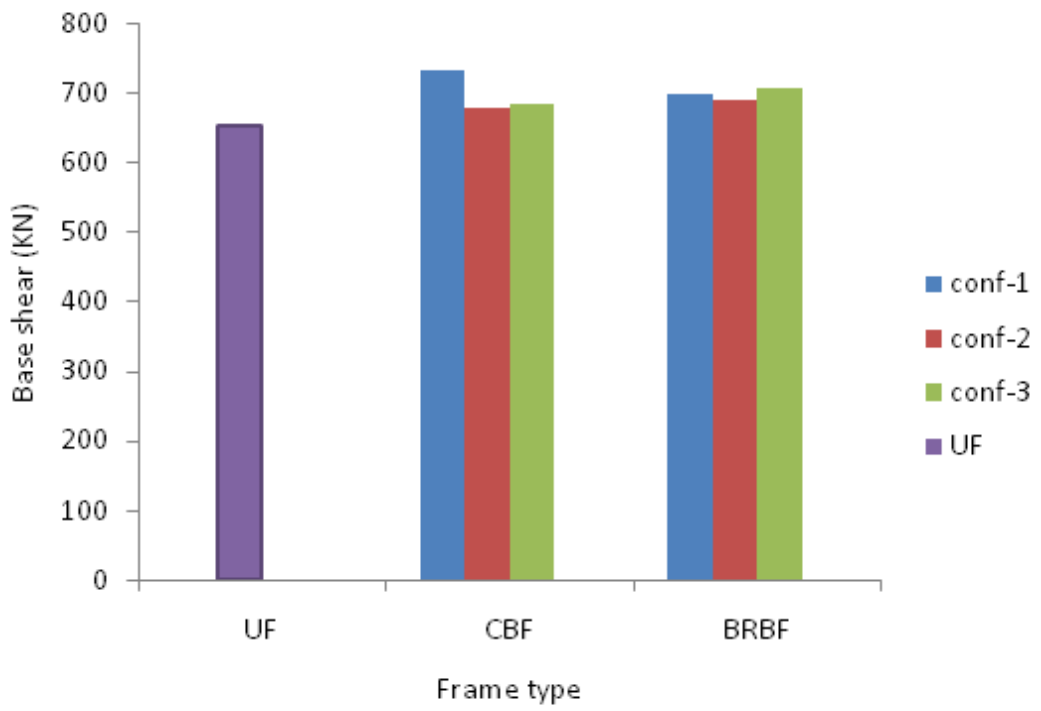
a)
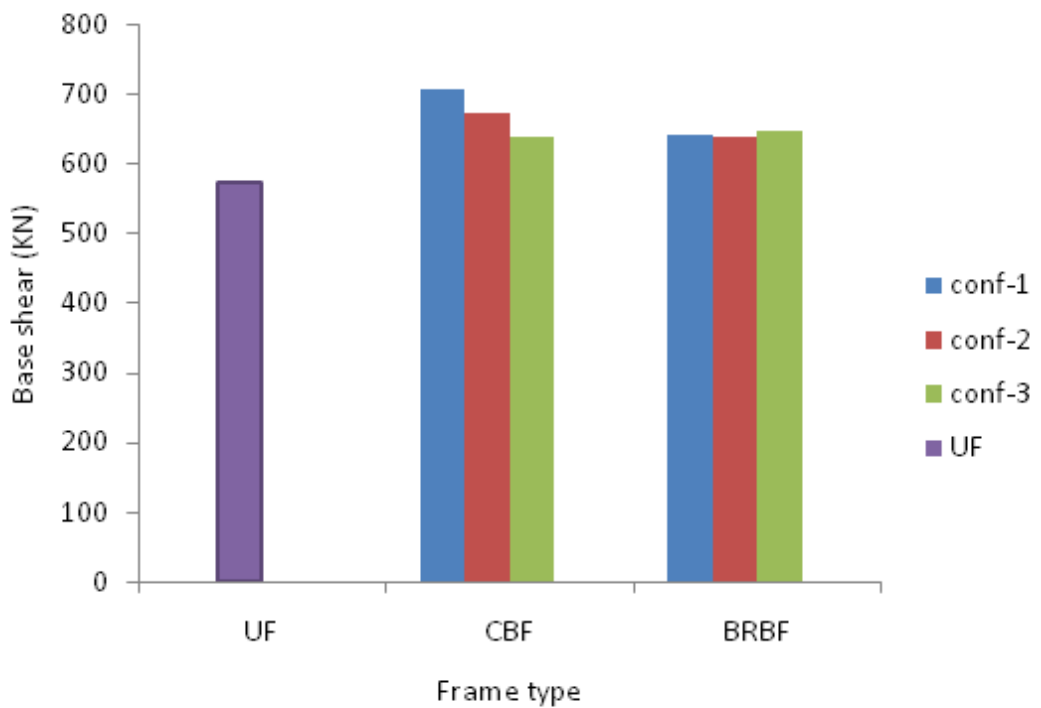
b)

Figure 4.10 Base shear for SMRF: a) T_p=1.4 s and b) T_p=0.9 s
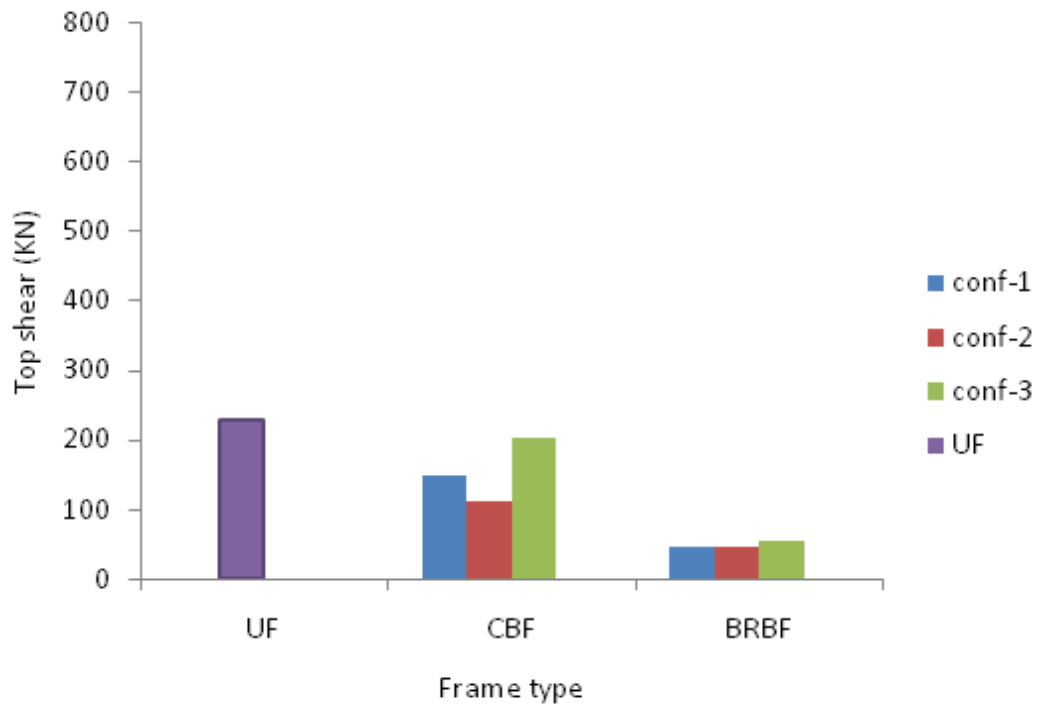
a)
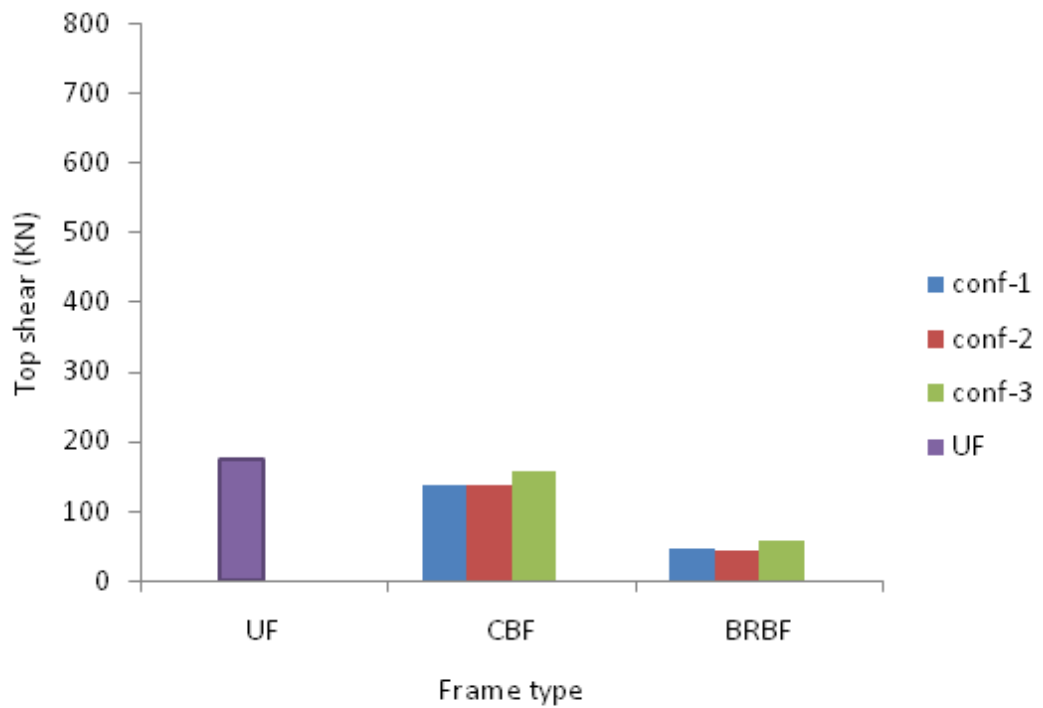
b)

Figure 4.11 Top shear for SMRF: a) T_p=1.4 s and T_p=0.9 s

4.1.5 Variation of roof displacement

Figures 4.12-4.13 show the deflected shape of OMRFs and SMRFs at various circumstances at the instance corresponding to the maximum roof displacement.

Both BRB and CB considerably decreased the value of maximum roof displacement and corresponding storey displacement compared to unbraced frames, especially in the case of BRBs, more uniform response of the frame along the height of the structure could be observed and there was not concentration of large deformation in one storey or without an abrupt changes in the drift pattern with respect to the level of deformation. Moreover, it was pointed out that the differences between performance of BRB and CB frames was much more apparent in severe ground motions (i.e. T_p=1.4 s). For example, the maximum roof displacement in the case of OMRF-Tp1.4-BRB was about 56% of that of OMRF-Tp1.4-CB. However, the maximum roof displacement in the case of OMRF-Tp0.9-BRB is approximately 68% of that of OMRF-Tp0.9-CB, results for the other frames subjected to equivalent pulses to Northridge and Kobe earthquakes showed the same tendency.

Moreover, the difference in performance of BRBFs and CBFs was less noticeable in ground motions with low or moderate seismicity (i.e. T_p=0.9 s) since both CBs and BRBs with the same cross-sectional had the same initial elastic stiffness. However, during severe earthquake excitations, most of the buildings were expected to undergo inelastic deformation such as in the case of high seismicity (i.e. T_p=1.4 s), the difference in performance of BRBFs and CBFs was more obvious because in the inelastic range CBs exhibited buckling deformation and strength degradation. However, BRBs remained unbuckled and supported larger seismic induced load.
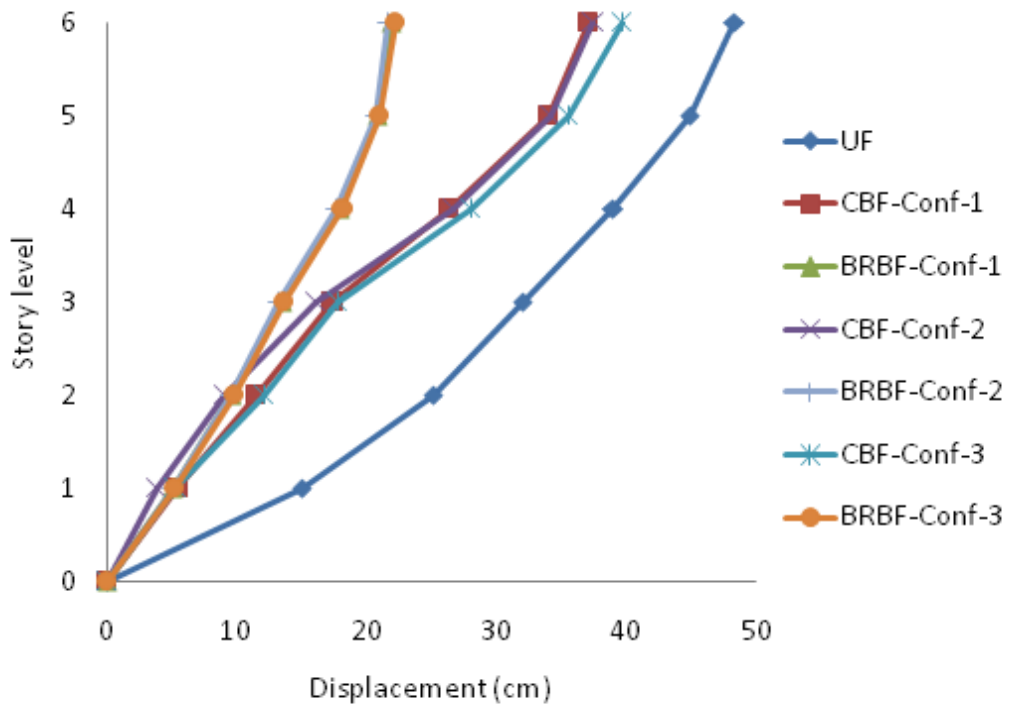
a)
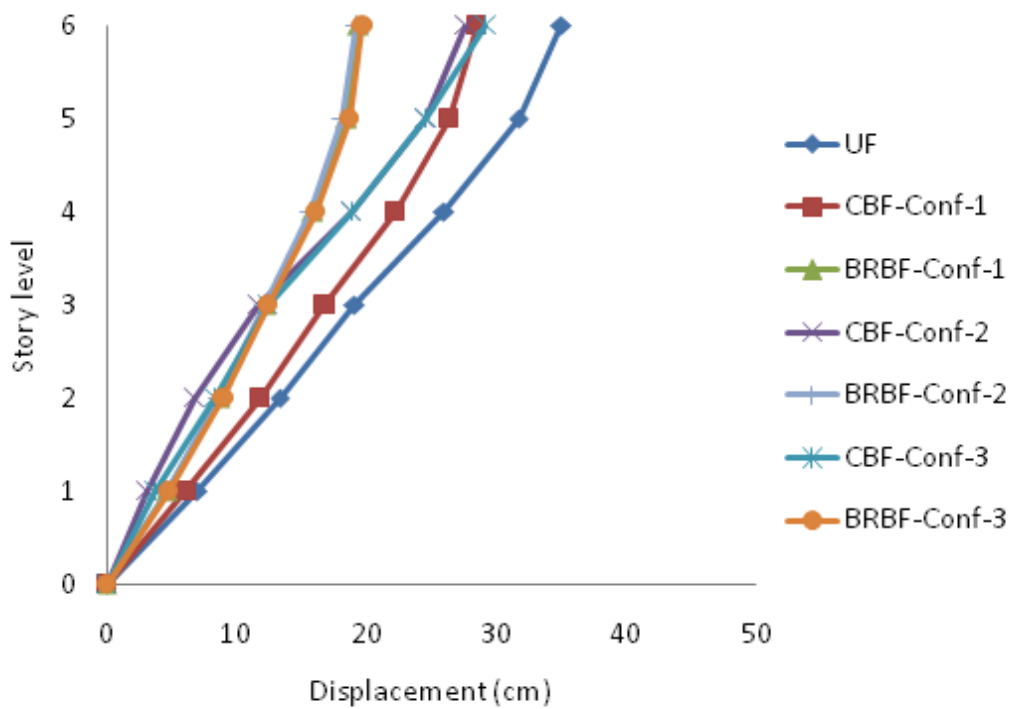
b)

Figure 4.12   Deflected shape at maximum roof displacement for OMRF: a) T_p=1.4 s and b) T_p=0.9 s
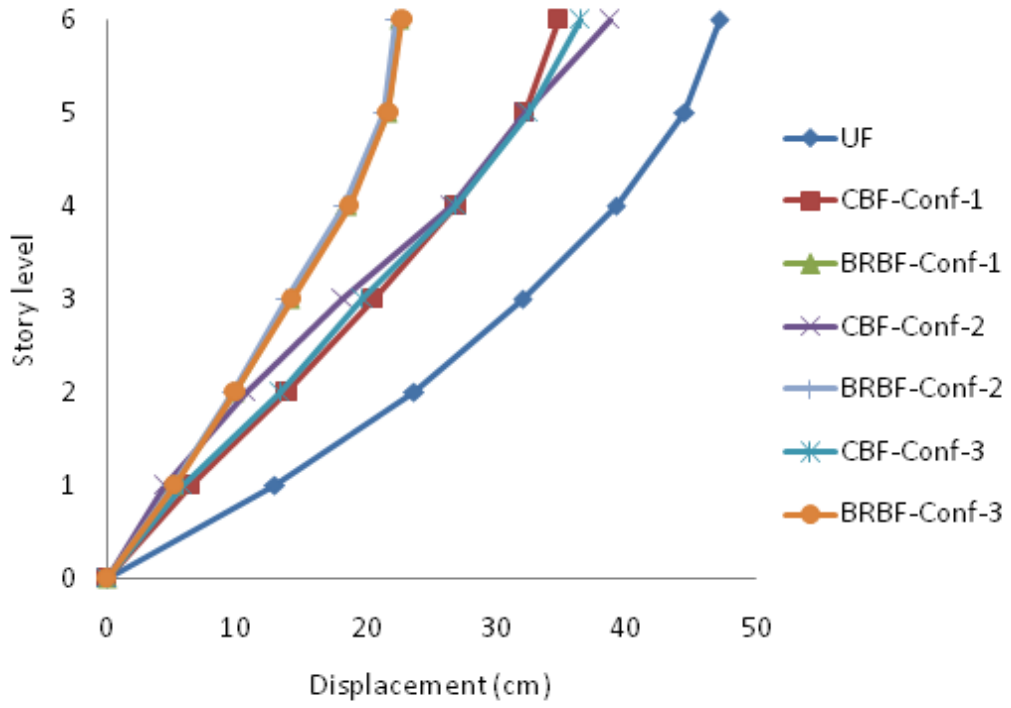
a)
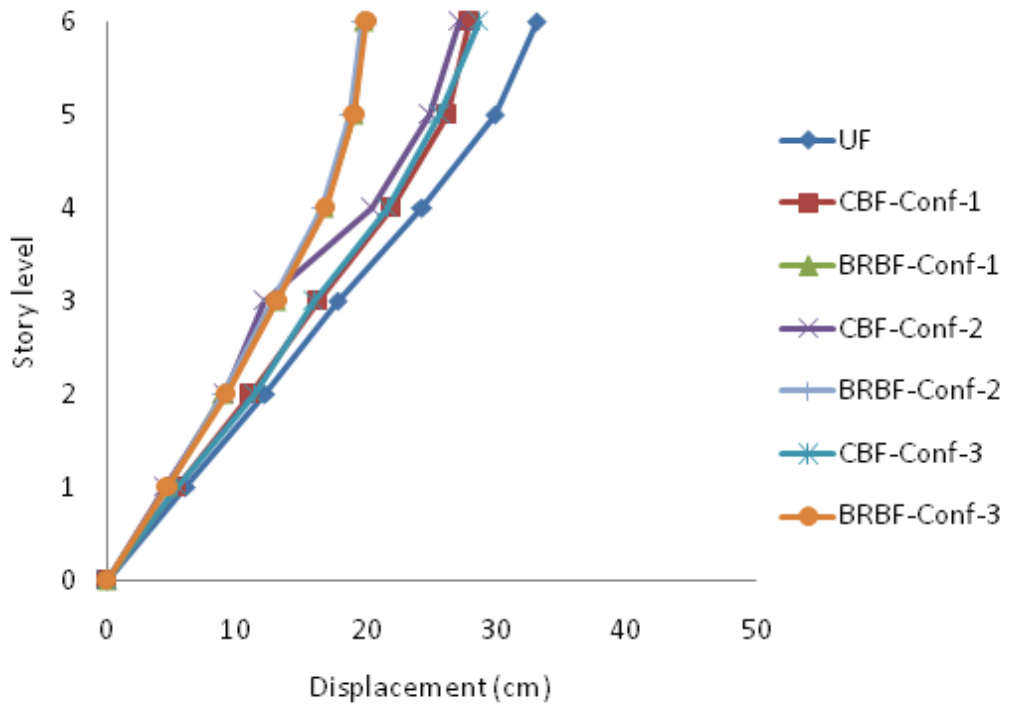
b)

Figure 4.13 Deflected shape at maximum roof displacement for SMRF: a) T_p=1.4 s and b) T_p=0.9 s

4.1.6 Variation of damage index

The value of effective damage index for different braced frame cases and the corresponding life safety limit as per Tables 5-8 of FEMA 273 (FEMA273, 1997) are given in Table 4.1.

The damage index is a parameter which indicates the level of damage to the structure due to inelastic deformation under earthquakes. The ductility damage index (D) can be defined as given in the equation below:

$$D = \frac{\varepsilon_{max}}{\varepsilon_u} \qquad\qquad (4.1)$$

For BRBs, the ultimate strain (ε_u) for the calculation of damage index was taken as $12\varepsilon_y$, as per Table 5.8 of FEMA273 (FEMA273, 1997). The damage index was taken as 1.0 for ultimate failure ($12\varepsilon_y$), 0.83 for collapse prevention (CP) (at $10\varepsilon_y$), 0.67 for life safety (LS) (at $8\varepsilon_y$) and 0.083 for immediate occupancy (IO) (at ε_y), as per Table 5.8 of FEMA273 (FEMA273, 1997). For CBs, the value of modeling parameters and acceptance criteria was different from BRBs and it depended on the properties of the cross-section.

Since a storey collapse is considered as a global collapse of the frame, the effective damage index of the frame, D_{eff}, is taken as the maximum of Di (the damage index of the ith storey), as given below:

$$D_{eff} = \text{Maximum of (Di)} \qquad\qquad (4.2)$$

Comparing the value of effective damage indexes for both CB frames and BRB frames given in Table 4.1, it could be noticed that in both tension and compression, this index was greater for the former than later, and they exceeded the admissible

value given by FEMA 273 (FEMA-273, 1997), especially when they were under compression loading. This might be explained as CBs typically buckle under compression force and exhibited large stiffness and strength degradation when loaded cyclically or monotonically in compression. However, due to the improved nonlinear behavior of BRBs, the damage indexes for the frames with BRBs were within the limit.

Table 4.1 Effective damage index (D_{eff}) of bracings

Sample no.	Designation of frame	Compression			Tension		
		Storey	Damage index	LS limit	Storey	Damage index	LS limit
1	OMRF-Tp0.9-BRB-Conf-1	1	0.45	0.67	4	0.39	0.67
2	OMRF-Tp0.9-BRB-Conf-2	1	0.45	0.67	4	0.41	0.67
3	OMRF-Tp0.9-BRB-Conf-3	1	0.45	0.67	2	0.43	0.67
4	OMRF-Tp0.9-CB-Conf-1	1	7.11	2.00	4	0.63	0.67
5	OMRF-Tp0.9-CB-Conf-2	4	8.96	3.92	5	0.56	0.67
6	OMRF-Tp0.9-CB-Conf-3	4	7.72	3.92	5	0.59	0.67
7	OMRF-Tp1.4-BRB-Conf-1	1	0.51	0.67	4	0.48	0.67
8	OMRF-Tp1.4-BRB-Conf-2	1	0.50	0.67	4	0.46	0.67
9	OMRF-Tp1.4-BRB-Conf-3	1	0.51	0.67	2	0.47	0.67
10	OMRF-Tp1.4-CB-Conf-1	1	10.49	2.00	4	0.94	0.67
11	OMRF-Tp1.4-CB-Conf-2	4	12.60	3.92	5	0.78	0.67
12	OMRF-Tp1.4-CB-Conf-3	4	11.95	3.92	5	0.76	0.67
13	SMRF-Tp0.9-BRB-Conf-1	1	0.48	0.67	1	0.43	0.67
14	SMRF-Tp0.9-BRB-Conf-2	1	0.48	0.67	1	0.42	0.67
15	SMRF-Tp0.9-BRB-Conf-3	1	0.48	0.67	2	0.46	0.67
16	SMRF-Tp0.9-CB- Conf-1	1	6.91	3.25	1	0.56	0.67
17	SMRF-Tp0.9-CB- Conf-2	4	7.95	3.11	2	0.50	0.67
18	SMRF-Tp0.9-CB- Conf-3	2	7.03	5.00	2	0.54	0.67
19	SMRF-Tp1.4-BRB- Conf-1	1	0.53	0.67	2	0.45	0.67
20	SMRF-Tp1.4-BRB- Conf-2	1	0.52	0.67	4	0.45	0.67
21	SMRF-Tp1.4-BRB- Conf-3	1	0.53	0.67	2	0.50	0.67
22	SMRF-Tp1.4-CB- Conf-1	1	8.43	3.25	2	0.77	0.67
23	SMRF-Tp1.4-CB- Conf-2	4	9.78	3.11	2	0.65	0.67
24	SMRF-Tp1.4-CB- Conf-3	1	9.27	3.25	3	0.64	0.67

In general, there was a slight difference between the damage indexes of the frames with different configurations. However, the damages in some brace configurations were lower compared to others. For example, the damage index in the braces in the second configuration (conf-2) was more compared to the other configurations (conf-1 and conf-3) and that was due to the fact that in the second configuration all the

brace were supporting the seismic loads in one direction or in other words they would either support compression load or tension load.

4.1.7 Plastification in the frames

From nonlinear dynamic analysis, the location of plastic hinges for both CB and BRB frames were evaluated for different frame type, brace type, and brace configurations. Basic principles and the theoretical backgrounds for nonlinear dynamic analysis and computing constant ductility spectra is presented in Appendix A. Figures 4.14-4.20 compare the location of plastic hinges for different case of structures subjected to artificial pulses that is equivalent to Kobe and Northridge earthquakes. Comparing the location and number of the plastic hinges given in the figures, the following observation can be made:

i.   Due to buckling and then strength and stiffness deterioration of the CBs, most of the critical actions have been transmitted to the structural members, and they entered the inelastic range of deformation. On contrary, in the case of BRBs, because of their perfect nonlinear behavior and absorbing more energy in the inelastic range, most of the structural members remained in the elastic range and plastic hinges were concentrated in the BRBs, which might be easily replaced after the earthquake.

ii.   As discussed previously, due to the sensitivity of the structural response with the pulse period value T_p, the ground motions with a smaller pulse period T_p resulted in less damage. As seen from the figures, it was pointed out that damage in the case of pulse with T_p=1.4 s was more compared to the pulse with T_p=0.9 s.

iii.   Comparison of the performance of SMRFs with OMRFs, it was observed that SMRFs were performing better than OMRFs. In the case of SMRFs, most of the plastic hinges were concentrated in the beam elements, and most of the columns remained in the elastic stage. However, in the case of OMRFs, many column elements entered the inelastic range that might lead to a catastrophic failure.

a)   b)   c)   d)

OMRF: a) subjected to Tp=1.4 s and b)   SMRF: c) subjected to Tp=1.4 s and d)
         subjected to Tp=0.9 s   subjected to Tp=0.9 s
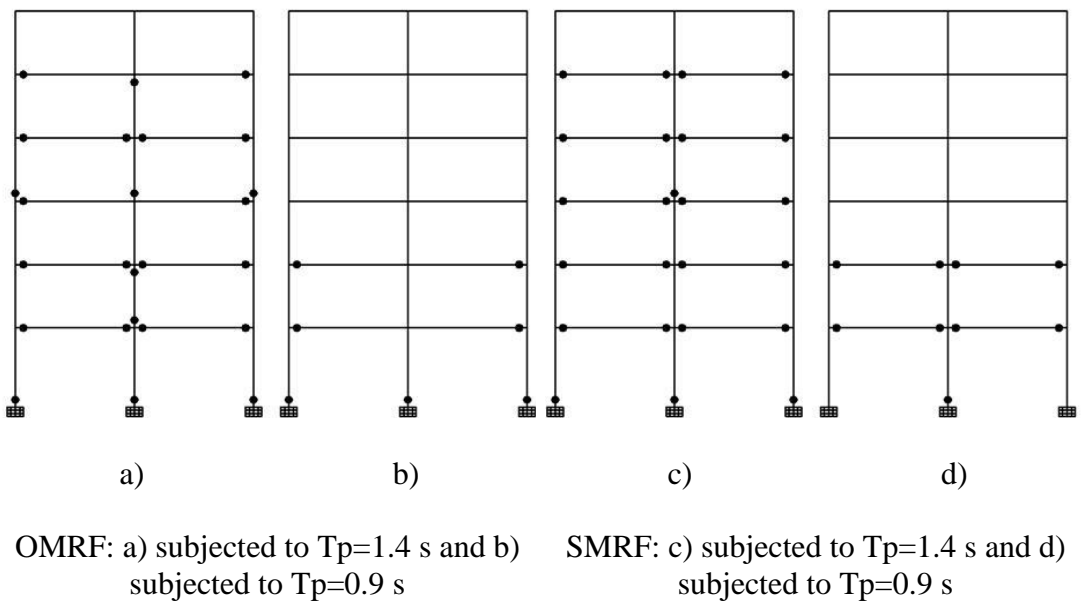
Figure 4.14 Plastic hinge formation for unbraced frames

Pulse P$_2$, T$_p$=1.4 s   Pulse P$_2$, T$_p$=0.9 s

a)   b)   c)   d)
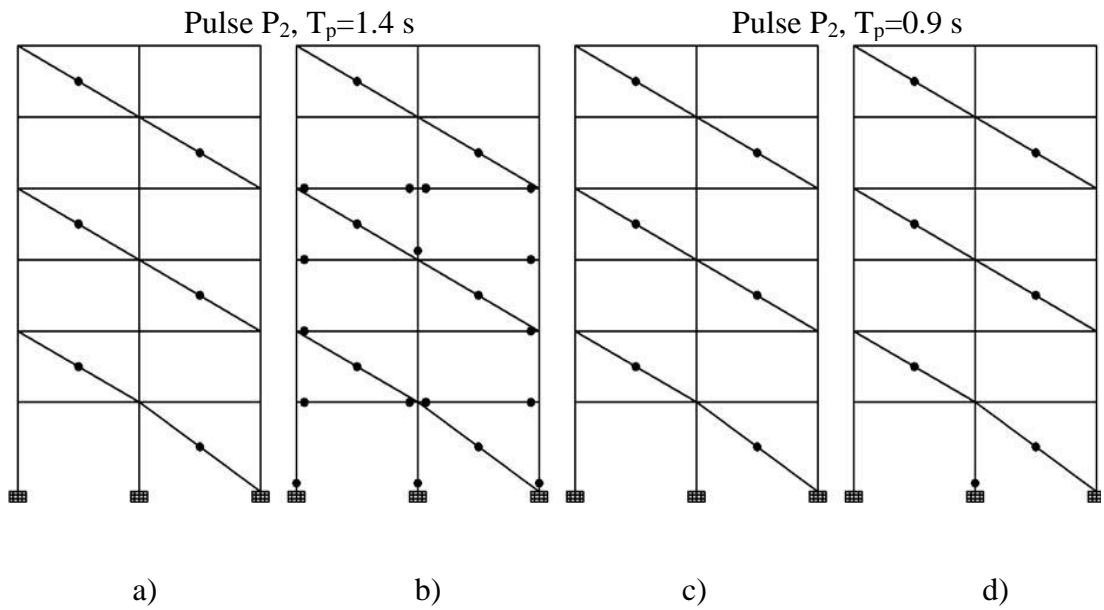
Figure 4.15 Plastic hinge formation for OMRFs with braces in configuration-1: a) BRB and b) CB subjected to Tp=1.4 s, and c) BRB and d) CB subjected to Tp=0.9 s

Pulse P$_2$, T$_p$=1.4 s   Pulse P$_2$, T$_p$=0.9 s

a)   b)   c)   d)
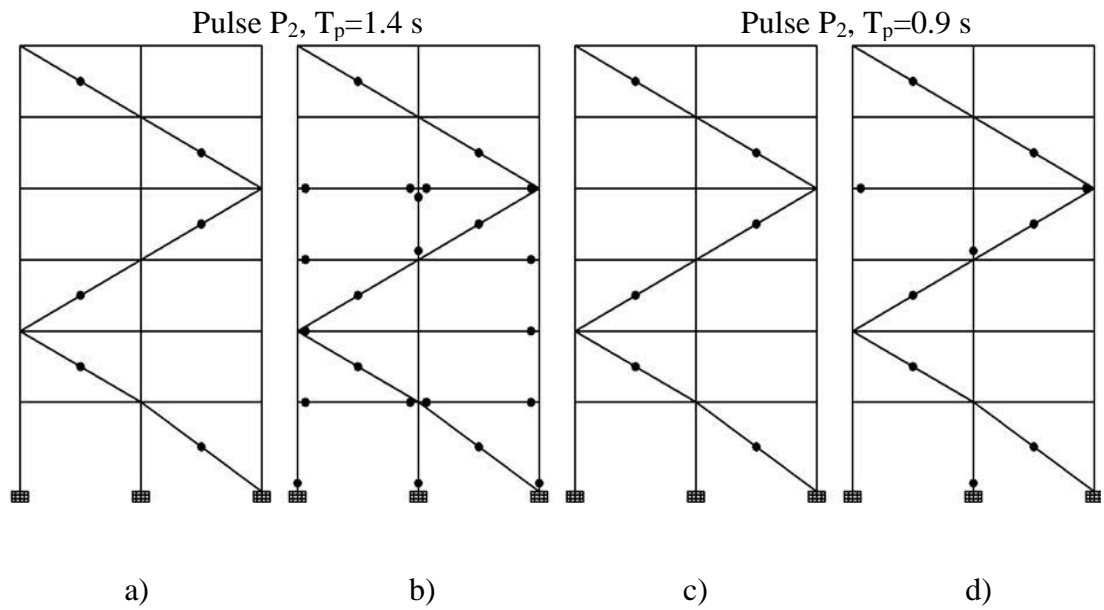
Figure 4.16 Plastic hinge formation for OMRFs with braces in configuration-2: a) BRB and b) CB subjected to T$_p$=1.4 s, and c) BRB and d) CB subjected to T$_p$=0.9 s

a)   b)   c)   d)
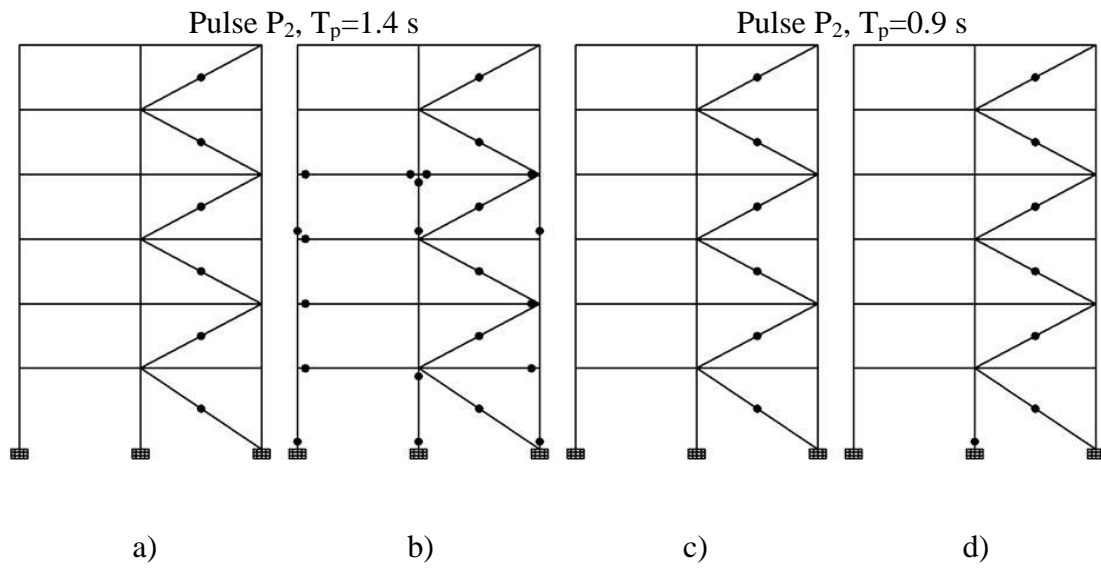
Figure 4.17 Plastic hinge formation for OMRFs with braces in configuration-3: a) BRB and b) CB subjected to T$_p$=1.4 s, and c) BRB and d) CB subjected to T$_p$=0.9 s

Pulse P$_2$, T$_p$=1.4 s   Pulse P$_2$, T$_p$=0.9 s

a)   b)   c)   d)
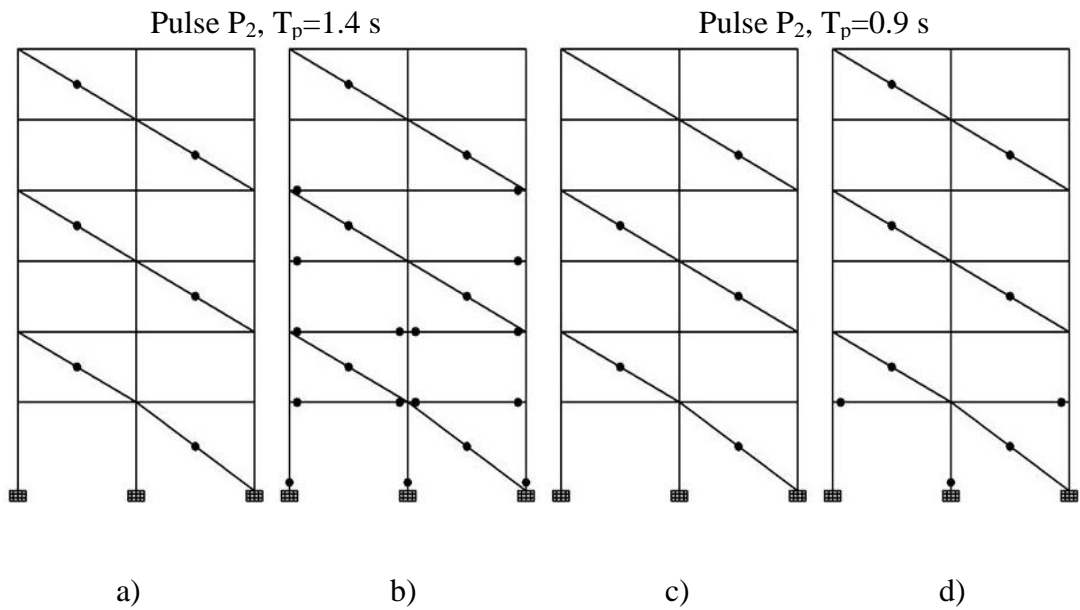
Figure 4.18 Plastic hinge formation for SMRFs with braces in configuration-1: a) BRB and b) CB subjected to T$_p$=1.4 s, and c) BRB and d) CB subjected to T$_p$=0.9 s

a)   b)   c)   d)
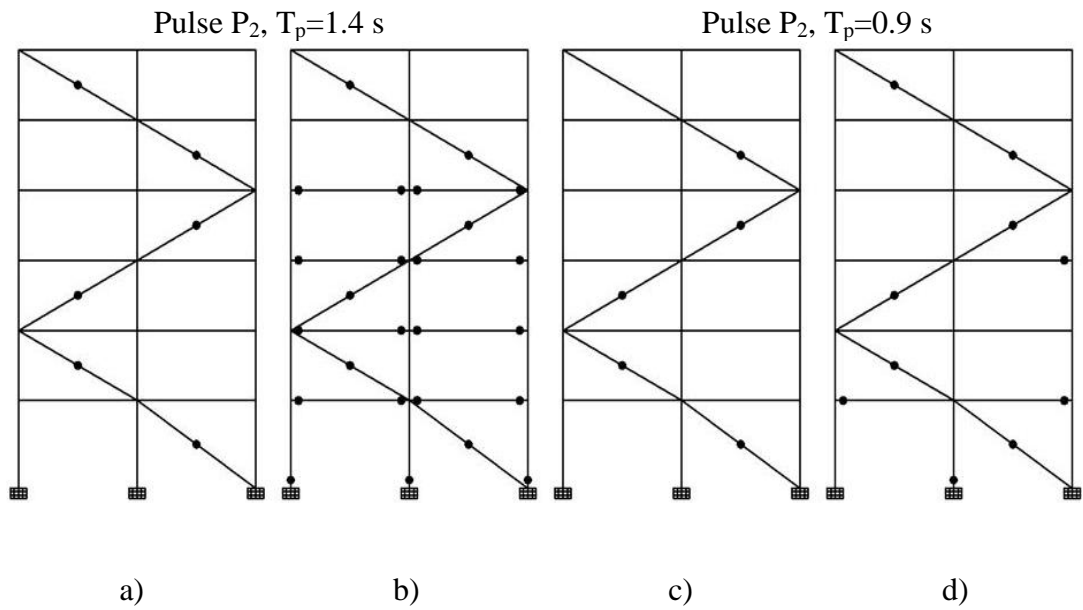
Figure 4.19 Plastic hinge formation for SMRFs with braces in configuration-2: a) BRB and b) CB subjected to T$_p$=1.4 s, and c) BRB and d) CB subjected to T$_p$=0.9 s

a)   b)   c)   d)
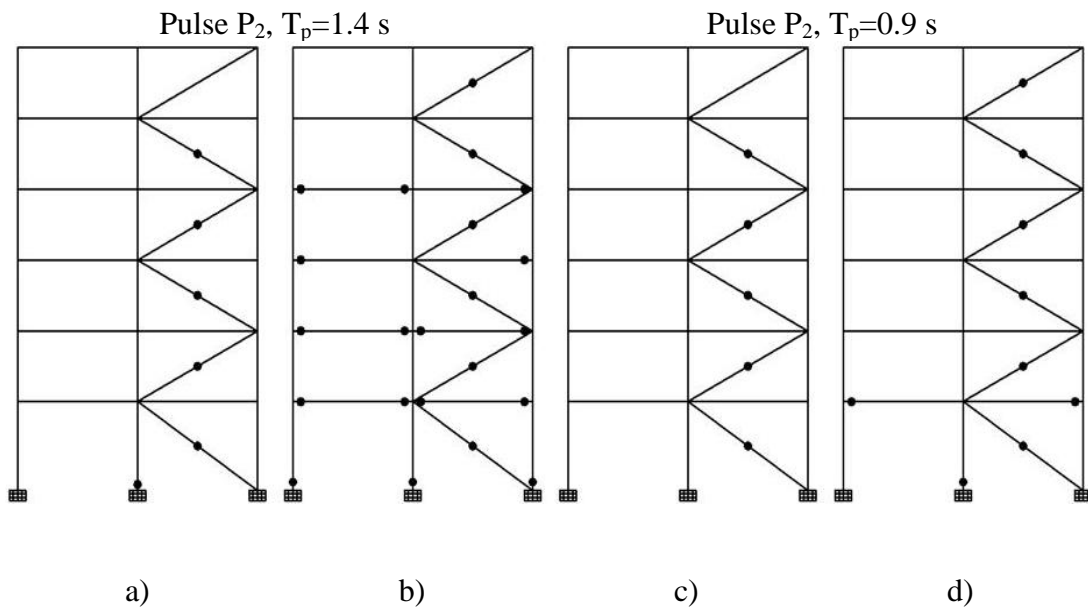
Figure 4.20 Plastic hinge formation for SMRFs with braces in configuration-3: a) BRB and b) CB subjected to T$_p$=1.4 s, and c) BRB and d) CB subjected to T$_p$=0.9 s

CHAPTER 5

CONCLUSION

The study described herein investigated the seismic performance of different type of moment resisting frame buildings equipped with diagonally conventional braces (CBs) and buckling restrained braces (BRBs) subjected to near-field ground motions. By comparing the procedures and results illustrated in this study, the following conclusions can be drawn:

1. BRBs provided smaller *interstorey drift index* compared to CBs. The results of the performed nonlinear dynamic analysis indicated that BRB frames were the most effective one because the reduction of interstorey drifts with respect to the original frames was on average equal to 50%. Whereas, in the case of CB frames, this reduction was only 13%, and on average lateral drift in BRBs was 42% lower than CBs.

2. Both CBs and BRBs considerably reduced the *global damage index* of the frames, especially in the case of the BRBs.

3. BRBs have provided more uniform response along the height and there wasn't a concentration of large deformation in one storey that might leads to formation of plastic hinges in the structural members.

4. In general, it was evident that the retrofitted frames with BRBs kept in the elastic range and plastification only occurred in the braces which might be

82

changed easily after the earthquake. On contrary, in the case of CBs, many structural members have undergone inelastic deformation.

5. Total *base shear* was increased in the presence of braces, but the columns would not be affected by this increment in the case of BRBFs, because most of the shear forces were supported by the BRBs. However, in the case of CBFs, some plastic hinges would be developed in the columns because when CBs exhibited buckling deformation their strength was degraded, and then most of the shear forces would be supported by the columns.

6. BRBFs were much stiffer and showed a better performance compared to CB frames, also putting the stiffness of the CB frames in perspective with unbraced frames it was apparent that in general the former was much stiffer than later.

7. Most of the seismic energy has been transmitted the structural component in the case of CBF because *damage index* in both tension and compression, was greater for the CB than BRB.

8. BRBs dissipated more energy compared to CB in the nonlinear range since they exhibited stable behavior and showed a spindle-hysteresis behavior. As a result, the system provided a better behavior in the nonlinear range of deformations. On contrary, due to the buckling of the conventional braces before reaching the maximum yield strength of the brace, less energy has been dissipated and unsymmetrical hysteresis behavior was developed.

9. Putting the performance of SMRFs in perspective with OMRFs, it was observed that SMRFs were performing better than OMRFs, in the case of SMRFs most of the plastic hinges were concentrated in the beam elements, and most of the columns remained in the elastic stage. However, in the case

of OMRFs, many column elements entered the inelastic range of deformation that might result in a catastrophic failure.

10. Increasing the lateral stiffness of the buildings made the earthquake excitation to induce a larger storey shear demand that might lead to failure. For example, in the case of OMRF with CBs in the second configuration subjected to Tp=0.9 s, it was pointed out that interstorey index was larger than OMRF without braces. So as a result, the selection of appropriate brace cross-section would contribute to avoid such dynamic responses.

11. Percent of tension and compression loads should be equally supported by the braces in order to provide a unique stiffness in both positive and negative directions, especially in the case of CBF. This is due to the fact that CBs have a smaller load carrying capacity in the compression loading compared to tension loading.

12. In general, the near fault ground motions with a large pulse period resulted in more damaging compared to ground motions with small pulse period. However, the location of the fundamental period of the structure on the response spectrum curve of the earthquake excitation may define the value shear forces experienced by the structural members.

REFERENCES

AIJ (Architectural Institute of Japan), Steel Committee of Kinki Branch, Reconnaissance report on damage to steel building structures observed from the 1995 Hyogoken-Nanbu (Hanshin/Awaji) earthquake), AIJ, Tokyo, May 1995, p.167.

AISC (2005a). ANSI/AISC 341-05. seismic provisions for structural steel buildings, American institute of steel construction, Inc., Chicago, IL.

AISC (2005b). ANSI/AISC 358-05. Prequalified connections for special and intermediate steel moment frames for seismic applications including supplement No. 1, American institute of steel construction, Inc., Chicago, IL.

Alavi B., Krawinkler H. (2004). Behavior of moment-resisting frame structures subjected to near-fault ground motions, *Journal of Earthquake engineering and structural dynamics*; **33**:687-706.

Altuntop MA. (2007). Analysis of building structures with soft stories, Msc thesis, Graduate School of Natural and Applied Sciences of ATILIM University, Ankara.

Asgarian B, Amirhesari N. (2008). A comparison of dynamic nonlinear behavior of ordinary and buckling restrained braced frames subjected to strong ground motion, *The structural design of tall and special buildings*; **17**:367-386.

ATC 40 (Applied Technology council). Seismic Evaluation and Retrofit of concrete buildings, volume 1-2, California, 1996.

AWS (2005), ANSI/AWS D1.8: 2005. Structural welding code-seismic supplement. American Welding Society, Miami, FL.

Black C, Makris N, Aiken I. (2002). Component testing, stability analysis and characterization of buckling restrained braces. Final Report to Nippon Steel Corporation, Japan.

Black C, Makris N, Aiken IA. (2004). Component testing, seismic evaluation and characterization of buckling-restrained braces. *Journal of Structural Engineering ASCE*; **130**(6):880–94.

Bozorgnia Y, Bertero VV. Earthquake engineering. From engineering seismology to performance-based engineering. Boca Raton (FL, USA): CRC Press; 2004.

Broderick BM, Elnashai AS, Ambraseys NN, Barr JM, Goodfellow RG, Higazy EM. The Northridge (California) earthquake of 17 January 1994: Observations, strong motion and correlative response analysis. Engineering seismology and earthquake engineering, Research report no. ESEE 94/4. London: Imperial College; 1994.

Broderick BM, Goggins JM, Elghazouli AY. (2005). Cyclic performance of steel and composite bracing members. *Journal of Constructional Steel Research*;**61**(4):493–514.

Bruneau M, Uang CM, Whittaker A. Ductile design of steel structures. New York (USA): McGraw-Hill; 1998.

Building Center of Japan (BCJ). Report on new building technologies approvals, applications and certification. Tokyo: BCJ; 2002 (in Japanese).

Chopra A. (1995). "Dynamics of Structures: Theory and Applications to Earthquake Engineering", Prentice Hall.

Corebrace (2002), West Jordan, Utah 84081. Available at: http://www.corebrace. com.

CSI Analysis Reference Manual for SAP2000, ETABS, and SAFE. (2009). Berkeley, California, USA.

Deulkar W N, Modhera C D, Patil H S (2010). Buckling restrained braces for vibration control of building structure. International Journal of Research and Reviews in Applied Sciences; 4:363-372.

Di Sarno, Elnashai AS, Nethercot DA. (2006). Seismic retrofitting of framed structures with stainless steel. *Journal of Constructional Steel Research*; **6**2(1–2):93–104.

Di Sarno, Elnashai AS. (2009). Bracing systems for seismic retrofitting of steel frames, *journal of constructional steel research*; **65**:452-465.

Elnashai AS, Bommer JJ, Baron I, Salama AI, Lee D. Selected engineering seismology and structural engineering studies of the Hyogoken Nanbu (Kobe, Japan) Earthquake of 17 January 1995. Engineering Seismology and Earthquake Engineering, Report no. ESEE/95-2. London: Imperial College; 1995.

FEMA (Federal Emergency Management Agency). (1997). NEHRP commentary on the guidelines for the seismic rehabilitation of buildings. **FEMA-274**, Washington, D.C.

FEMA (Federal Emergency Management Agency). (1997). NEHRP guidelines for seismic rehabilitation of buildings, **FEMA-273**.Washington (DC).

FEMA (Federal Emergency Management Agency). (2000). Prestandard and commentary for the seismic rehabilitation of building. **FEMA-356**, D.C.

FEMA (Federal Emergency Management Agency). (2000). State of art report on past performance of steel moment frame buildings in earthquakes. Report no. **FEMA 355E**. Washington (DC, USA).

FEMA (Federal Emergency Management Agency). (2003). Recommended provisions for seismic regulations for new buildings and other structures, **FEMA-450**. Washington (DC).

Fujimoto M, Wada A, Saeki E, Watanabe A, Hitomi Y. (1988). A study on the unbonded brace encased in buckling restraining concrete and steel tube, *Journal of Structural and Construction Engineering*; **34**: 249–58.

Güneyisi EM. (2012). Seismic reliability of steel moment resisting framed buildings retrofitted with buckling restrained braces, *Earthquake engineering and structure dynamics*; **41**: 853-874.

Hisatoku T. Reanalysis and repair of a high-rise steel building damaged by the 1995 Hyogoken-Nanbu earthquake. Proceedings, 64th Annual Convention, Structural

Engineers Association of California, Structural Engineers Assn. of California, Sacramento, CA, 1995, pages 21-40.

Inoue K, Sawaizumi S, Higashibata Y (1992). Bracing design criteria of the reinforced concrete panel including unbonded steel diagonal braces. *Journal of Structural and Construction Engineering, Architectural Institute of Japan*; **432:**41–9.

Inoue K, Sawaizumi S, Higashibata Y (1993). Stiffening design at the edge of the reinforced concrete panel including unbonded steel diagonal braces. *Journal of Structural and Construction Engineering, Architectural Institute of Japan*; **443**:137–46.

Inoue K, Sawaizumi S, Higashibata Y. (2001). Stiffening requirements for unbonded braces encased in concrete panels. *Journal of Structural Engineering*, ASCE;**127**(6):712–9.

Iwata M, Kato T, Wada A. Buckling-restrained braces as hysteretic dampers. Proceeding of Behavior of Steel Structures in Seismic Areas. Rotterdam: Balkema; 2000.

Jain AK, Goel SC, Hanson RD. (1980). Hysteretic cycles of axially loaded steel members. *J. Struct Div ASCE*; **106** (ST8):1777–1795

Kalyanaraman V, Mahadevan K, Thairani V. (1988b). Core loaded earthquake resistant bracing system. *Journal of Constructional Steel Research*; **46**(1–3):437–9.

Kalyanaraman V, Ramachandran B, Prasad BK, Sridhara BN. Analytical study of sleeved column buckling resistant braced system. In: SEAOC Convention Proceedings. 2003. p. 713–20.

Kalyanaraman V, Sridhara BN, Mahadevan K. Sleeved column systems. In: SSRC 50th anniversary conference. Lehigh University. 1994.

Kalyanaraman V, Sridhara BN, Ramachandran B. (1988a). A sleeved bracing system for earthquake resistant design of tall buildings. In: Proceedings of the 11th symposium on earthquake engineering. University of Roorkee; 1998. p. 713–20.

Kim H, Goel S. Seismic evaluation and upgrading of braced frame structures for potential local failures. UMCEE 92-24, Dept. of Civil Engineering and Environmental Engineering, Univ. of Michigan, Ann Arbor, Oct. 1992, p.290.

Kim J., Choi H. (2005) Response modification factors of chevron-braced frames. *Journal of Engineering Structures*; **27**:285–300.

Kim Jinkoo, Lee Y., Choi H. (2011). Progressive collapse resisting capacity of braced frames. *The structural design of tall and special buildings*; **20**:257-270

Kimura, Yoshioka K, Takeda, Fukuya Z, Takemoto K. Tests on braces encased by mortar in-filled steel tubes. Summaries of technical papers of annual meeting. Architectural Institute of Japan; 1976. p. 1041– 2 (in Japanese).

Krawinkler H, et al. Northridge earthquake of January 17, 1994: reconnaissance report, Vol. 2—steel buildings. Earthquake Spectra, 11, Suppl. C, Jan. 1996, p.25-47.

Kumar G. R., Kumar S. R. S., Kalyanaraman V. (2007). Behavior of frames with non-buckling bracings under earthquake loading, *Journal of constructional steel research*; **63**: 254-262.

Kumar GR, Kumar SRS, Kalyanaraman V. (2007). Behaviour of frames with Non Buckling bracings under earthquake loading. *Journal of Constructional Steel Research*; **63**(2):254–262.

Lin KC, Lin CCJ, Chen JY, Chang HY. (2010). Seismic reliability of steel framed buildings, *Structural Safety*; **32**(3):174–182.

Mahin SA. (1998). Lessons from damage to steel buildings during the Northridge earthquake, *Engineering Structures*; **20**(4):261–270.

Mahmoudi M , Zaree M (2010). Evaluating response modification factors of concentrically braced steel frames, *Journal of constructional steel research*; 66:1196-1204.

Martinelli, Mulas MG, Perotti F. (1998). The seismic behavior of steel moment resisting frames with stiffening braces. *Journal of Engineering Structures*; **20**(12):1045–62.

Mochizuki S, Murata Y, Andou N, Takahashi S. Experimental study on buckling of unbonded braces under axial forces: Parts 1 and 2. Summaries of technical papers of annual meeting. Architectural Institute of Japan; 1979. p. 1623–6 (in Japanese).

Mochizuki S, Murata Y, Andou N, Takahashi S. Experimental study on buckling of unbonded braces under axial forces: Part 3. Summaries of technical papers of annual meeting. Architectural Institute of Japan; 1980. p. 1913–4 (in Japanese).

Mochizuki S, Murata Y, Andou N, Takahashi S. Experimental study on buckling of unbonded braces under axial forces: Part 4. Summaries of technical papers of annual meeting. Architectural Institute of Japan; 1982. p. 2263–4 (in Japanese).

Naeim F, Kelly JM. Design of seismic isolated structures: From theory to practice. New York: John Wiley & Sons Inc.; 1999.

Naeim F, Lew M, Huang CH, Lam HK, Carpenter LD. (2000). The performance of tall buildings during the 21 September 1999 Chi-Chi earthquake Taiwan. *The Structural Design of Tall Buildings*; **9**(2):137–160.

Nagao T, Mikuriya K, Matsumoto Y, Takahashi S. An experimental study on the elasto-plastic behavior of unbonded composite bracing (part 1–4). Summaries of technical papers of annual meeting, vol. II. Architectural Institute of Japan, Structural Engineering Section; 1988. p. 1329–36 (in Japanese).

Nagao T, Mikuriya K, Takahashi S, Yuki S. An experimental study on the elasto-plastic behavior of unbonded composite bracing (part 5–7). Summaries of technical papers of annual meeting, vol. II. Architectural Institute of Japan, Structural Engineering Section; 1989. p. 1501–6 (in Japanese).

Nagao T, Sera S, Nakamura S, Ouchi H, Otani K, Fukutajima K. A study on the RC encased H-section steel brace (part 1. general description, part 2 results and discussion). Summaries of technical papers of annual meeting, vol. II. Architectural Institute of Japan. Structural Engineering Section; 1992. p. 1773–6 (in Japanese).

Nagao T, Takahashi S. (1990). A study on the elasto-plastic behavior of unbonded composite bracing (part 1 experiments on isolated members under cyclic loading).

Journal of Structural and Construction Engineering, Architectural Institute of Japan;**415**:105–15.

Nagao T, Takahashi S. (1991). A study on the elasto-plastic behavior of unbonded composite bracing (part 2 analytical studies). *Journal of Structural and Construction Engineering, Architectural Institute of Japan*;**422**:45–56.

Nakashima, Inoue K, Tada M. (1998) Classification of damage to steel buildings observed in the 1995 Hyogoken-Nanbu earthquake. *Engineering Structures*; **20**(4–6):271–281.

Nakashima, Inoue K, Tada M. (1998). Classification of damage to steel buildings observed in the 1995 Hyogoken-Nanbu earthquake. *Engineering Structures*; **20**(4–6):271–281.

Nakashima, Roeder CW, Maruoka Y. (2000). Steel moment frames for earthquakes in United States and Japan. *Journal of Structural Engineering*, ASCE;**126**(8):861–8.

Osteraas J, Krawinkler H. (1989). The Mexico earthquake of September 19, 1985 behavior of steel buildings. *Earthquake Spectra*; **5**(1):51–88.

Qiang X. (2005). State of the art of buckling-restrained braces in Asia. *Journal of Constructional Steel Research*; **61**:727–748.

Rai DC, Goel SC. (2003) Seismic evaluation and upgrading of chevron braced frames, *Journal of Constructional Steel Research*;**59**(8):971_94.

Ren Ch.C., Ou J.P., and Jia J.F. (2008), "Fuzzy Seismic Damage Assessment of Steel Frame Structures with Buckling Restrained Braces under Near-field Ground Motions," *The 14Th World Conference on Earthquake Engineering*, Beijing, China.

Ronald O. H., Helmut K., James O. M., Scott M. A., NEHRP seismic design technical brief No.2, seismic design of steel special moment frames, national institute of standards and technology (NIST) June 2009.

Sabelli R., Mahin S., Chang C. (2003). Seismic demands on steel braced frame buildings with buckling restrained braces. *Journal of Engineering structures*; **25**:655-666.

Saeki E, Maeda Y, Nakamura H, Midorikawa M, Wada A. (1995) Experimental study on practical-scale unbonded braces. *J Struct Constr Eng AIJ*; **476**:149–58.

SEAOC (Structural Engineers Association of California) (1999). Recommended Lateral Force Requirements and Commentary. seventh edition. Sacramento, California.

Sermin O. (2005). Evaluation of pushover analysis procedures for frame structures, Msc Thesis submitted to the graduate school of natural and applied sciences of Middle East Technical University, Ankara.

Soong TT, Dargush. Passive energy dissipation systems in structural engineering. Chichester (UK): John Wiley & Sons; 1998.

Takeda T, Kimura Experimental study on precast concrete shear walls — Part 6. Summaries of technical papers of annual meeting. Architectural Institute of Japan; 1979. p. 1677–8 (in Japanese).

Tirca L and Tremblay R (2004), "Influence of building height and ground motion type on the seismic behavior of zipper concentrically braced steel frames," 13th World Conference on Earthquake Engineering, Vancouver, B.C., Canada; Paper No. 2894.

Tirca LD., Foti D., Diaferio M. (2003). Response of middle-rise steel frames with and without passive dampers to near-field ground motions. *Journal of Engineering Structures*; **25**:169-179.

Tremblay R et al. (1995). Performance of steel structures during the 1994 Northridge earthquake. *Canadian Journal of Civil Engineering*; **22**(2):338–360.

Tremblay R et al. (1996). Seismic design of steel buildings: lessons from the 1995 Hyogo-ken Nanbu earthquake. *Canadian Journal of Civil Engineering*; **23**(3):727–756.

Tremblay R. (2002). Inelastic seismic response of steel bracing members. *Journal of Constructional Steel Research*; **58**(5–8):665–701.

Wakabayashi M, Nakamura T, Katagihara A, Yogoyama H, Morisono T (1973a). Experimental study on the elastoplastic behavior of braces enclosed by precast concrete panels under horizontal cyclic loading—Parts 1 & 2. Summaries of technical papers of annual meeting, vol. 10. Architectural Institute of Japan, Structural Engineering Section. p. 1041–4 (in Japanese).

Wakabayashi M, Nakamura T, Katagihara A, Yogoyama H, Morisono T (1973b). Experimental study on the elastoplastic behavior of braces enclosed by precast concrete panels under horizontal cyclic loading—Parts 1 & 2. Summaries of technical papers of annual meeting, vol. 6. Kinki Branch of the Architectural Institute of Japan. p. 121–128 (in Japanese).

Walterio A. López, S.E. (2008). On Designing with Buckling-Restrained Braced Frames STRUCTURE MAGAZINE. Available at: http://www.structuremag.org/ Archives /2008-7/C-InSights-Lopez-July08.pdf.

Watanabe A, Hitomi Y, Saeki E, Wada A, Fujimoto M. (1988a) Properties of brace encased in buckling-restraining concrete and steel tube. In: Proc. of ninth world conf. on earthquake eng, vol. IV. p. 719–724.

Watanabe E, Sugiura K, Nagata K, Kitane Y. (1998b) Performances and damages to steel structures during 1995 Hyogoken-Nanbu earthquake. *Engineering Structures*; **20**(4–6):282–290.

Yamaguchi M, et al. Earthquake resistant performance of moment resistant steel frames with damper. Proceeding of Behavior of Steel Structures in Seismic Areas. Rotterdam: Balkema; 2000.

Yoshino T, Karino Y. Experimental study on shear wall with braces: Part 2. Summaries of technical papers of annual meeting, vol. 11. Architectural Institute of Japan, Structural Engineering Section; 1971. p. 403–4 (in Japanese).

Youssef N, Bonowitz D, Gross J. A survey of steel moment-resisting frame buildings affected by the 1994 Northridge earthquake. Research report no. NISTIR 5625. Gaithersburg (MD, USA): National Institute of Science and Technology (NIST); 1995.

APPENDIX

The governing equation of an inelastic SDOF system is as follows:

$$m\ddot{u} + c\dot{u} + f_s(u, \dot{u}) = -m\ddot{u}_g \qquad (A-1)$$

where m is the mass, c is the viscous damping constant, and $f_s(u, \dot{u})$ is the resisting force of an elasto-plastic SDOF system as shown in Figure A-1.
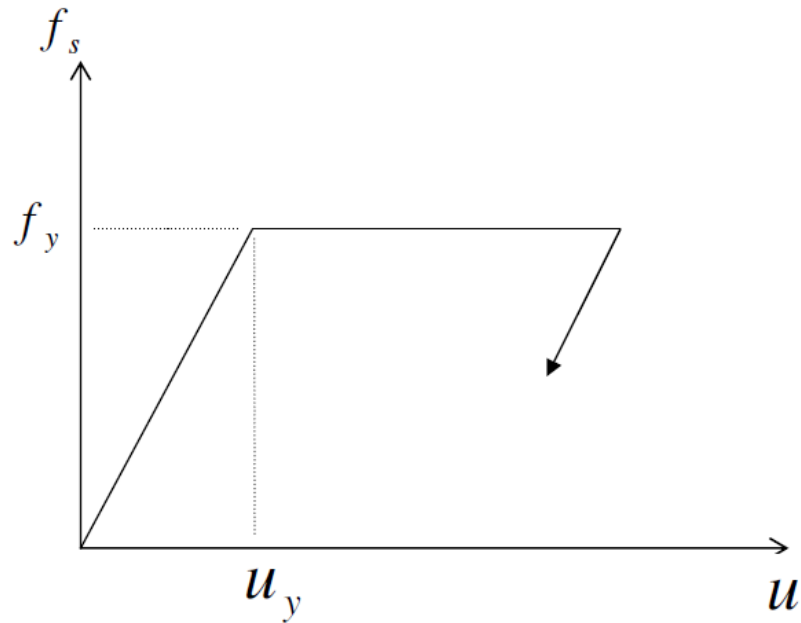
Figure A-1 Typical elasto-plastic system

In general, for a given $\ddot{u}_g$, $u(t)$ depends on ω_n, ξ, u_y and the form of the force deformation relation. If eq. (A-1) is divided by m one can obtain:

$$\ddot{u} + 2\xi\omega_n\dot{u} + \omega_n{}^2 u_y \tilde{f}_s(u, \dot{u}) = -\ddot{u}_g(t) \qquad (A-2)$$

$$\omega_n = \sqrt{\frac{k}{m}}, \qquad \xi = \frac{c}{2m\omega_n}, \qquad \tilde{f}_s(u,\dot{u}) = \frac{f_s(u,\dot{u})}{f_y} \qquad\qquad (A\text{-}3)$$

The function $\tilde{f}_s(u,\dot{u})$ describes the force-deformation relation in a partially dimensionless form as shown in Figure A-2.
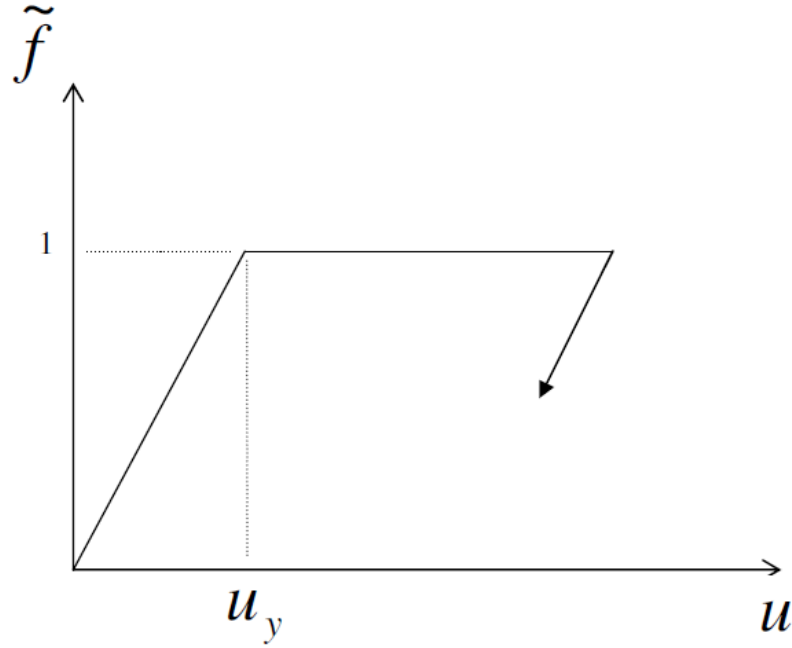
Figure A-2 Force deformation relation in normalised form

Furthermore, for a given $\ddot{u}_g$, the ductility factor μ depends on $\omega_n, \xi, \bar{f}_y$ where $\bar{f}_y$ is the normalized yield strength of the elasto-plastic system defined as:

$$\bar{f}_y = \frac{f_y}{f_e} = \frac{u_y}{u_e} \qquad\qquad (A\text{-}4)$$

where f_e and u_e are the elastic strength and displacement of the corresponding linear SDOF system. The procedure for this proof is as follows. Equation (A-2) is rewritten In term of $\mu(t) = \frac{u(t)}{u_y}$. Therefore, substituting for $u(t) = u_y \mu(t)$, $\dot{u}(t) = u_y \dot{\mu}(t)$, and $\ddot{u}(t) = u_y \ddot{\mu}(t)$ into equation (A-2) and dividing by u_y, yields:

$$\ddot{\mu} + 2\xi\omega_n\dot{\mu} + \omega_n{}^2\tilde{f}_s(\mu,\dot{\mu}) = -\omega_n{}^2\frac{\ddot{u}_g(t)}{a_y} \tag{A-5}$$

where $a_y = \frac{f_y}{m}$ can be interpreted as the acceleration of the mass necessary to produce the yield force f_y, and $\tilde{f}_s(\mu,\dot{\mu})$ is the force-deformation relationship in dimensionless form (Figure A-3).
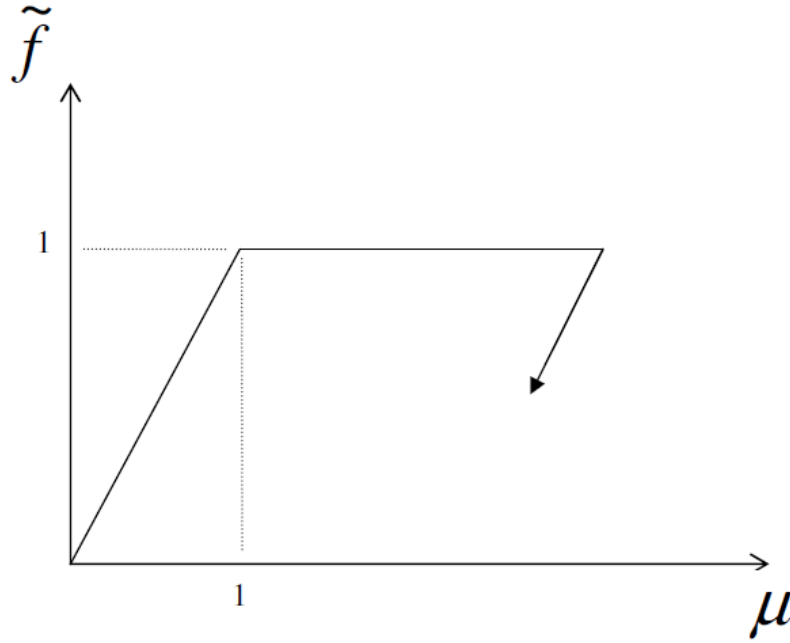
Figure A-3 Force deformation relation in normalized form

Equation A-5 shows that for a given $\ddot{u}_g$ and for a given $\tilde{f}_s(\mu,\dot{\mu})$ relationship, $\mu(t)$ depends on ω_n, ξ, a_y. In turn a_y depends on ω_n, ξ.

Appendix B: Interstorey drift time history
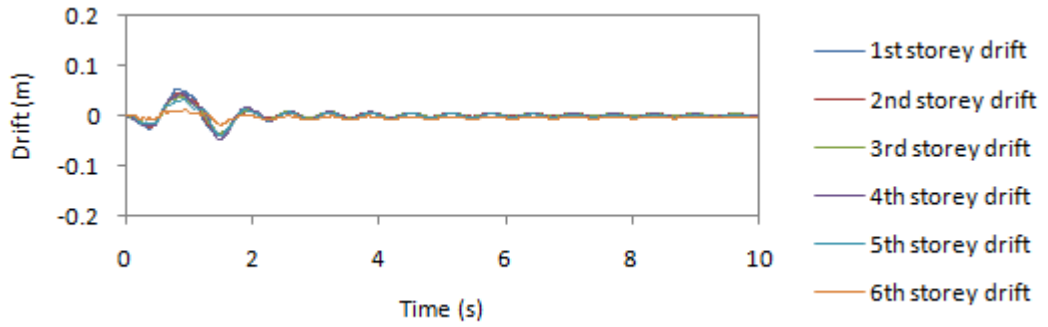
Figure B-1 Storey drift time history of OMRF-Tp1.4-BRB-conf-1
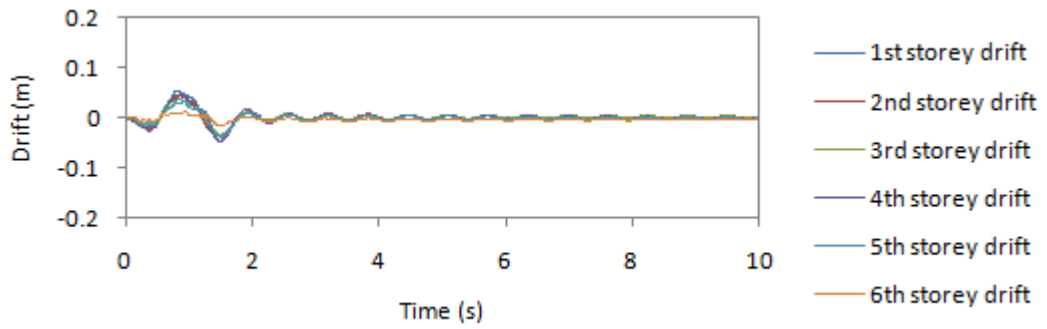
Figure B-2 Storey drift time history of OMRF-Tp1.4-BRB-conf-2
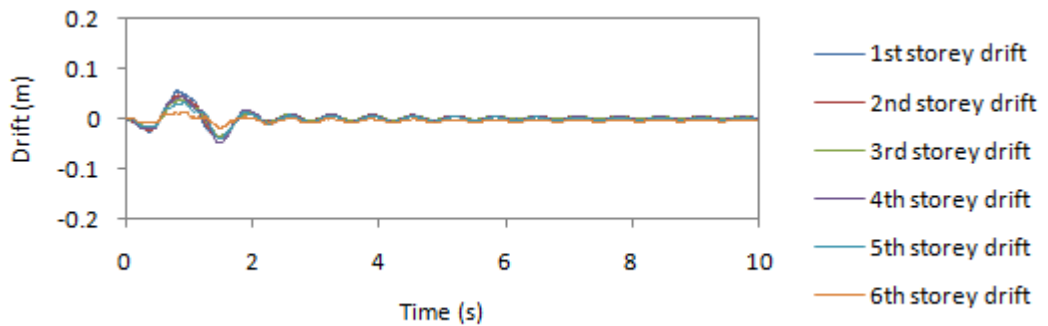
Figure B-3 Storey drift time history of OMRF-Tp1.4-BRB-conf-3
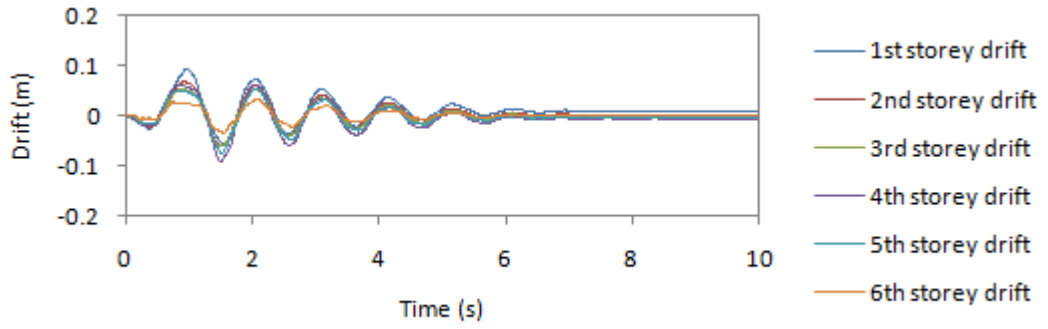
Figure B-4 Storey drift time history of OMRF-Tp1.4-CB-conf-1
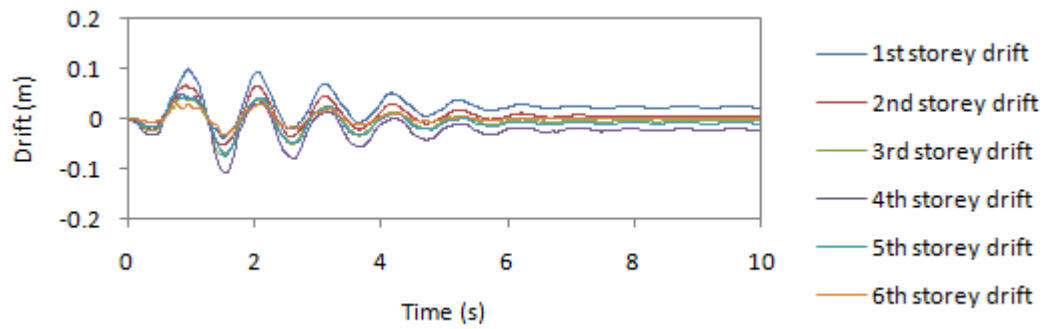
Figure B-5 Storey drift time history of OMRF-Tp1.4-CB-conf-2
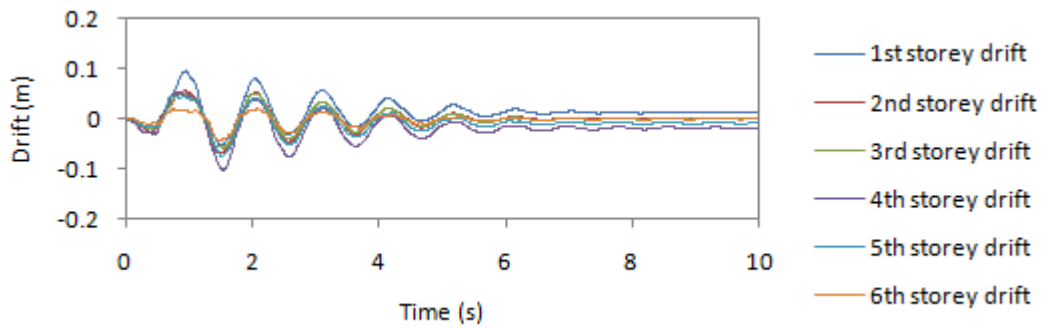
Figure B-6 Storey drift time history of OMRF-Tp1.4-CB-conf-3
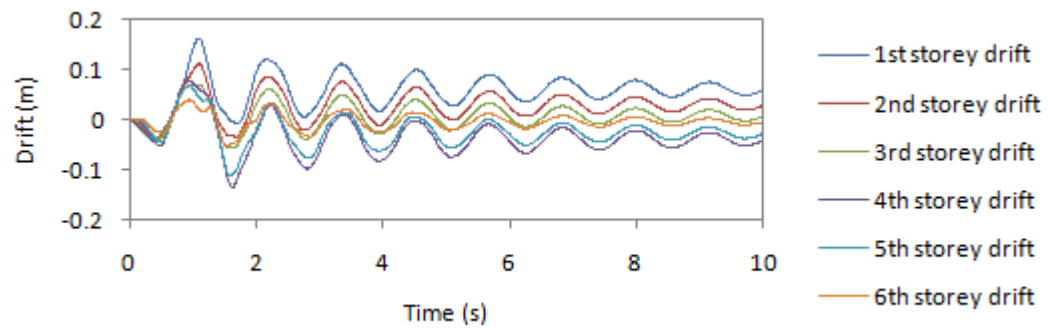
Figure B-7 Storey drift time history of OMRF-Tp1.4-UF
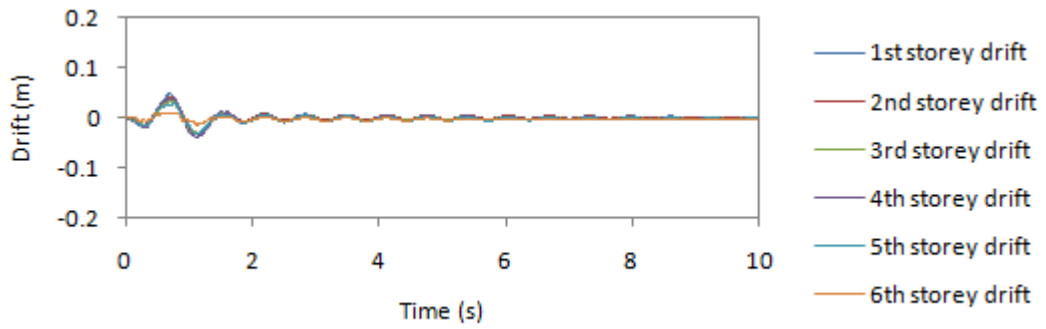
Figure B-8 Storey drift time history of OMRF-Tp0.9-BRB-conf-1
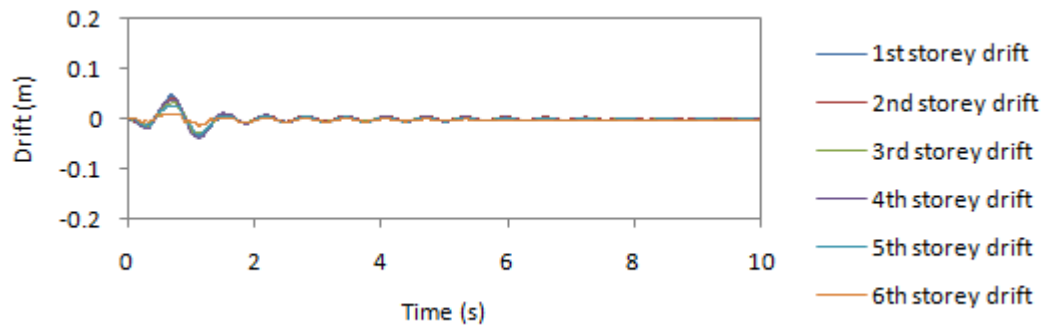
Figure B-9 Storey drift time history of OMRF-Tp0.9-BRB-conf-2
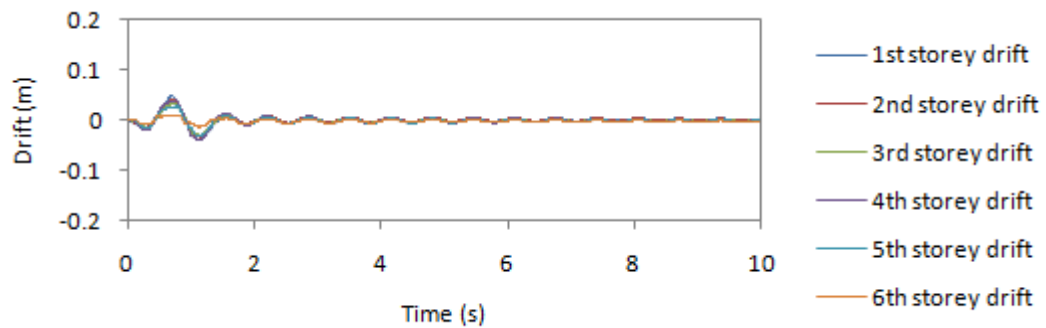
Figure B-10 Storey drift time history of OMRF-Tp0.9-BRB-conf-3
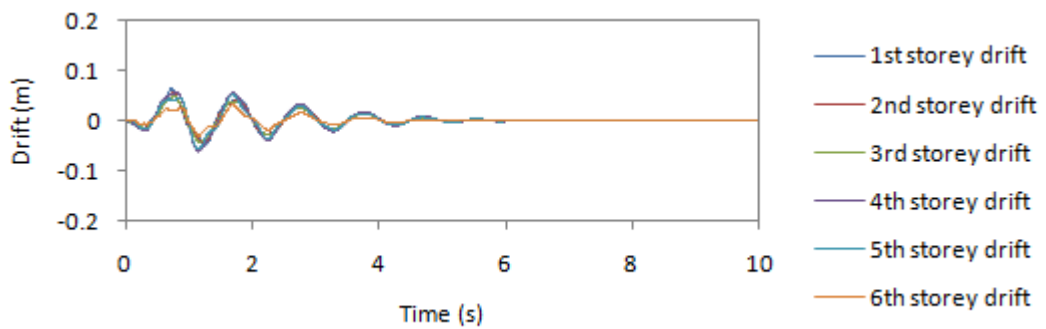
Figure B-11 Storey drift time history of OMRF-Tp0.9-CB-conf-1
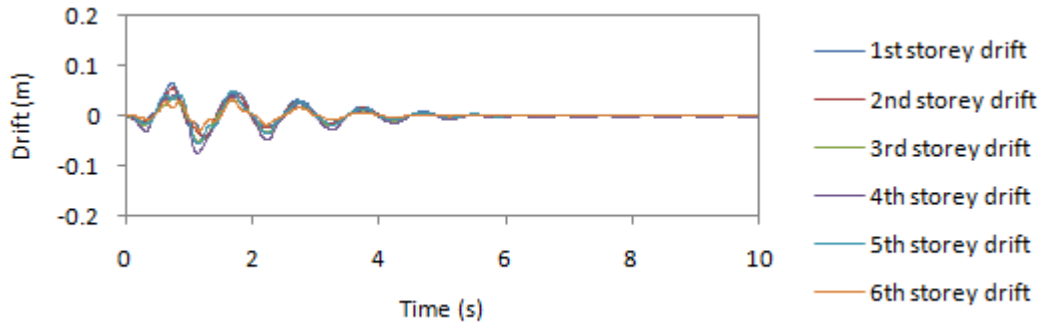
Figure B-12 Storey drift time history of OMRF-Tp0.9-CB-conf-2
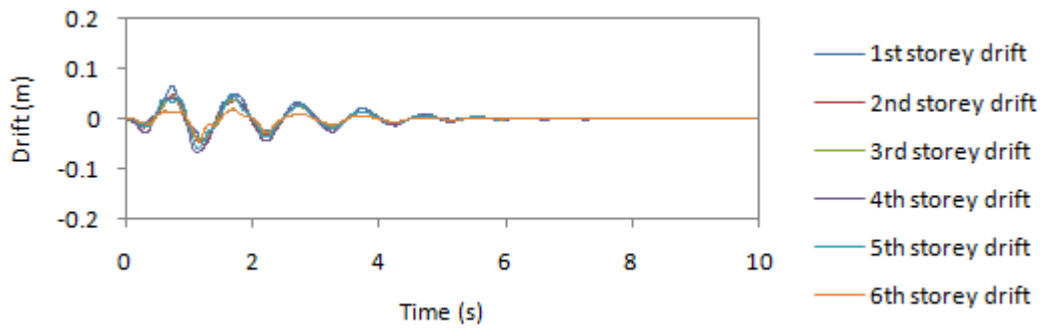
Figure B-13 Storey drift time history of OMRF-Tp0.9-CB-conf-3
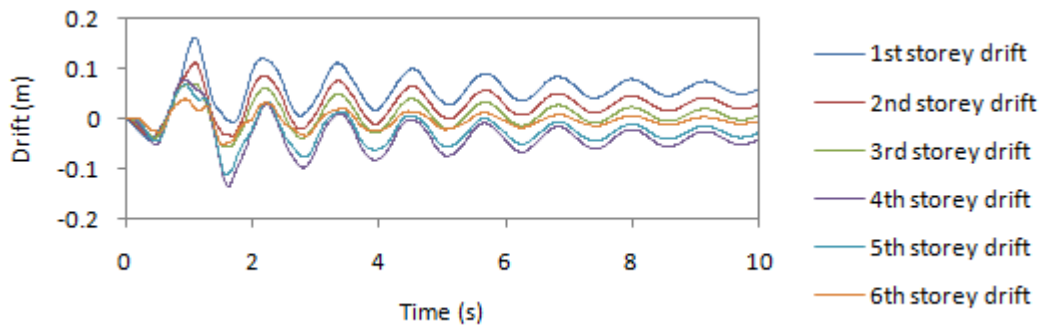
Figure B-14 Storey drift time history of OMRF-Tp0.9-Un
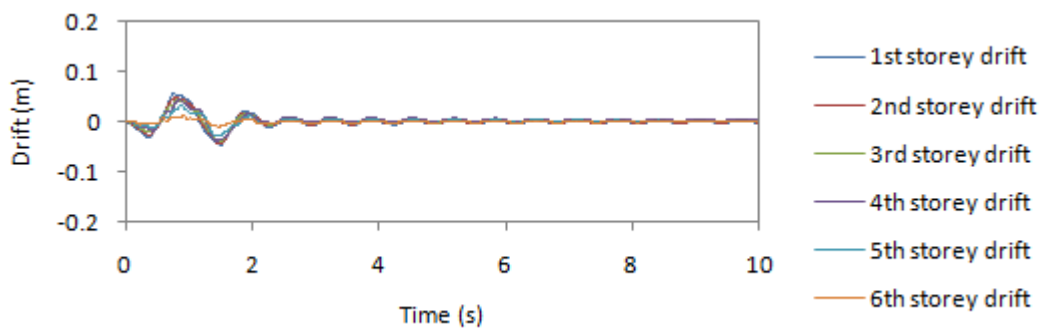
Figure B-15 Storey drift time history of SMRF-Tp1.4-BRB-conf-1
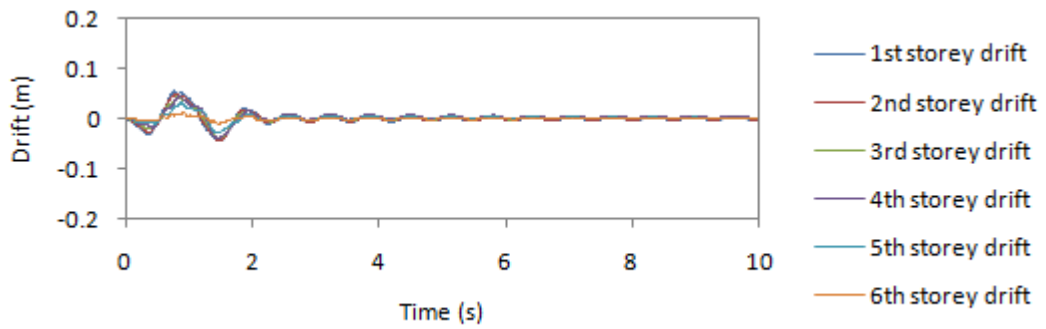
Figure B-16 Storey drift time history of SMRF-Tp1.4-BRB-conf-2
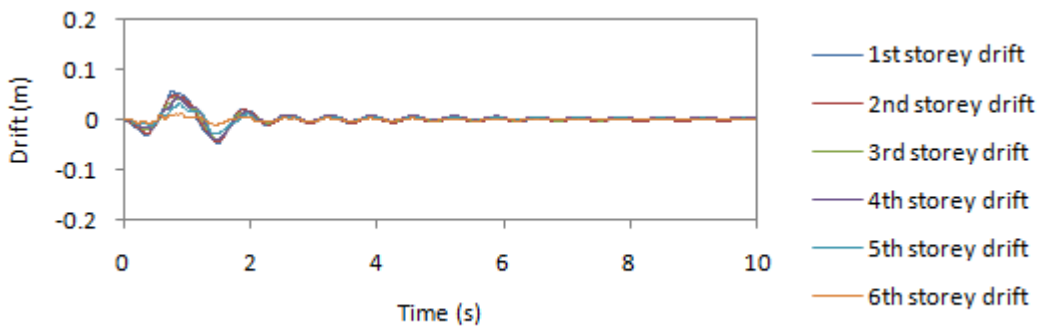
Figure B-17 Storey drift time history of SMRF-Tp1.4-BRB-conf-3
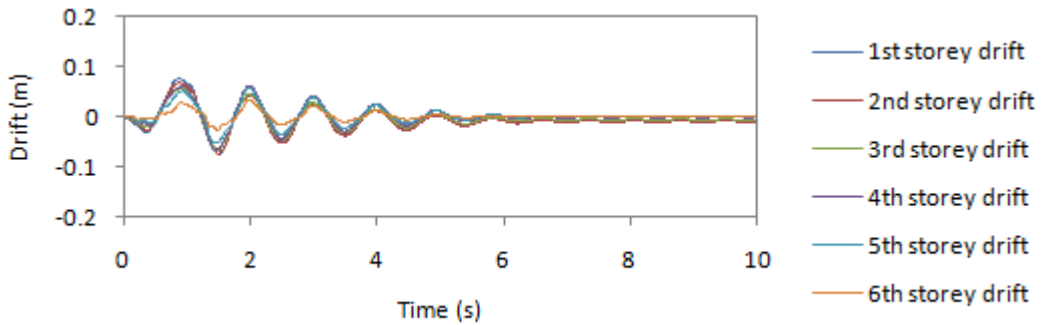
Figure B-18 Storey drift time history of SMRF-Tp1.4-CB-conf-1
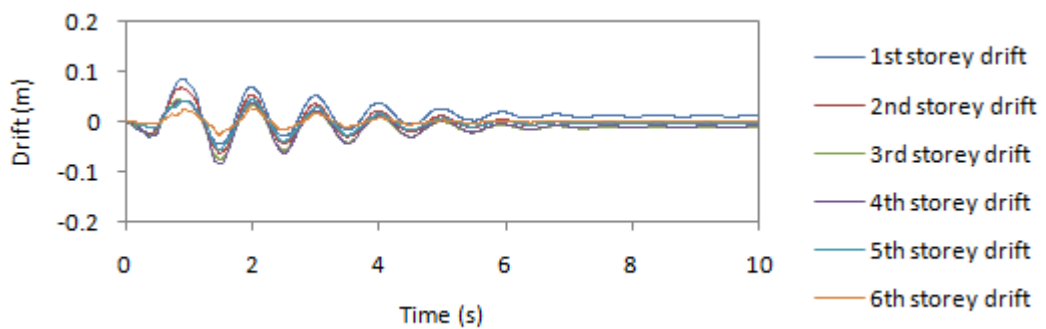
Figure B-19 Storey drift time history of SMRF-Tp1.4-CB-conf-2
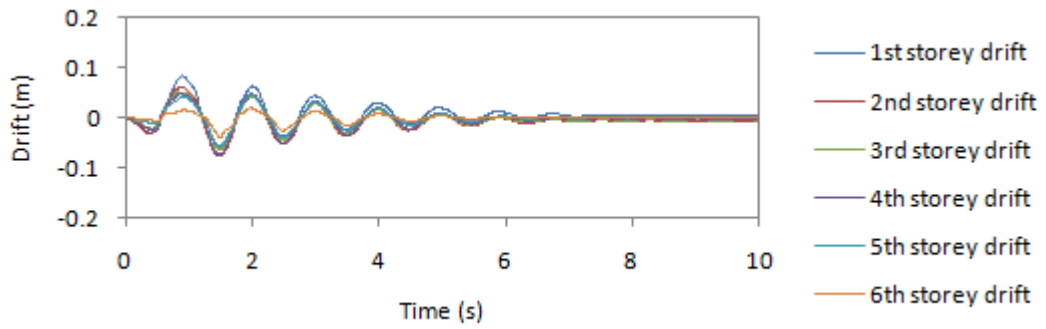
Figure B-20 Storey drift time history of SMRF-Tp1.4-CB-conf-3
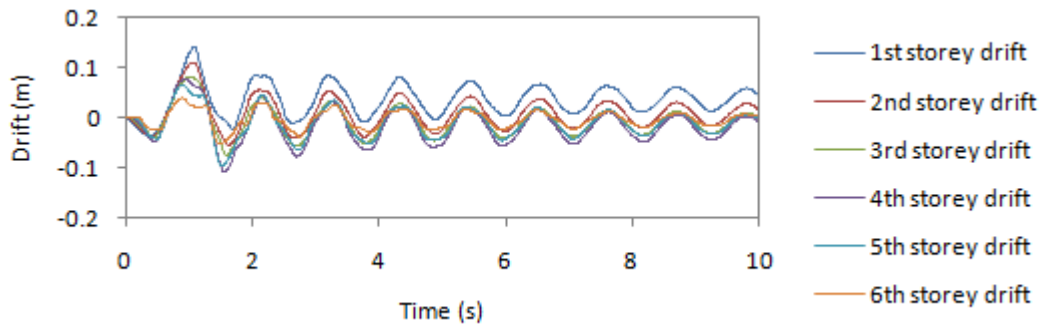
Figure B-21 Storey drift time history of SMRF-Tp1.4-UF
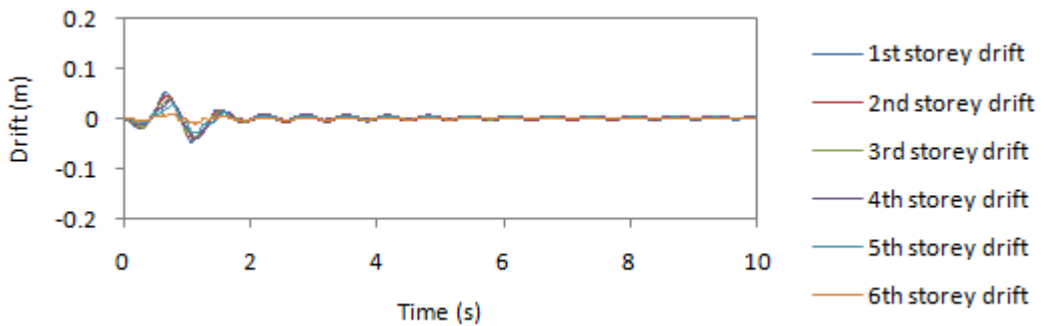
Figure B-22 Storey drift time history of SMRF-Tp0.9-BRB-conf-1
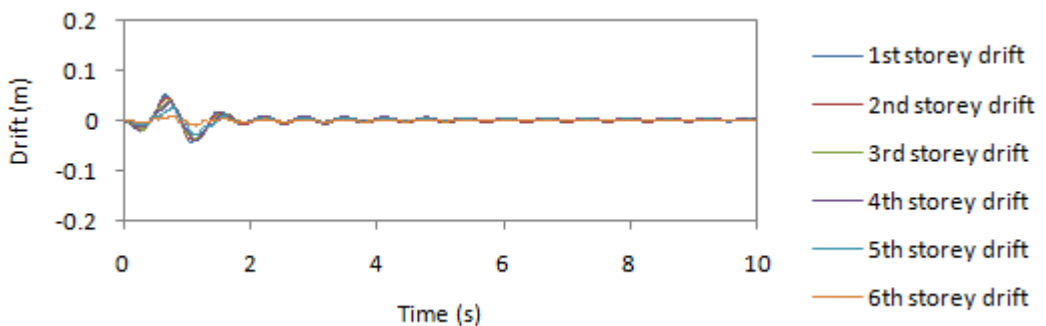
Figure B-23 Storey drift time history of SMRF-Tp0.9-BRB-conf-2
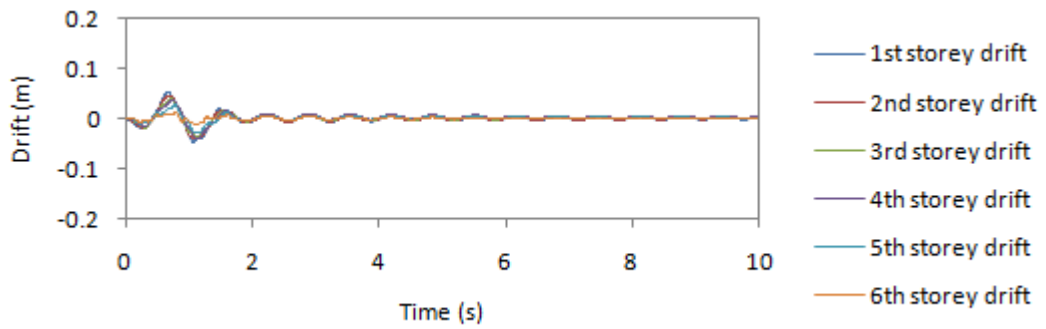
Figure B-24 Storey drift time history of SMRF-Tp0.9-BRB-conf-3
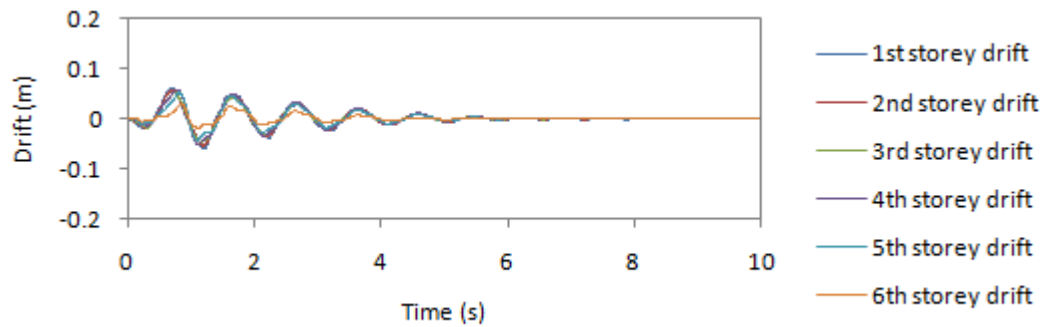
Figure B-25 Storey drift time history of SMRF-Tp0.9-CB-conf-1
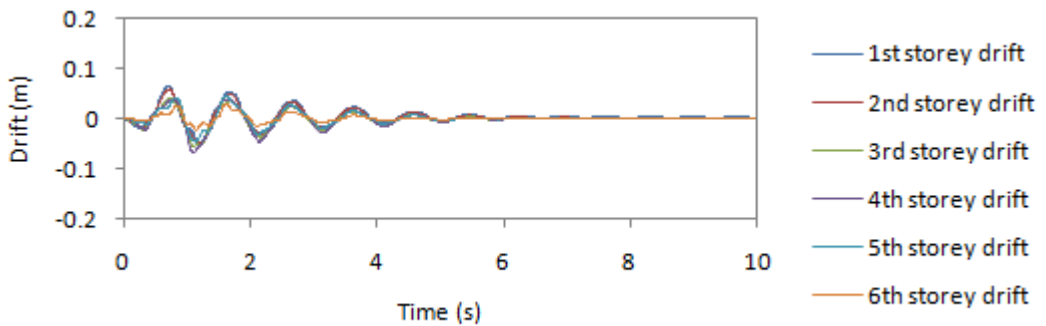
Figure B-26 Storey drift time history of SMRF-Tp0.9-CB-conf-2
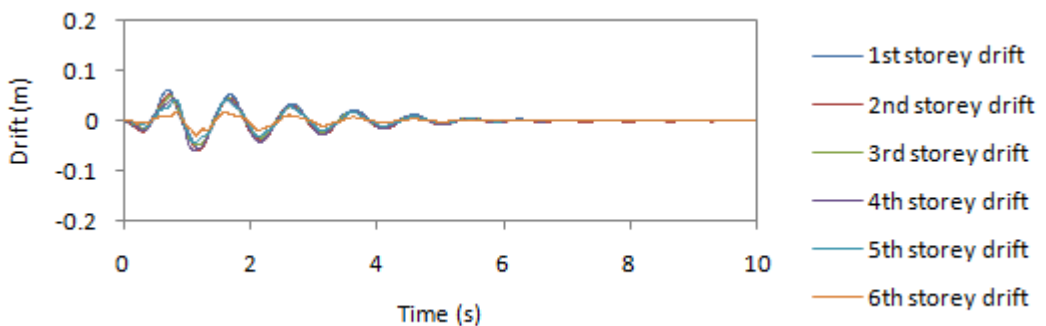
Figure B-27 Storey drift time history of SMRF-Tp0.9-CB-conf-3
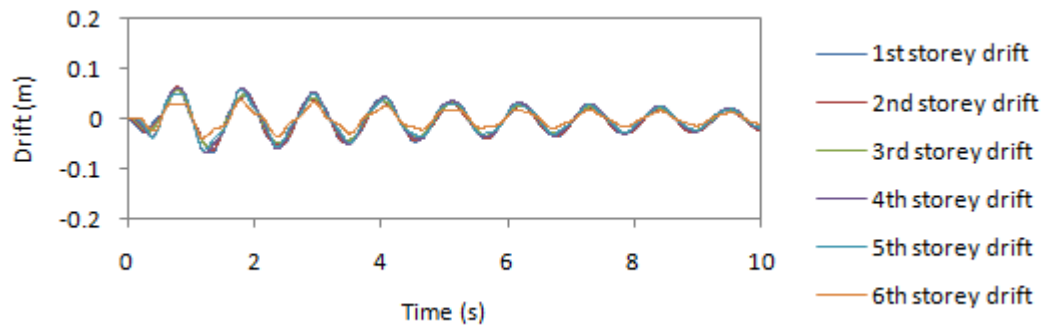
Figure B-28 Storey drift time history of SMRF-Tp0.9-UF

Appendix C: Roof displacement time history
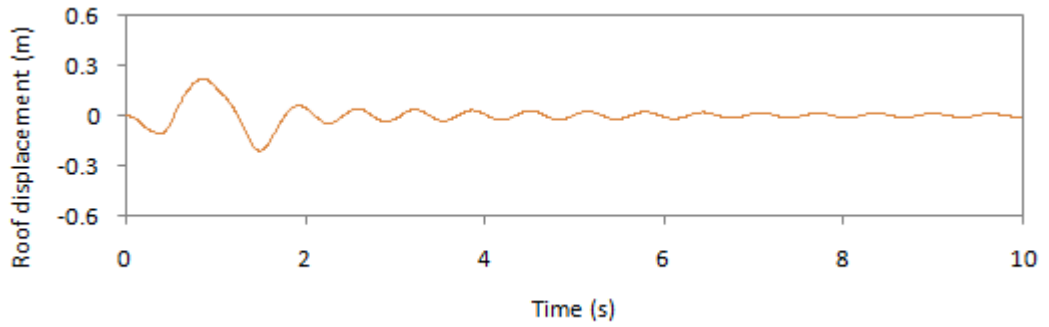
Figure C-1 Roof displacement time history of OMRF-Tp1.4-BRB-conf-1
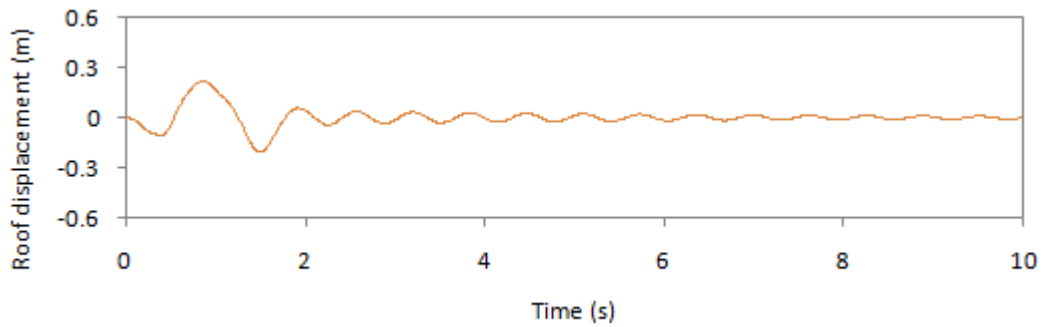
Figure C-2 Roof displacement time history of OMRF-Tp1.4-BRB-conf-2
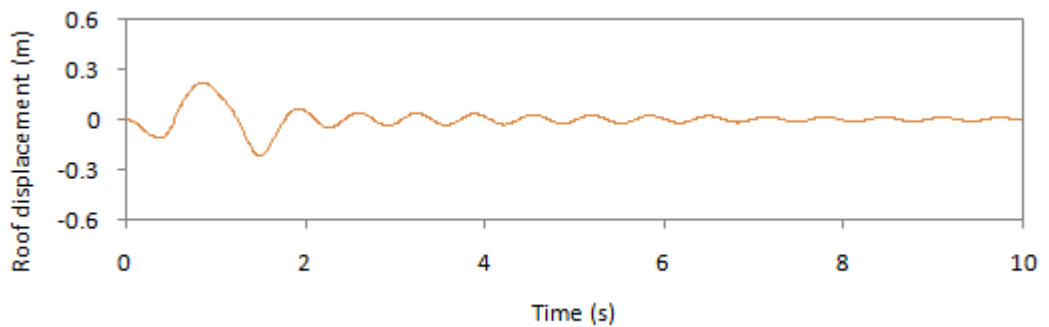
Figure C-3 Roof displacement time history of OMRF-Tp1.4-BRB-conf-3
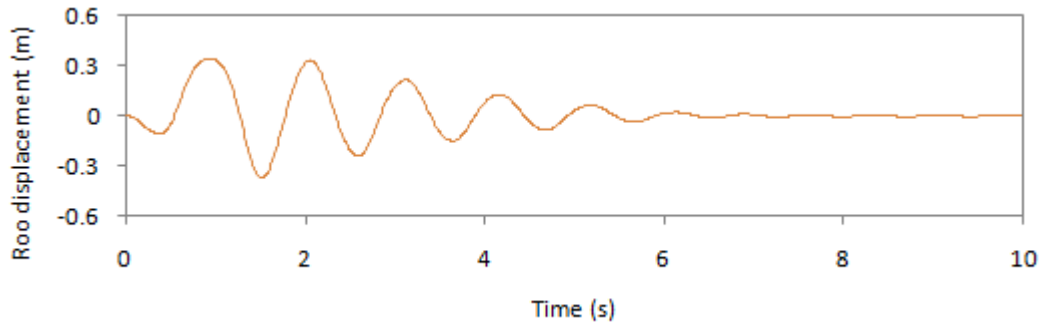
Figure C-4 Roof displacement time history of OMRF-Tp1.4-CB-conf-1
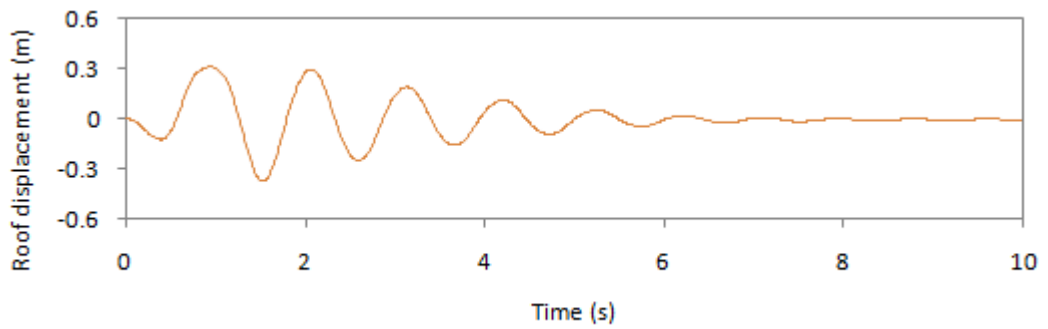
Figure C-5 Roof displacement time history of OMRF-Tp1.4-CB-conf-2
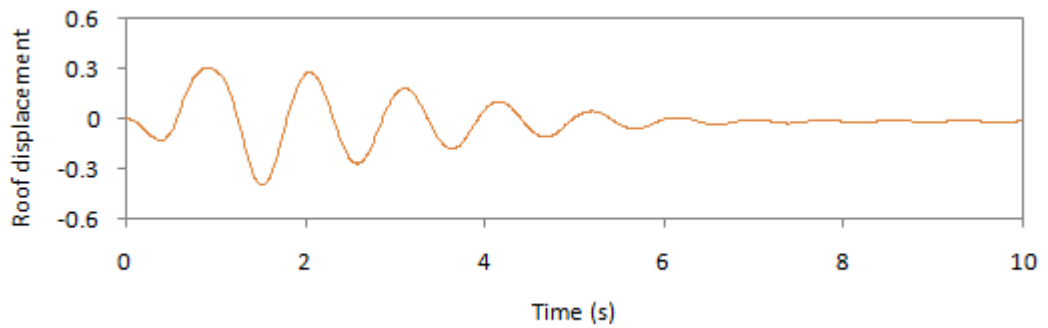
Figure C-6 Roof displacement time history of OMRF-Tp1.4-CB-conf-3
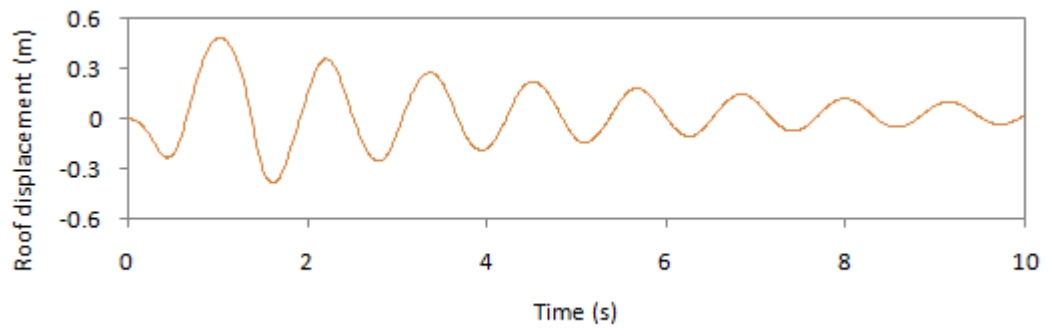
Figure C-7 Roof displacement time history of OMRF-Tp1.4-UF

107
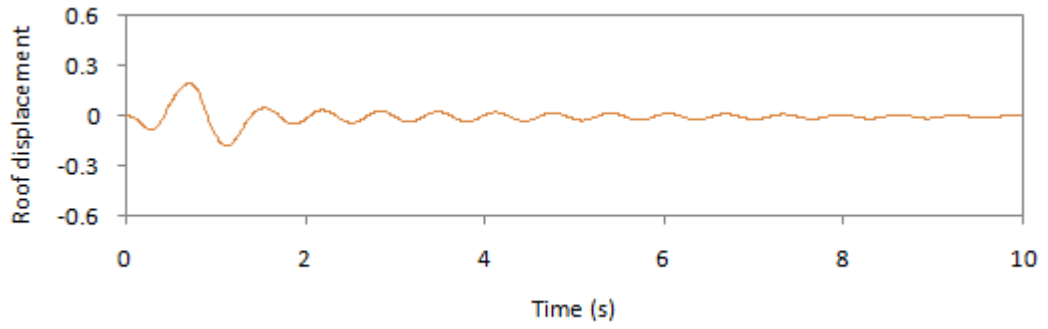
Figure C-8 Roof displacement time history of OMRF-Tp0.9-BRB-conf-1
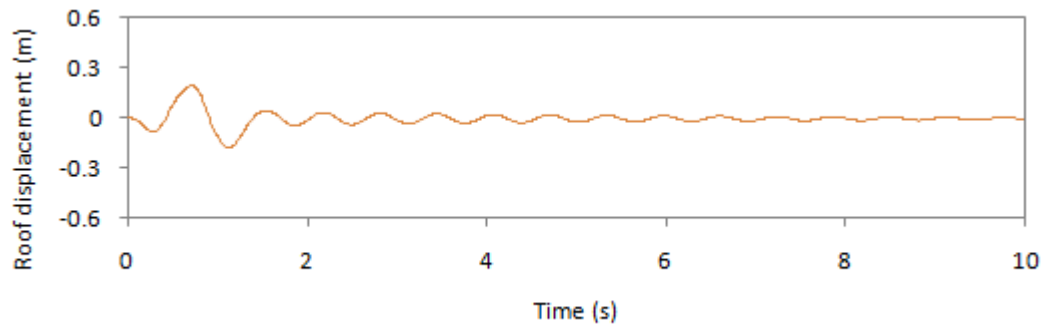
Figure C-9 Roof displacement time history of OMRF-Tp0.9-BRB-conf-2
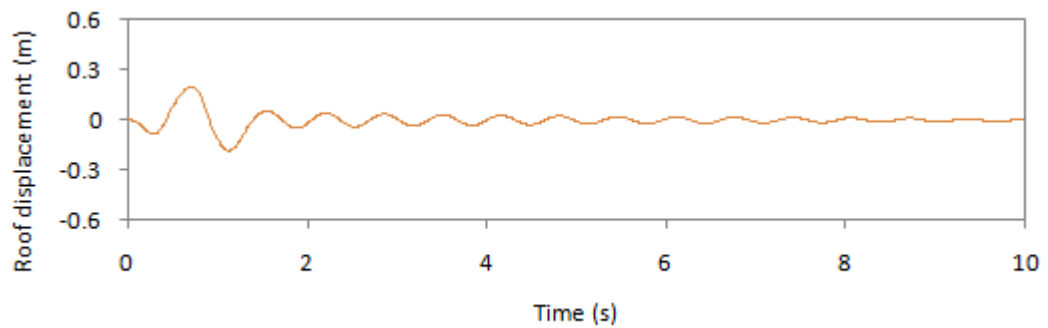
Figure C-10 Roof displacement time history of OMRF-Tp0.9-BRB-conf-3
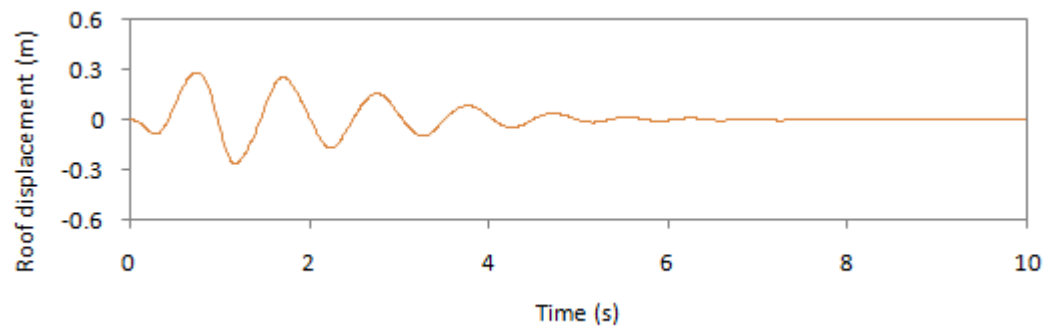
Figure C-11 Roof displacement time history of OMRF-Tp0.9-CB-conf-1
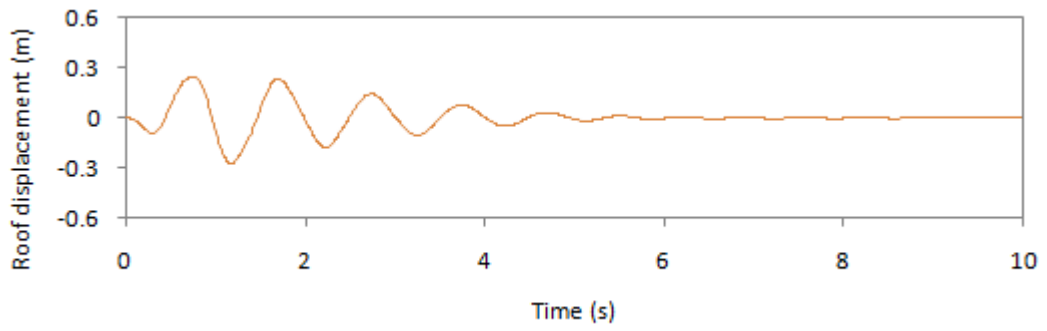
Figure C-12 Roof displacement time history of OMRF-Tp0.9-CB-conf-2
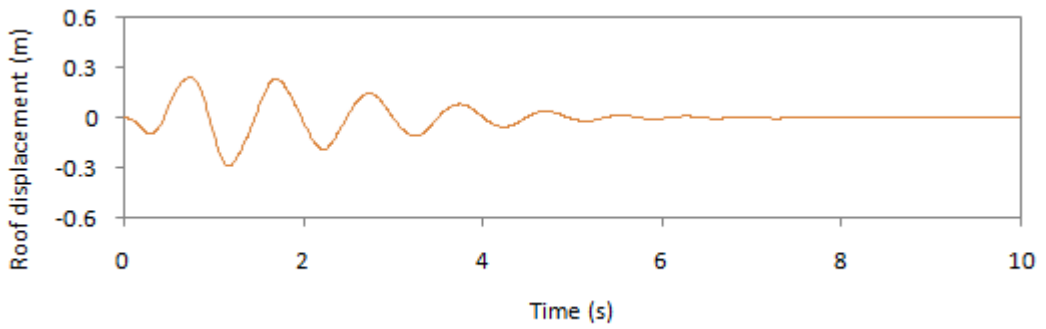
Figure C-13 Roof displacement time history of OMRF-Tp0.9-CB-conf-3
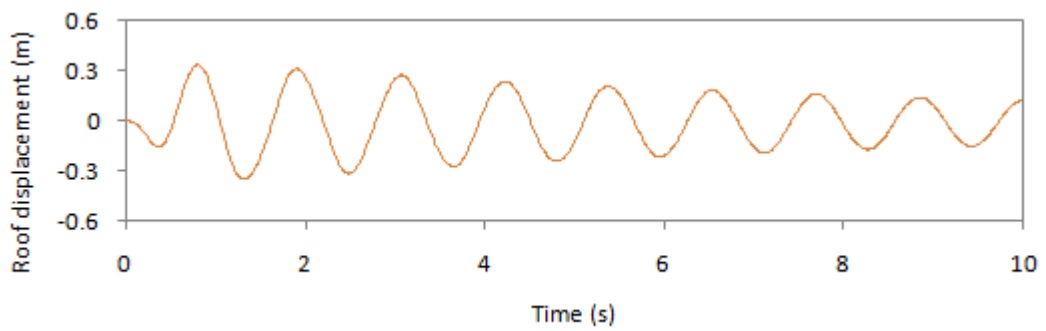
Figure C-14 Roof displacement time history of OMRF-Tp0.9-UF
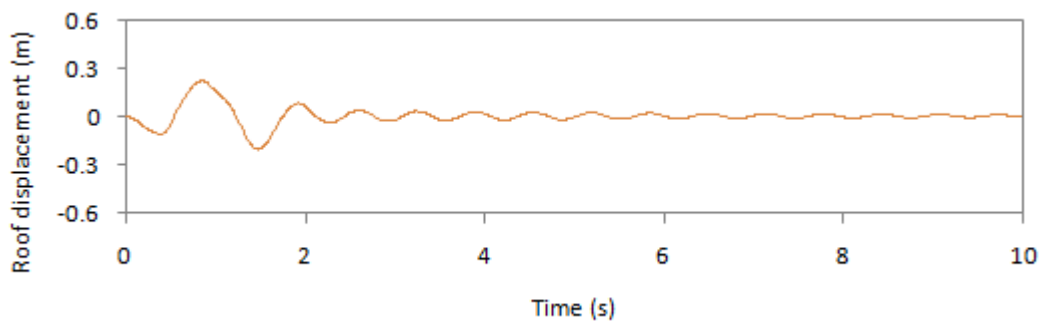
Figure C-15 Roof displacement time history of SMRF-Tp1.4-BRB-conf-1
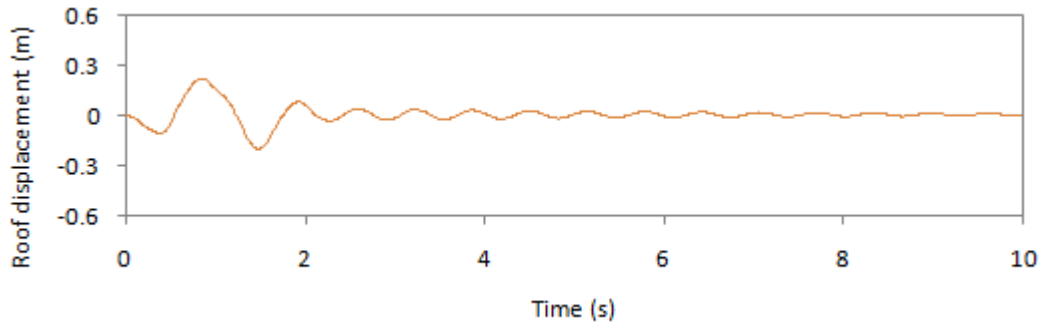
Figure C-16 Roof displacement time history of SMRF-Tp1.4-BRB-conf-2
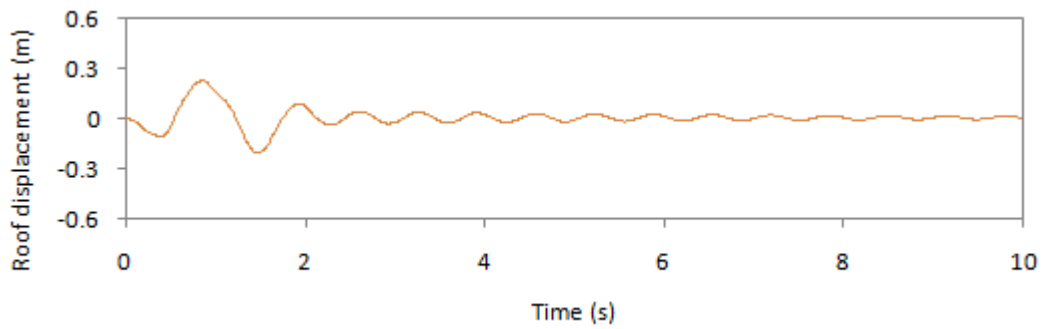
Figure C-17 Roof displacement time history of SMRF-Tp1.4-BRB-conf-3
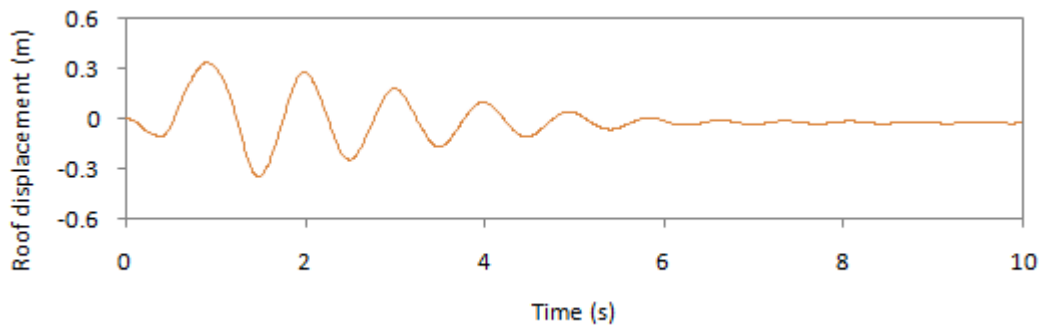
Figure C-18 Roof displacement time history of SMRF-Tp1.4-CB-conf-1
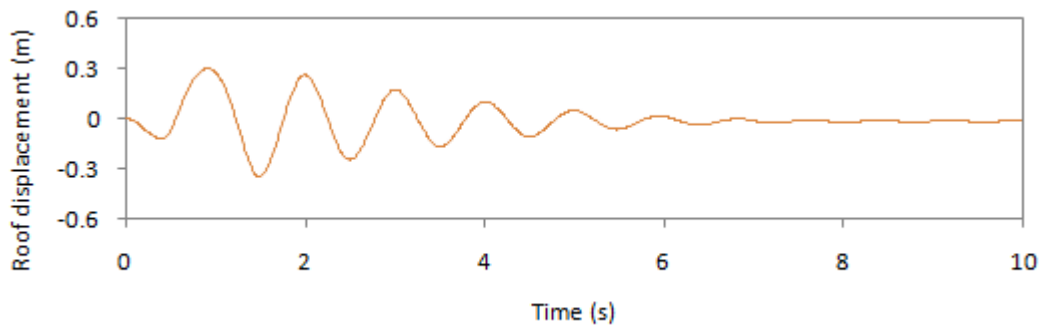
Figure C-19 Roof displacement time history of SMRF-Tp1.4-CB-conf-2
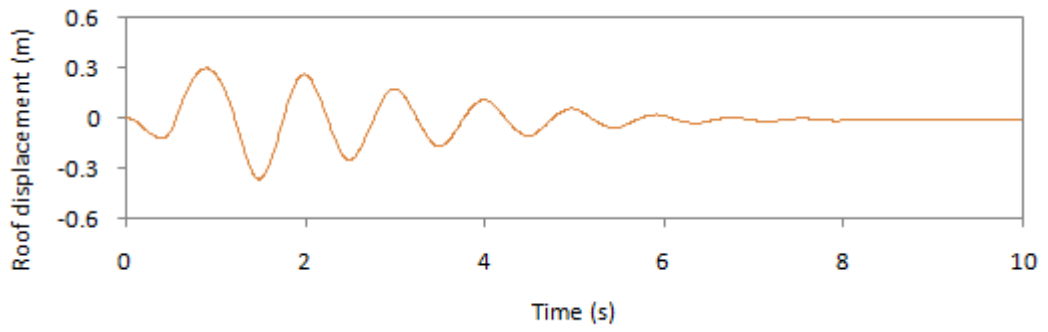
Figure C-20 Roof displacement time history of SMRF-Tp1.4-CB-conf-3
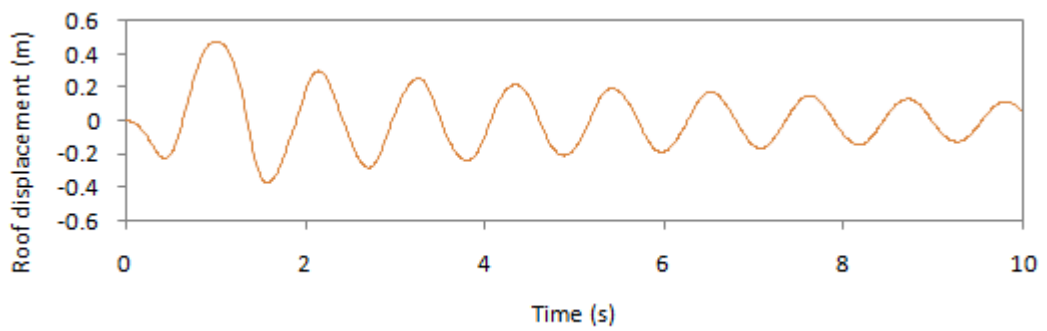
Figure C-21 Roof displacement time history of SMRF-Tp1.4-UF
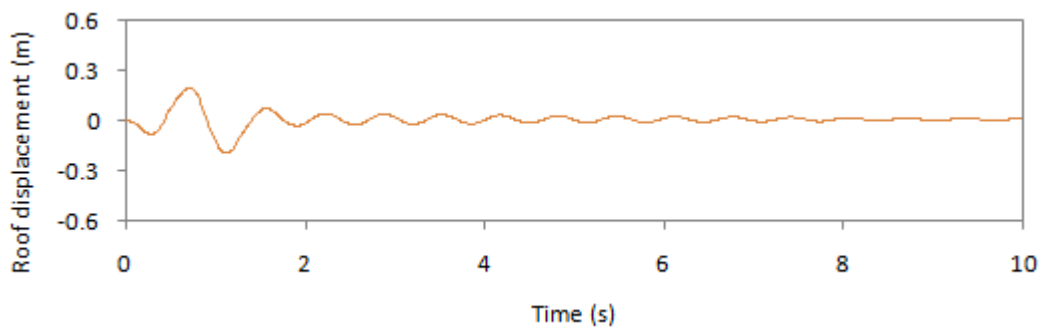
Figure C-22 Roof displacement time history of SMRF-Tp0.9-BRB-conf-1
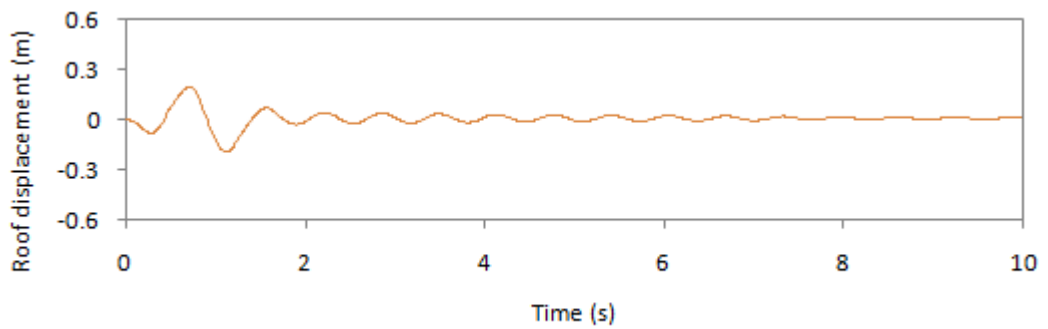
Figure C-23 Roof displacement time history of SMRF-Tp0.9-BRB-conf-2

111
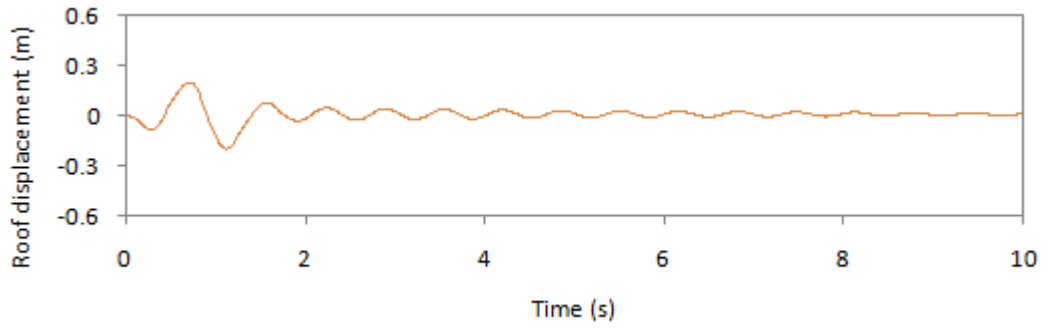
Figure C-24 Roof displacement time history of SMRF-Tp0.9-BRB-conf-3
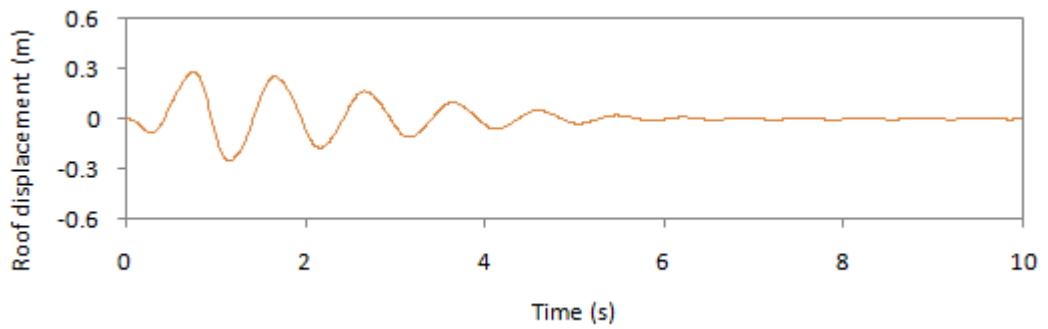
Figure C-25 Roof displacement time history of SMRF-Tp0.9-CB-conf-1
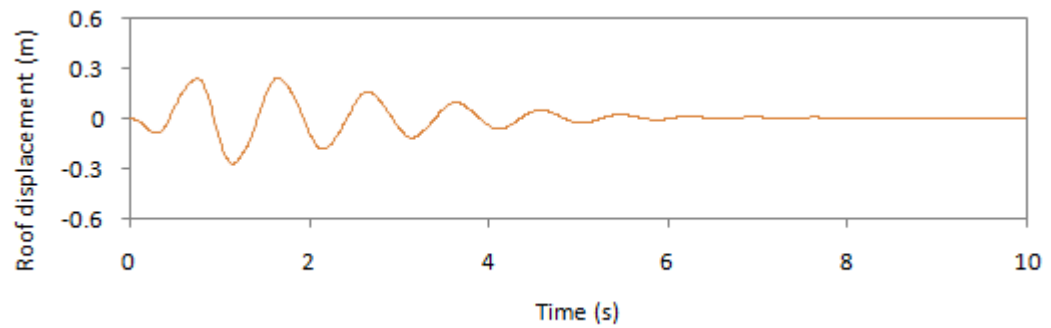
Figure C-26 Roof displacement time history of SMRF-Tp0.9-CB-conf-2
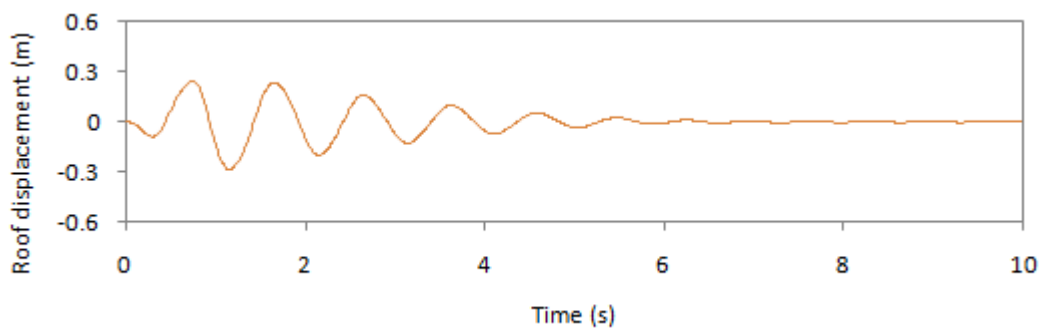
Figure C-27 Roof displacement time history of SMRF-Tp0.9-CB-conf-3
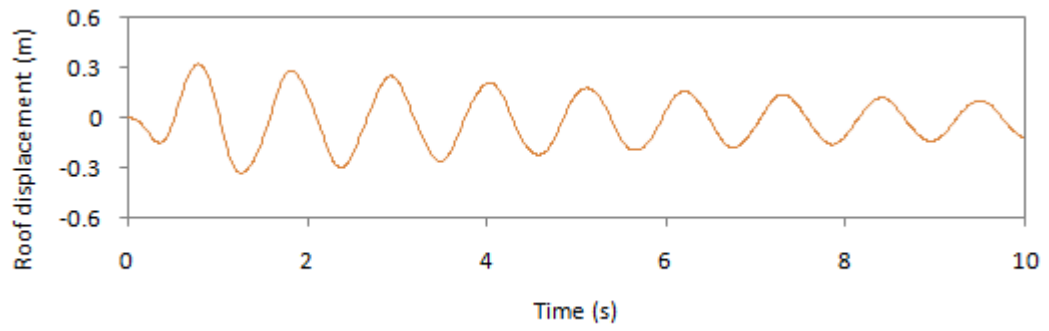
Figure C-28 Roof displacement time history of SMRF-Tp0.9-UF

Appendix D: Base shear and top shear time history
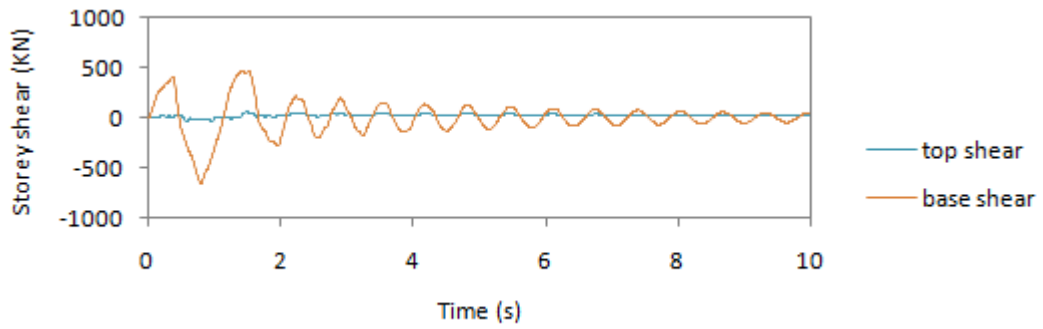
Figure D-1 Base and top shear time history of OMRF-1.4-BRB-conf-1
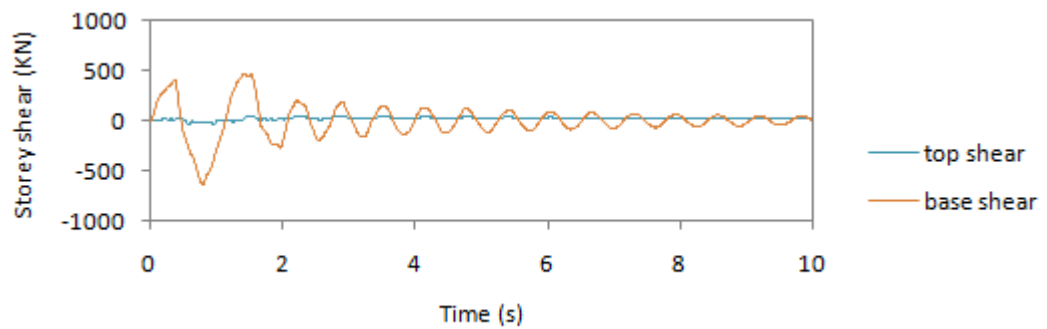
Figure D-2 Base and top shear time history of OMRF-1.4-BRB-conf-2
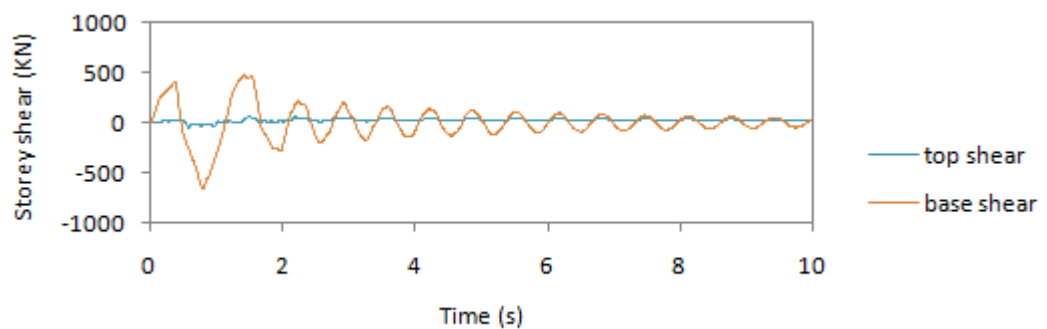
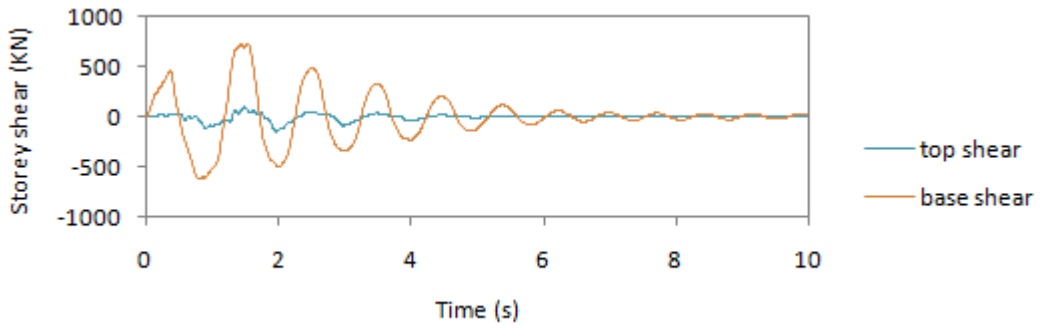Figure D-3 Base and top shear time history of OMRF-1.4-BRB-conf-3
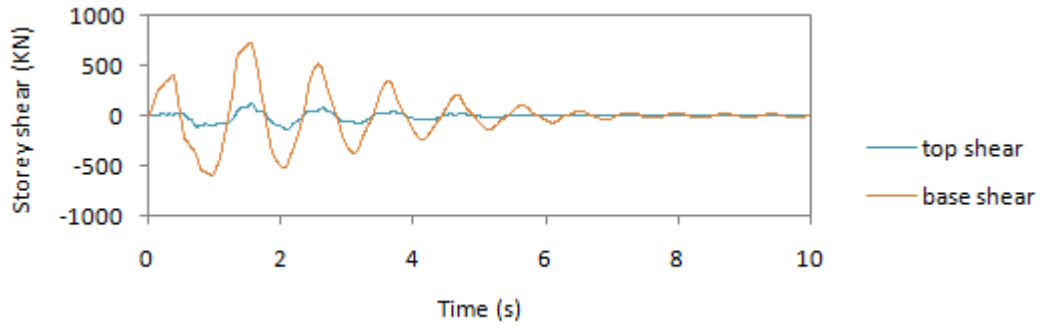
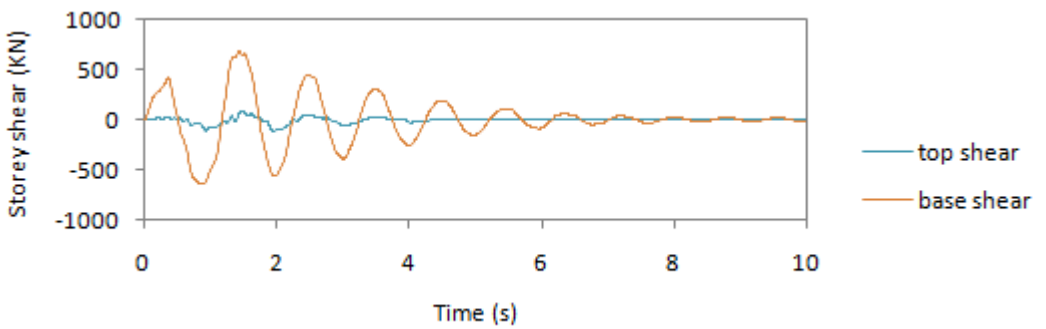Figure D-4 Base and top shear time history of OMRF-1.4-CB-conf-1
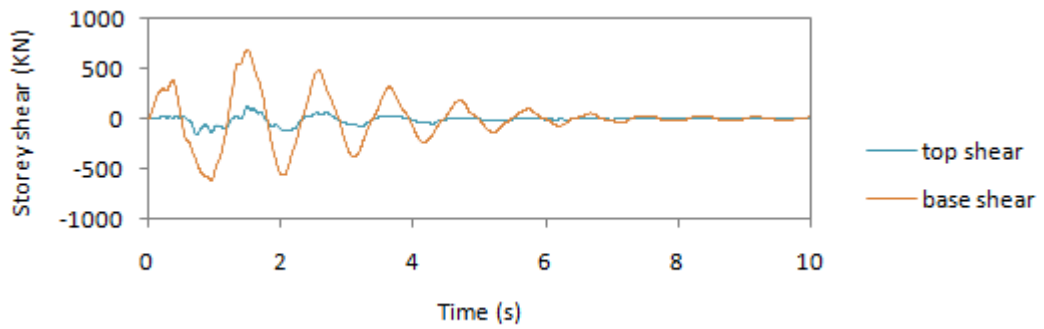
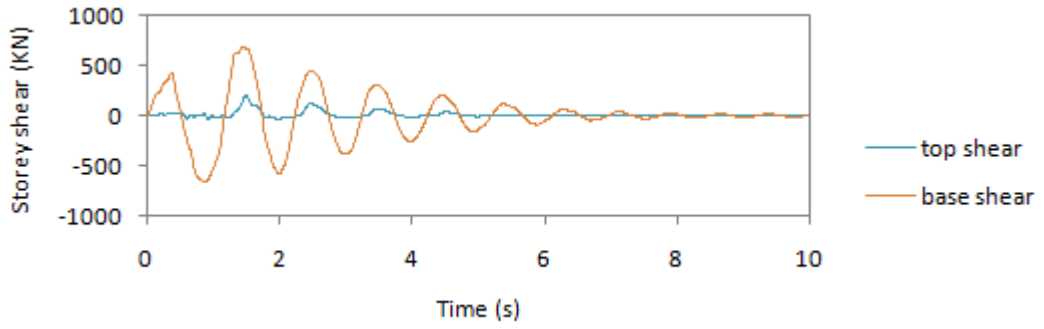Figure D-5 Base and top shear time history of OMRF-1.4-CB-conf-2
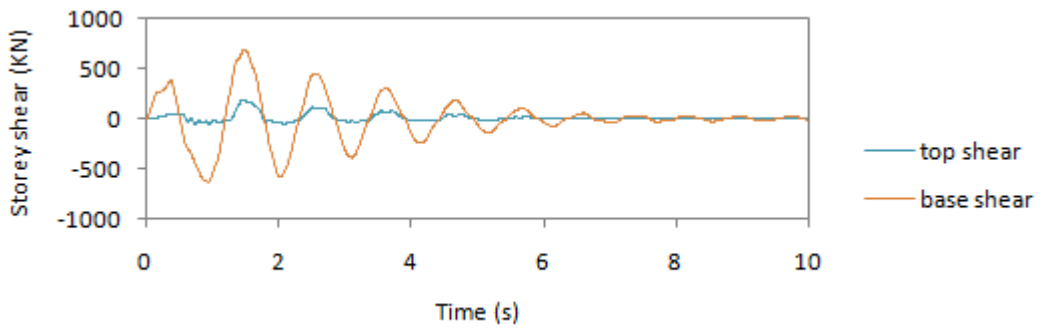
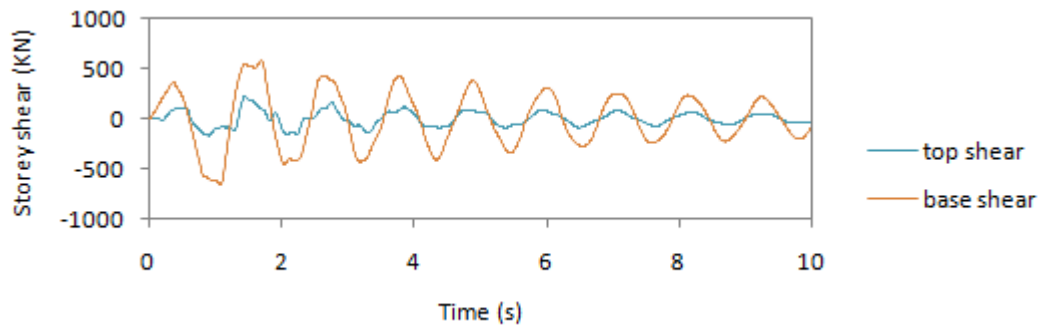Figure D-6 Base and top shear time history of OMRF-1.4-CB-conf-3
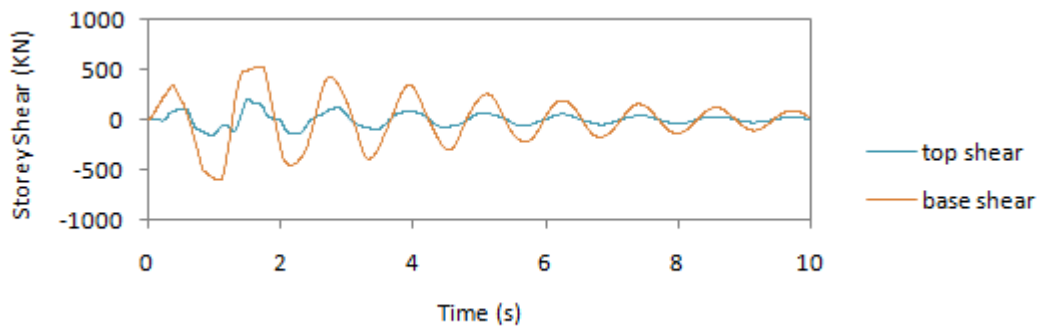
Figure D-7 Base and top shear time history of OMRF-1.4-UF
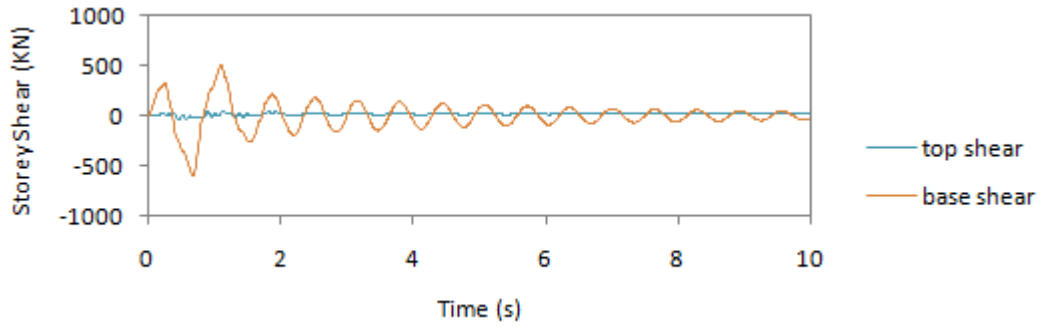
Figure D-8 Base and top shear time history of OMRF-0.9-BRB-conf-1
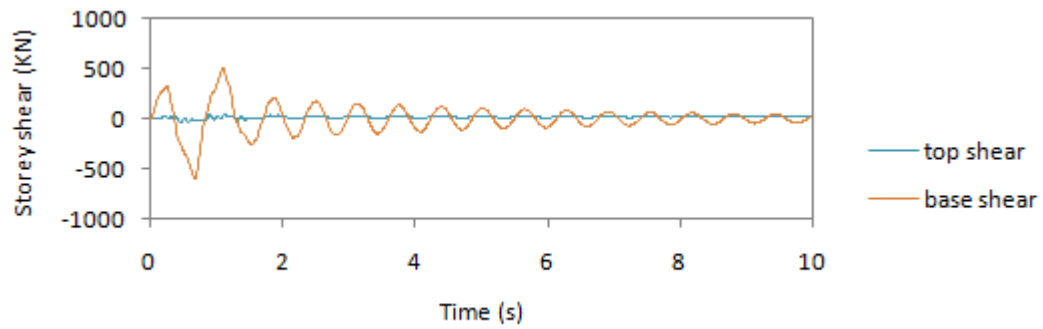
Figure D-9 Base and top shear time history of OMRF-0.9-BRB-conf-2
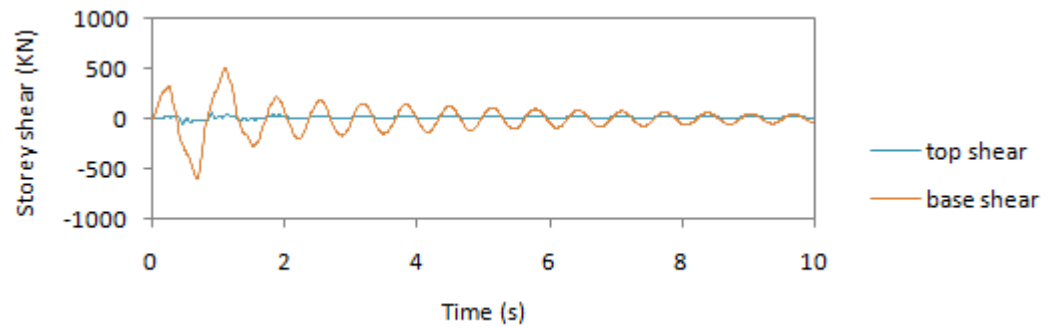
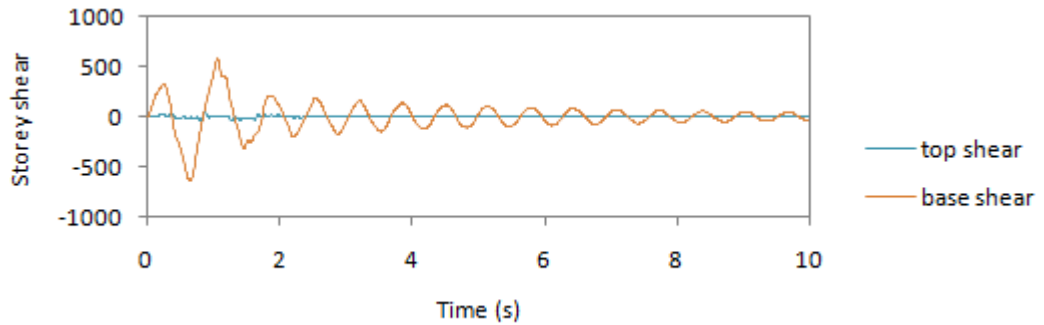Figure D-10 Base and top shear time history of OMRF-0.9-BRB-conf-3
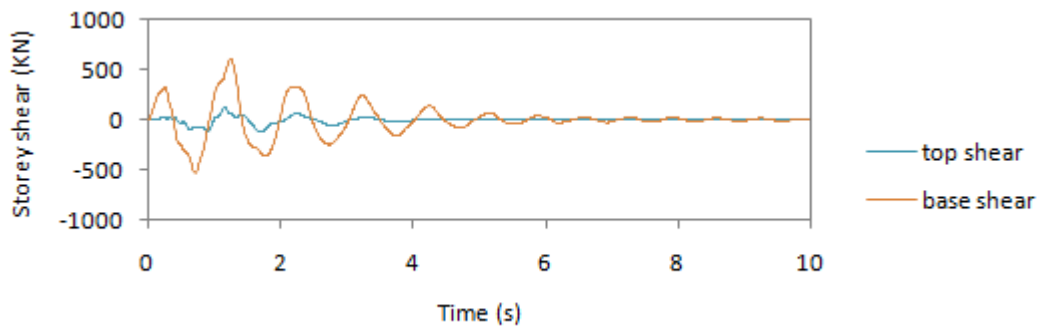
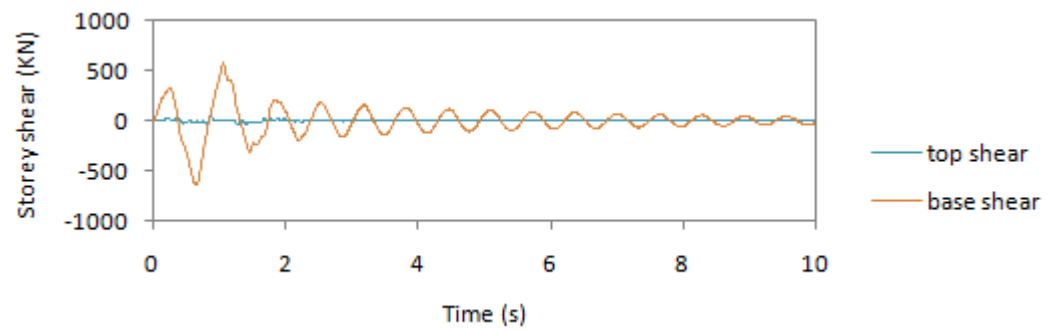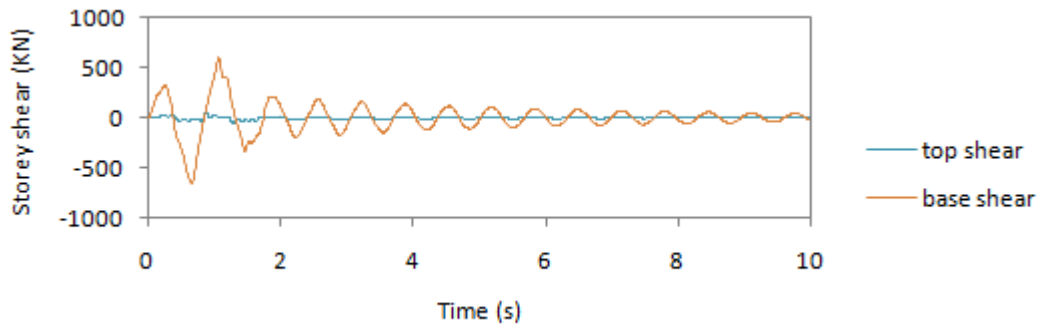Figure D-11 Base and top shear time history of OMRF-0.9-CB-conf-1
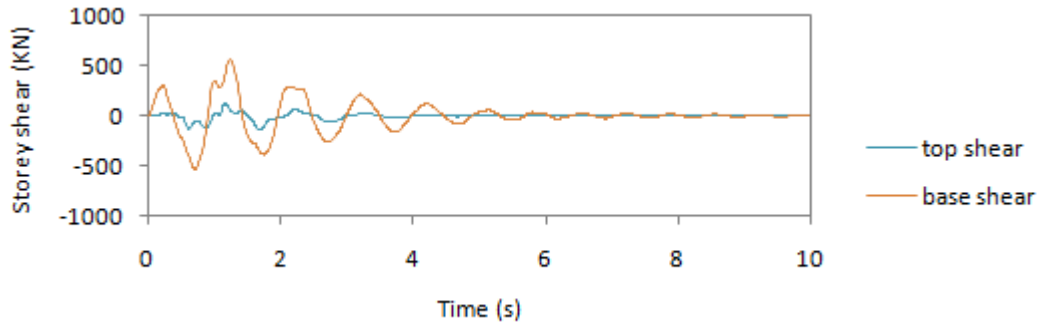
Figure D-12 Base and top shear time history of OMRF-0.9-CB-conf-2
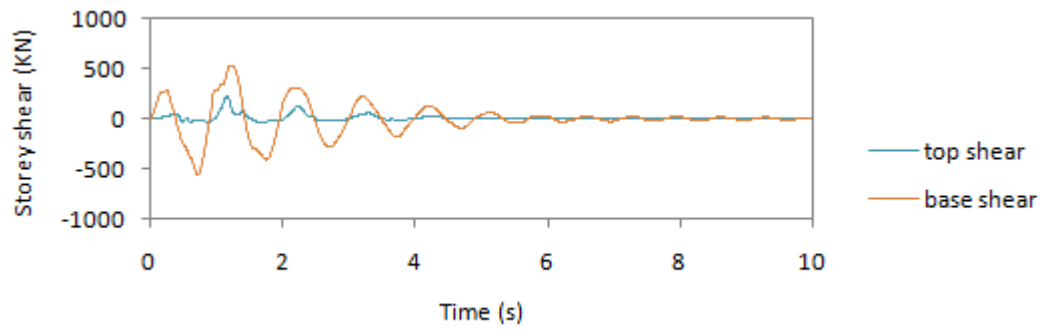
Figure D-13 Base and top shear time history of OMRF-0.9-CB-conf-3
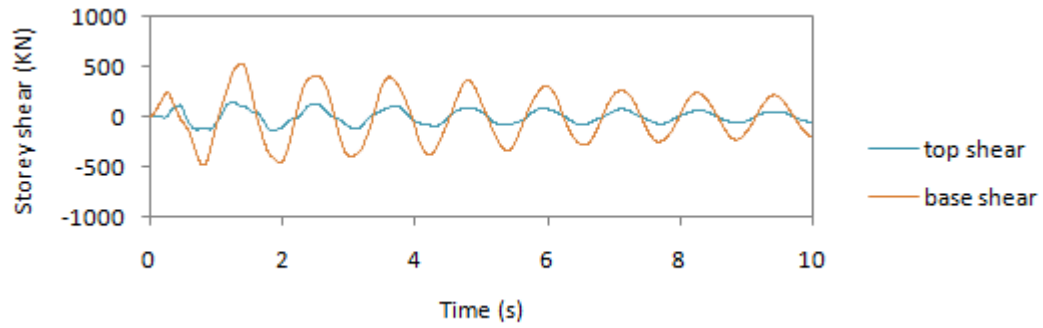
Figure D-14 Base and top shear time history of OMRF-0.9-UF
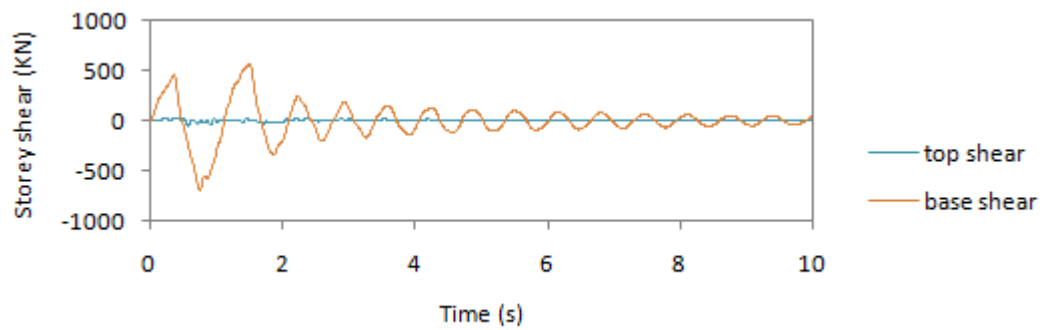
Figure D-15 Base and top shear time history of SMRF-1.4-BRB-conf-1

117
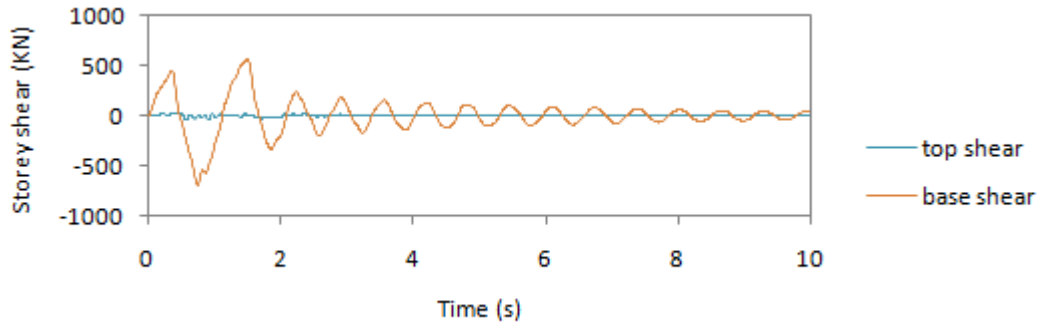
Figure D-16 Base and top shear time history of SMRF-1.4-BRB-conf-2
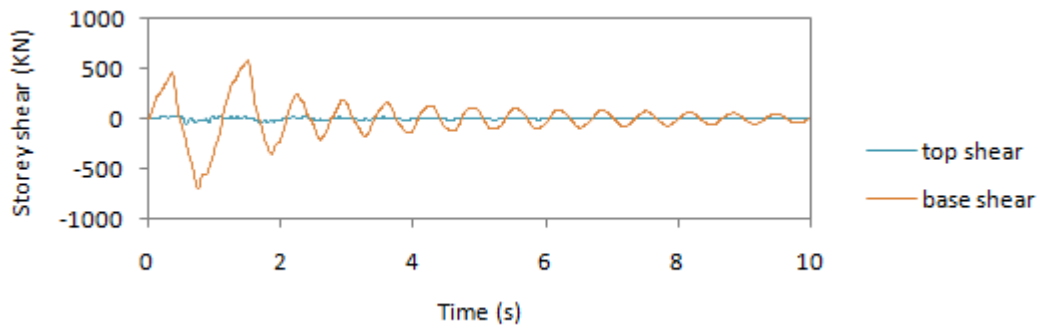
Figure D-17 Base and top shear time history of SMRF-1.4-BRB-conf-3

Figure D-18 Base and top shear time history of SMRF-1.4-CB-conf-1

Figure D-19 Base and top shear time history of SMRF-1.4-CB-conf-2

Figure D-20 Base and top shear time history of SMRF-1.4-CB-conf-3

Figure D-21 Base and top shear time history of SMRF-1.4-UF

Figure D-22 Base and top shear time history of SMRF-0.9-BRB-conf-1

Figure D-23 Base and top shear time history of SMRF-0.9-BRB-conf-2

119

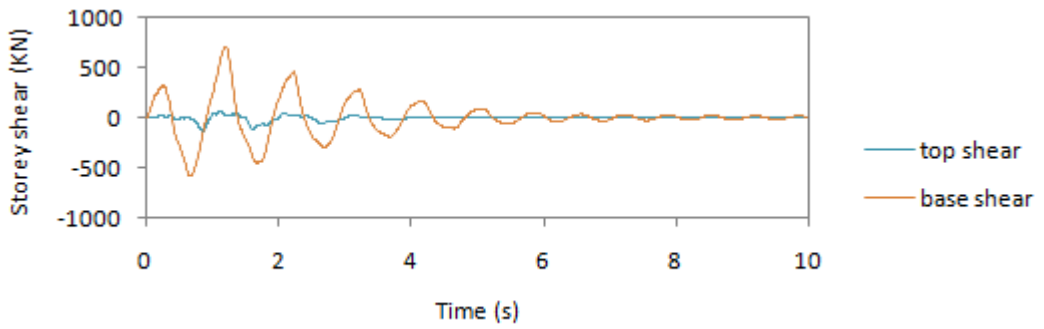Figure D-24 Base and top shear time history of SMRF-0.9-BRB-conf-3

Figure D-25 Base and top shear time history of SMRF-0.9-CB-conf-1
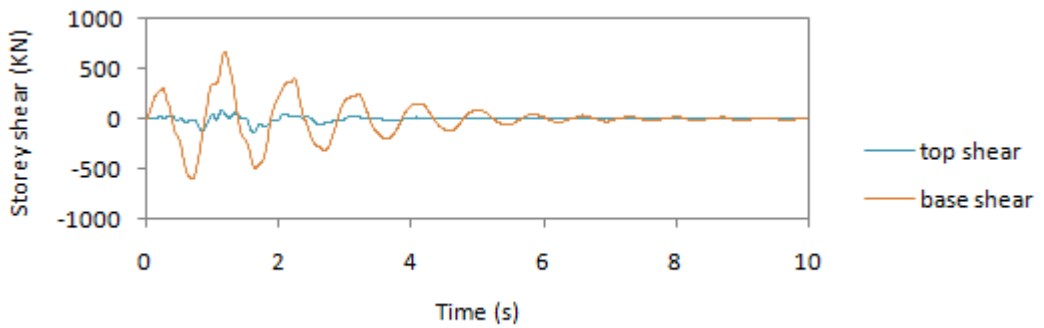

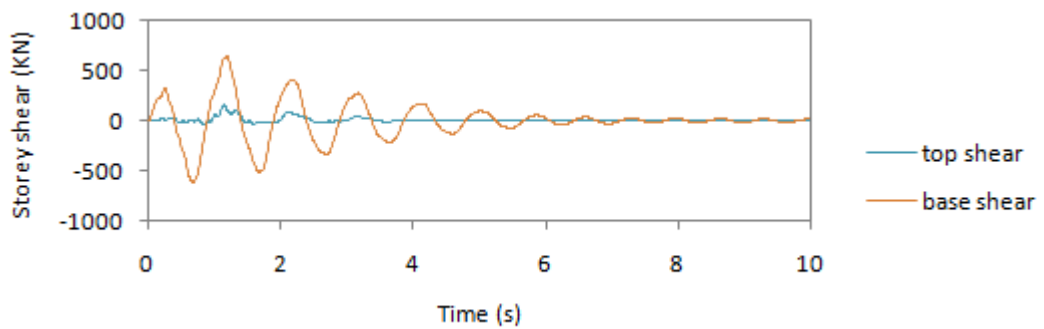Figure D-26 Base and top shear time history of SMRF-0.9-CB-conf-2
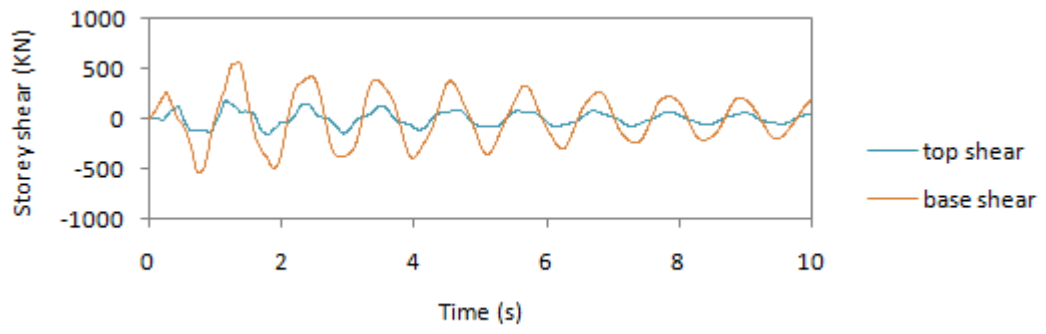

Figure D-27 Base and top shear time history of SMRF-0.9-CB-conf-3

Figure D-28 Base and top shear time history of SMRF-0.9-UF